Medical University of Gdansk

Katarzyna Kaczor

Antitumor activity of newly synthesized ebselen derivatives

Doctoral Dissertation

Supervisor prof. Jędrzej Antosiewicz

Gdańsk 2019

To begin, I would like to express my sincere thanks to Professor Jędrzej Antosiewicz, who gave me the opportunity to conduct scientific work, and for his care and help.

A very special thanks to all of my colleagues from the Departments of Bioenergetics and Physiology of Exercise and Medical Chemistry. Additionally, to my colleagues and doctors from the University of Ancona in Italy: I thank you all for your kindness and friendly welcome.

I wish to express my thanks to Michał for his love, patience and optimism.

I also want to thank to my close friends, especially Patrycja and Kasia for positive motivation, and Monica for linguistic help.

Last, but not least, I am very grateful to my dear parents, who have always believed in me, and offered me endless support and encouragement. Many thanks to my dad for helping me choose this scientific career path and for his valuable suggestions.

Thank you to all those who contributed to this work.

This work was supported by National Science Centre, Poland, grant no. 2015/17/B/NZ7/03058.

Table of Contents

List of Abbreviations 7
1. Abstract in Polish 8
2. Abstract 10
3. Introduction 12
3.1. Prostate cancer 12
3.1.2. PTEN 13
3.2. Oxidative stress 14
3.2.1. Reactive oxygen and nitrogen species 14
3.2.2. Lipid Peroxidation 17
3.2.3. Protein modification 17
3.2.4. DNA damage 18
3.3. Antioxidant defense 19
3.3.1. Enzymatic antioxidants 19
3.3.2. Non-enzymatic Antioxidants 20
3.3.3. Repair line 21
3.4. Oxidative stress and signaling pathways 21
3.5. Akt 22
3.5.1. Akt and its anti-apoptotic mechanism in cancers 23
3.6. The cell cycle 25
3.7. Mechanisms of cell death 25
3.7.1. Apoptosis 25
3.7.2. Necrosis 26
3.7.3. Ferroptosis 27
3.8. PARP 27
3.9. Anticancer and chemopreventive activities of organoselenium compounds ... 28
3.9.1. Antioxidant and cytoprotective activites of ebselen 29
4. Aims 31
5. Materials 32
5.1. Cell lines 32
5.2. Tested chemical compounds 32
5.3. Reagents 33
5.3.1. Cell culture media and reagents 33

5.3.2. Supplements: 33
5.4. Buffers and reagents: 33
5.4.1. SRB assay: 33
5.4.2. Commercial assay kits: 33
5.4.3. Western blot analysis: 33
5.4.4. Primary antibodies: 35
5.4.5. Secondary antibodies: 35
5.4.6. Comet assay: 35
5.5. Other reagetns: 36
5.6. Evaluation of maximum tolerated dose (MTD) 36
6. Methods 36
6.1. Cell culture 36
6.2. Cell treatment 36
6.3. Cell viability assay using Sulforhodamine B (SRB) 37
6.4. Cell cycle assay 37
6.5. Assessment of cell death using Muse Anaylzer 38
6.6. Cell viability assay 38
6.7. Detection of intracellular reactive oxygen species (ROS) by flow cytometry 38
6.8. Protein lysate preparation 39
6.8.1. Protein concentration using Bradford protein assay 39
6.9. Western blotting - One gel electrophoresis 40
6.9.1 Transfer protein from gel to membrane 40
6.10. Comet assay 41
6.10.1 Evaluation of DNA damage 41
6.11. Statistical analysis 42
7. Animal study 42
7.1. Determination of Maximum Tolerated Dose (MTD) after single administration 42
7.2. Evaluation of Maximum Tolerated Dose – study design 42
7.2.1 Drug preparation 43
8. Results 44
8.1. 1. Antitumor activity of *N*-substituted ebselen derivatives 45
8.2. Cytotoxic activity of *N*-allyl-BS in DU 145, PC-3 and PNT1A cells 46
8.2.1. Influence of *N*-allyl-benzisoselenazol-3(*2H*)-one on cell viability in prostate cancer cell lines DU 145 and PC-3, and in the non-cancer cell line PNT1A 46

8.2.2. Influence of *N*-allyl-BS on the cell cycle in prostate cancer cells 48
8.2.3. Influence of *N*-allyl-BS on apoptosis and necrosis in prostate cancer cells .. 50
8.2.4. Effect of DFO and Ferr-1 on cell death induced by *N*-allyl-BS 52
8.2.5. Influence of *N*-allyl-BS on ROS generation in prostate cancer cells 54
8.2.6. Influence of *N*-allyl-BS on DNA damage in prostate cancer cells 56
8.2.7. Influence of *N*-allyl-BS on the level of the active form of Akt in prostate cancer cells 58
8.2.8. Cytotoxic activity of *N*-allyl-BS in PC-3 cells-effects of different oxygen tension 60
8.3. Cytotoxic activity of *N*-(3-m)-b-BS in DU 145 and PC-3 cells and PNT1A 62
8.3.1. The influence of *N*-(3-methyl)-butyl- benzisoselenazol-3(*2H*)-one on cell viability in prostate cancer cell lines DU 145 and PC-3, and in the non-cancer PNT1A 62
8.3.2. Influence of *N*-(3-m)-b-BS on the cell cycle in prostate cancer cells 64
8.3.3 Influence of *N*-(3-m)-b-BS on apoptosis and necrosis in prostate cancer cells 65
8.3.4 Effect of DFO and Ferr-1 on cell death induced by *N*-(3-m)-b-BS 68
8.3.5. Influence of *N*-(3-m)-b-BS on ROS generation in prostate cancer cells 69
8.3.6. Influence of *N*-(3-m)-b-BS on DNA damage in prostate cancer cells 71
8.3.7. Influence of *N*-(3-m)-b-BS on the level of active form of Akt in prostate cancer cells 72
8.3.8. Cytotoxic activity of *N*-(3-m)-b-BS in PC-3 cells-effects of different oxygen tension 74
8.3.9. Influence of *N*-allyl-BS and *N*-(3-m)-b-BS on DNA damage in PNT1A 75
8.4. Result of MTD determination of *N*-allyl-BS *in vivo* 77
8.4.1. Evaluation of MTD of *N*-allyl-BS *in vivo* 77
9. Discussion 80
10. Conclusions 89
11. Bibliography 90

List of Abbreviations

PSA - prostate specific antigen

PTEN - phosphatidylinositol phosphatase-3,4,5-triphosphate

ROS - reactive oxygen species

RNS - reactive nitrogen species

GSH - glutathione

ATP - adenosine triphosphate

8-OH-2'dG - 8-hydroxy-2-deoxyguanine

GPx - glutathione peroxidase

Akt/PKB - kinase Akt, protein kinase B

PI3K - phosphatidyl inositol 3 kinase

PARP - Poly (ADP-ribose) polymerase-1

***N*-allyl-BS** - *N*-allyl-benzisoselenazol-3(*2H*)-one

***N*-(3-m)-b-BS** - *N*-(3-methyl)-butyl- benzisoselenazol-3(*2H*) one

DFO - desferoxamine

Ferr-1 - ferrostatin-1

MTD – maximum tolerated dose

1. Abstract in Polish

Nowotwór prostaty plasuje się na drugim miejscu pod względem zachorowalności oraz na piątym miejscu pod względem śmiertelności u mężczyzn. W związku z tym, kluczowe znaczenie ma poszukiwanie nowych i skutecznych chemioterapeutyków w leczeniu raka prostaty. Jakkolwiek, przez ostatnie dziesięciolecia, badania w tym aspekcie są wciąż niewystarczające. Podjęto wiele prób aby opracować nowe i skuteczne leki przeciwnowotworowe, które wykazują mniejszą toksyczność względem normalnych, ludzkich komórek.

Zainteresowanie cząsteczaką ebselenu zaczęło się już w latach 80 i jest on jednym z najszerzej badanych związków organicznych selenu. Wykazano, iż ebselen posiada wysoką aktywność antyoksydacyjną. Naśladuje on działanie enzymu GPx, który odpowiada za równowagę pomiędzy reaktywnymi formami tlenu a antyoksydantami. Zatem, usuwa nadmiar silnego utleniacza, nadtlenku wodoru i chroni komórki przed wolonorodnikowym uszkodzeniem makrocząsteczek. Ponadto, wykazuje on działanie przeciwzapalne, neuroprotekcyjne oraz przeciwnowotworowe.

W niniejszej pracy postawiono hipotezę, iż przeciwnowotworowe działanie *N*-allilo-BS i *N*-(3-m)-b-BS oparte o (indukcja apoptozy i /lub zatrzymanie cyklu komórkowego, produkcja ROS) może być związane z regulacją szlaku sygnałowego kinazy Akt.

Głównym celem niniejszej rozprawy doktorskiej było zweryfikowanie postawionej hipotezy oraz zbadanie potencjalnego mechanizmu działania przeciwnowotworowego dwóch wybranych *N*-podstawionych pochodnych ebselenu, mianowicie *N*-allilo-BS i *N*-(3-m)-b-BS, na dwóch liniach komórek raka prostaty, różniących się od siebie podłożem genetycznym DU 145 i PC-3. Wpływ badanych pochodnych ebselenu na parametr żywotności komórek oceniono również na normalnej linii komórkowej prostaty PNT1A.

Otrzymane wyniki badań w ramach rozprawy doktorskiej wykazały, że oba związki organiczne selenu wywierały działanie cytotoksyczne w stosunku do komórek nowotworu prostaty oraz hamowały proliferację komórek, podczas gdy normalne komórki były mniej wrażliwe na działanie pochodnych ebselenu. Dodatkowo, oba związki indukowały zatrzymanie cyklu komórkowego w fazie G2 /M i promowały śmierć komórki na drodze apoptozy. Zostało to potwierdzone przez pomiar ciętej formy

PARP, który jest markerem apoptozy i uszkodzenia DNA. Ponadto, *N*-allilo-BS i *N*- (3-m) -b-BS indukowały generację ROS, w obu liniach komórek raka prostaty. Wzmożoną produkcję ROS można powiązać z indukcją stresu oksydacyjnego i genotoksycznym uszkodzeniem DNA. *N*-allil-BS statystycznie indukował uszkodzenie DNA w komórkach PC-3 po traktowaniu 8h i 24h. Co więcej, przedstawione dane potwierdziły, że poziom aktywnej formy Akt (p-Akt) był istotnie statystycznie zmniejszony w komórkach DU145 i komórkach PC-3 traktowanych *N*-allilo-BS i *N*-(3-m)-b-BS. Wyniki te podkreślają, że komórki PC-3 wykazują większą wrażliwość, niż komórki DU145 na działanie *N*-allilo-BS i *N*-(3-m)-b-BS. Może to być związane z inaktywacją ścieżki sygnałowej kinazy Akt. Dodatkowo, *N*-allilo-BS wykazał silniejsze działanie cytotoksyczne względem komórek raka prostaty niż *N*-(3-m)-b-BS i zatem został wybrany do badań *in vivo.* W badaniach na myszach, wyznaczono maksymalna tolerowaną dawkę (MTD) jednokrotnego podania dla *N*-allilo-BS, która wynosiła 100mg/kg. Wyznaczenie dawki MTD jest głównym celem badań klinicznych w 1 fazie, gdzie kolejno w dalszych etapach wyznaczana się MTD wielopodaniową oraz parametry farmakokinetyczne.

Podsumowując, dane uzyskane w niniejszej rozprawie doktorskiej pokazują, że nowo zsyntetyzowane *N*-allilo-BS i *N*-(3-m)-b-BS zmniejszają przeżywalność komórek raka prostaty oraz indukują śmierć komórki poprzez apoptozę. Może to być wynikiem zatrzymania cyklu komórkowego, zwiększonej produkcji ROS, uszkodzenia DNA oraz zahamowania szlaku sygnałowego Akt. Zatem, *N*-allilo-BS i *N*-(3-m)-b-BS można uwzględnić jako nowe i silne chemioterapeutyki przeciwko rakowi gruczołu krokowego.

2. Abstract

Prostate cancer has been listed as the second most prevalent cancer worldwide behind lung cancer, and the fifth leading cause of mortality in men. Due to this fact, the search for novel and potent chemotherapeutics against prostate malignancies has become crucial. In particular, over the last decades, much effort has been made to develop new and effective anticancer drugs that exhibit less toxicity towards normal human cells.

Ebselen has been one of the most extensively studied organoselenium compounds since the1980s. It was shown to reveal a broad spectrum of biological activities, including chemopreventive, anti-inflammatory, neuroprotective, and anticancer activity. Moreover, ebselen exhibits potent antioxidant activity as it mimics GPx, and therefore possesses the ability to regulate redox homeostasis and protect the cells against oxidative stress.

We hypothesized that some of the *N*-allyl-BS and *N*-(3-m)-b-BS anticancer activities (apoptosis induction and/or cell-cycle arrest, and ROS production) could be associated with the down-regulation of the Akt-dependent signaling pathway.

The main purpose of this doctoral dissertation was to verify the hypothesis and to investigate the anticancer potential mechanism of two selected N-substituted ebselen derivatives, namely *N*-allyl-BS and *N*-(3-m)-b-BS, on two cancer cell lines, which are the phenotypically different from each other DU 145 and PC-3. The influence of the analyzed compounds on the cell viability parameter was also assessed on normal prostate cell line PNT1A.

The results demonstrated that both organoselenium compounds exerted cytotoxic activity towards prostate tumor cells and inhibited cell proliferation, whereas normal cells were less sensitive to ebselen analogues. Moreover, both compounds induced G2/M cell cycle arrest, and promoted cell death through apoptosis. This was confirmed by the measurement of PARP-cleavage, which is the marker of apoptosis and DNA damage. Moreover, *N*-allyl-BS and *N*-(3-m)-b-BS induced ROS production in both cancer cell lines. Extensive ROS generation can be associated with the induction of oxidative stress and DNA damage. In addition, *N*-allyl-BS statistically induced DNA damage in PC-3 cells. What is more, the presented data confirmed that the levels of the active form of Akt (p-Akt) were significantly reduced in DU145 and PC-3 cells treated

with *N*-allyl-BS and *N*-(3-m)-b-BS. These results highlight that higher sensitivity of PC-3 than DU145 cells to *N*-allyl-BS *N*-(3-m)-b-BS may be associated with Akt inactivation.

N-allyl-BS exhibited a stronger cytotoxic effect towards prostate cancer cells than *N*-(3-m)-b-BS, and therefore was selected for *in vivo* studies. The maximum tolerated dose (MTD) of a single oral administration for *N*-allyl-BS in mice was determined as 100mg/kg. Determination of single MTD administration is one of the main goals in the first phase of clinical trials, in order to further establish multiple MTD administration and pharmacokinetic parameters.

In conclusion, the data presented in this doctoral dissertation demonstrate that newly synthesized *N*-allyl-BS and N -(3-m)-b-BS decreased the survival of cancer cells and promoted cell death through apoptosis. This may be an outcome of cell cycle arrest, higher ROS generation, DNA damage, and inactivation of the Akt signaling pathway. Taken together, *N*-allyl-BS and N -(3-m)-b-BS may be elucidated as novel and potent chemotherapeutics against prostate cancers.

3. Introduction

3.1. Prostate cancer

The prostate is the male gland located between the penis and the bladder and located in front of the rectum. Its main function is to support the production of semen. However, in the presence of dysfunction or morphological change (e.g. hypertrophy of the prostate gland), there is a potential for cancer cell formation. Adenocarcinoma is one of the most common malignant prostate tumors that develop from gland cells. According to the GLOBOCAN study, there were 1,1 million diagnosed cases, and 307,000 deaths, in 2012. (Ferlay, Soerjomataram et al. 2015) The data show that prostate cancer morbidity and mortality numbers have increased, with 1,3 million (7.0 %) cases of prostate cancer and 359,000 (3.8 %) deaths estimated worldwide, in 2018 (Bray, Ferlay et al. 2018). Due to this fact, prostate cancer has been listed as the second most prevalent cancer worldwide behind lung cancer, and the fifth leading cause of mortality in men. What is more, in the United States, it is estimated that 1 man in 9 will be diagnosed with a prostate tumor and 1 out of 40 will die because of cancer (Ferlay, Colombet et al. 2018). The risk of cancer increases with age. It is evaluated that 6 incidences out of 10 of prostate tumors are diagnosed in men over 60 years old. In men under 55, prostate cancer can develop asymptomatically. In contrast, men under 40 are at lower risk of cancer morbidity. The average age of diagnosis in men is 66 (American Society of Cancer). Notwithstanding, life expectancy is related with an early diagnosis among men developing prostate tumor.

The number of men developing prostate cancer in Poland is particularly high. It was evaluated that there were 14,211 prostate cancer cases among men, which was 17.4 % of all cancer cases followed by 4 876 deaths, which is 8.8% of all deaths in 2015 (Didkowska, Wojciechowska 2015). It is worth to mention that between the 1980s and 2015, the morbidity and mortality rates significantly increased. Furthermore, the prognostics for the years 2010-2025 estimate that there will be an increase in the cases of prostate cancer-associated deaths among different age groups (Didkowska, Wojciechowska et al.2009). Hence, it is important to take an interest in understanding prostate cancer. It is also important to note that life expectancy increases with early diagnosis of prostate cancer.

The clinical screening of prostate specific antigen (PSA) is one of the factors used in diagnosing prostate cancer in asymptomatic individuals (Tikkinen, Dahm et al. 2018; Vernooij, Lytvyn et al. 2018). Nevertheless, according to the American Society of Cancer, the PSA test is not precise in all cases of prostate cancer (American society of Cancer). Another diagnostic approach is the detection of latent cancer in tissue removed during prostatectomy or at autopsy. Unfortunately, there is little information about the ethology of prostate cancer. Genetic background is considered one of the factors involved in the development of carcinogenesis. In particular, tests of abnormal prostate cancer genes which are inherited from both parents may improve the identification of prostate cancer (Perdomo, Zapata-Copete et al. 2018). Another theory is that it is linked with obesity and a decreased intake of vitamins and antioxidants in the daily diet (Daniyal, Siddiqui et al. 2014). Above all, isoflavonoids such as genistein and quercetin have been shown to play an important role in chemoprevention from prostate cancer through antioxidant and hormonal capacity (Aufderklamm, Miller et al. 2014; Ward, Mir et al. 2018). Singh and co-authors reported that sulforaphane also exhibited chemopreventive activities in a prostate tumor mouse model (Singh, Kim et al. 2018). A deficiency in nutritional elements also leads to a higher risk of neurodegenerative diseases and cancers (Avery and Hoffmann 2018). It is worth mentioning that selenium is one of the essential nutrients that plays an important role in various biological and physiological processes in cells. Due to this fact, selenium has been shown to reveal chemopreventive and anticancer activities against prostate cancer (Vinceti, Filippini et al. 2018), which will be discussed in the next chapter in detail.

3.1.2. PTEN

Phosphatase and tensin homolog (PTEN) is defined as the multi-functional “tumor suppressor” that is frequently lost in many cancers. PTEN modulates cell cycle progression and cell survival through downregulating the intracellular levels of phosphatidylinositol-3,4,5-trisphosphate by its dephosphorylation, thus the Akt signaling pathway (Hopkins, Hodakoski et al. 2014). In many cancer cell lines such as prostate, breast glioblastoma or lung cancer, the mutations or deletions in this gene encoding Pl3K signaling pathway lead to higher activity of serine/threonine kinase (Akt) (Hollander, Blumenthal et al. 2011; Chiang, Chen et al. 2015; Naderali, Khaki et

al. 2018). Moreover, the loss of the expression of PTEN and the loss of its function result in over-activation of Akt by its constant phosphorylation. Akt regulates many processes including the cell cycle, apoptosis, cell migration, nutrient metabolism or angiogenesis (Naderali, Khaki et al. 2018). Inhibition of Akt signaling leads to apoptosis and growth inhibition, particularly in tumor cells characterized by elevated Akt activity. Due to this fact, most commonly studied prostate cancer cell lines are DU 145 and PC-3, which are phenotypically different from each other. Namely, PTEN-positive DU 145 is characterized by normal Akt kinase activity and PTEN-negative PC-3 by elevated Akt kinase activity. Hence, PTEN-negative tumors demonstrate amplified metastatic potential and a higher resistance to chemotherapeutics as compared to PTEN-positive tumors (Choi, Xie et al. 2017).

3.2. Oxidative stress

According to Helmut Sies' definition "oxidative stress " refers to an imbalance between pro-oxidant and anti-oxidant reactions, leaning towards pro-oxidant excess (Sies 1997). Oxidative stress is described as the disturbance of homeostasis between reactive oxygen species (ROS) and reactive nitrogen species (RNS) formation, and a decreased antioxidant ability to remove them. It has been shown that oxidative stress is one of the main factors involved in aging, arteriosclerosis, neurodegenerative disease, and the induction of cancers and other conditions (Sies and Cadenas 1985; Halliwell 1992; Coyle and Puttfarcken 1993; Klaunig and Kamendulis 2004; Burton and Jauniaux 2011).

3.2.1. Reactive oxygen and nitrogen species

At homeostatic levels ROS and RNS remain the normal products of cell metabolites. It is demonstrated that in physiological conditions, ROS play an important role in, and has a beneficial impact on biological functions (Lenaz 2012) They are responsible for the activation of protein kinases and act as the second messengers in many intracellular signaling pathways. ((Burton and Jauniaux 2011). Furthermore, the superoxide anion ($O_2^{\bullet -}$), produced by neutrophils plays a vital role in hosting defense against pathogens. Another one, nitric oxide (NO) is an important signaling molecule in

human body, that modifies the regulation of blood pressure, immune system in the cell and neuronal transmitting. The main ROS are: singlet oxygen ($^1O_2$), ozone (O_3), superoxide anion ($O_2^{\bullet -}$), hydrogen peroxide (H_2O_2), and hydroxyl radical ($OH^\bullet$). Hydrogen peroxide in the presence of reduced metal ions undergoes Fenton (1) or Haber-Weiss (2) reaction and generates the most dangerous and destructive $OH^\bullet$ (Wardman and Candeias 1996).

$$Fe^{2+} + H_2O_2 \longrightarrow OH^\bullet + OH^- + Fe^{3+} \quad (1)$$

$$H_2O_2 + O_2^- \longrightarrow OH^\bullet \quad OH^- + O_2 \quad (2)$$

The term reactive nitrogen species (RNS) describes nitrogen species and includes nitric oxide ($NO^\bullet$), nitrogen peroxide ($NO_2^\bullet$), peroxynitrite ($ONOO^-$) and peroxide radicals ($ROO^\bullet$).

The generation of ROS and RNS may be formed from either exogenous or endogenous sources. Exogenous sources include: UV light, visible light and ionizing radiation, which is the most dangerous, as it can lead to cell damage and the development of cancer (Weinstein 1991; Churg 2003). Other factors are : smoking, improper diet, environmental and industrial toxins and many others (Fang, Yang et al. 2002). These factors may trigger ROS and RNS formation through the basic metabolism of the cell or through the activation of endogenous sources (Churg 2003).

The major endogenous source of ROS generation is referred to as the mitochondrial respiratory chain, complex I and III, located in the inner mitochondrial membrane, and it is considered to produce around 90% of ROS (Chen, Vazquez et al. 2003). To this fact, mitochondria are considered the main source of ROS generation. What's more, the electron transport chain (ETC) promotes the four electron oxygen reduction reaction, which in the end forms a water molecule (Turrens 2003). However, 1-3 % of electrons undergo a partial reduction of oxygen, resulting in the "leakage of electrons" and inducing ROS generation. Another source of ROS, superoxide anions are enzymatic reactions catalyzed by oxidoreductases such as xanthine oxidase, which catalyzes hypoxanthine to xanthine, and further xanthine to uric acid, and plasma membrane NADPH oxidase, existing majorly in the phagosome membrane (Javeshghani, Magder et al. 2002; Gomez-Cabrera, Borras et al. 2005). Cytochrome P-450 enzymes, present in the endoplasmic reticulum and peroxisomal flavin oxidases, contribute to the formation of superoxide anion (Valko, Izakovic et al. 2004; Hrycay and Bandiera 2015). It is important to note that in the inflammatory stage

a rapid increase in oxygen consumption by phagocytic cells generates an "oxygen burst", which is another source of endogenous ROS generation (Lenaz and Genova 2009; Lenaz 2012). Extensive ROS generation leads to damage of these macromolecules: lipids, proteins and nucleic acids. Besides the macromolecules, ROS oxidize small molecules such as glutathione (GSH), ascorbate and NAD, etc. (Sies and Cadenas 1985; Das and White 2002). Moreover, ROS elevate the level of intracellular calcium ions due to stimulation of the calcium channel and inactivation of the membrane calcium pump. They decrease the level of ATP since ROS inhibit the glycolysis process and oxidative phosphorylation. (Marnett 2000; Lenaz and Genova 2009) Taken together, amplified ROS generation promotes various harmful effects and induces oxidative stress. (Laurent, Nicco et al. 2005). The simplified scheme of the dangerous action of free radicals is presented in Fig. 1

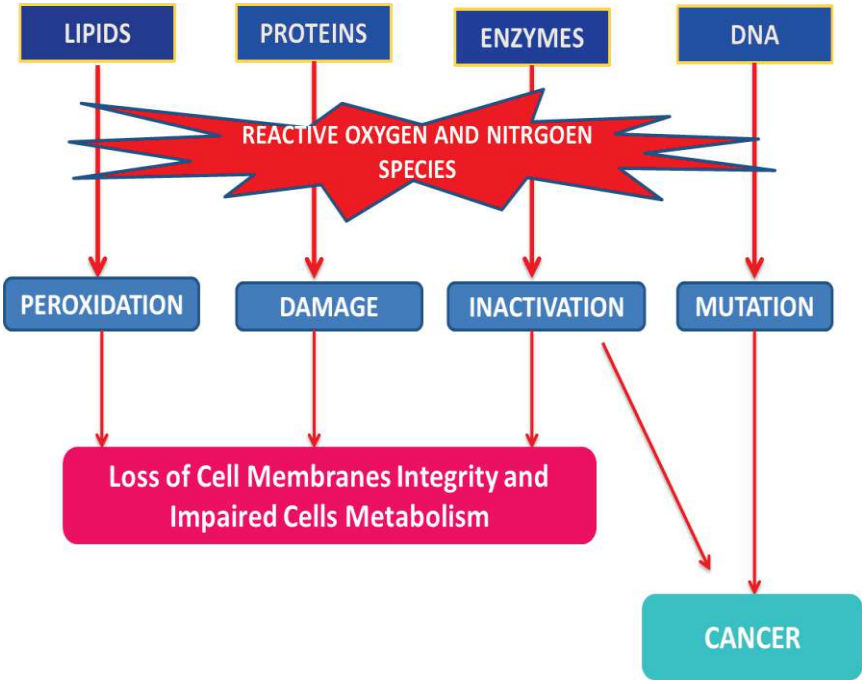

Fig. 1 Deleterious effect of ROS and RNS on macromolecules

3.2.2. Lipid Peroxidation

Lipid peroxidation is a chain reaction and is initiated by free radicals oxidizing polyunsaturated fatty acid side chains in cell membranes, leading to their damage. The modification of cellular membrane causes loss of membrane integrity, depolarization, and decreases oxidative phosphorylation. Lipid peroxidation can be either enzymatic or non-enzymatic. Principal markers detected in this process are: malondialdehyde, 4-hydroxy-2-nonenal, 8-izoprostane and others (Mylonas and Kouretas 1999; Yoshida, Umeno et al. 2013; Shichiri 2014).

3.2.3. Protein modification

Hydroxyl radicals formed by ionizing radiation or by the Fenton reaction may directly react with amino acids, both free and in proteins, causing cleavage of the polypeptide backbone of proteins, modification of amino acid side chains, and conversion of the protein to derivatives that are highly sensitive to proteolytic degradation (Naskalski and Bartosz 2000; Beal 2002) .In particular, most aromatic groups and especially sulfhydryl groups (-SH) are sensitive to the oxidation of free radicals. They undergo modification in the reaction with free radicals, and they generate protein carbonylation and there is a decrease in the level of sulfhydryl groups, leading to protein inactivation. What is more, the elevated level of carbonyl groups and the decreased level of sulfhydryl groups are commonly used markers of protein oxidation, both *in vitro* and in pathological conditions (Dalle-Donne, Giustarini et al. 2003). Despite direct alteration of proteins by ROS oxidation, indirectly, proteins may be covalently changed by products of lipid and carbohydrate peroxidation (Klaunig, Kamendulis et al. 2010). The above mentioned modifications contribute to the inactivation of enzymes, destruction of transport proteins, and haemoglobin and myoglobin oxidation, and further cause the induction of carcinogenesis (Smith, Carney et al. 1992; Stadtman 1992; Davies 2016).

3.2.4. DNA damage

The integrity of DNA is one of the important factors in maintaining biological and physiological cell function. Interestingly, it is estimated that human cells undergo daily exposure to hydroxyl radical "oxidative attacks" at 1.5 x 10^5. Of note, more than 100 oxidative products, including single or double strand DNA cleavage, have been identified. Furthermore, the permanent oxidative alternations of genetic material result in the induction of mutagenesis, carcinogenesis and aging.(Valko, Izakovic et al. 2004). The hydroxyl radical is determined as the most reactive and dangerous ROS. This is due to the fact, that the molecule reacts with all components of the DNA, modifying the purine and pyrimidine bases and the deoxyribose backbone leading to the breaking of the phosphodiester strands that link nucleotides (Wiseman and Halliwell 1996; Cooke, Evans et al. 2003). It is associated with DNA- induced damage of single or double DNA strand breaks, and the formation of abnormal cross-links between DNA and DNA strands and proteins. The above mentioned DNA damage can trigger inhibition or induction of transcription, stimulation of transduction-signaling pathways, replication errors or genome instability (Valko, Rhodes et al. 2006; Lenaz 2012). Overall, these chemical modifications are strictly associated with the initiation of neurodegenerative diseases such as Parkinson's and Alzheimer's, and principally with carcinogenesis.(Marnett 2000; Cooke, Evans et al. 2003). All things considered, the hydroxyl radical seems to be the main source of DNA damage in the cell. The most common base modification among over 20 base alterations is 8-hydroxy-2-deoxyguanine (8-OH-2'dG). The formation of 8-OH-2'dG is used as the biomarker of oxidative DNA damage. It is easily formed and gives an insight into mutagenic and carcinogenic properties. What is more, it has been detected in many types of cancer, therefore it is used as the biomarker of oxidative DNA damage and a potential biomarker of cancer (Shigenaga and Ames 1991).

There are distinguished nuclear and mitochondrial DNA. Mitochondrial DNA (mtDNA) seems to be more susceptible than nuclear DNA to oxidative damage(Yakes and Van Houten 1997). It is affected by the close proximity of the respiratory chain and a deficient amount of protective histones showing that 8-OH-2'dG is 10-20 fold higher in mtDNA than in nuclear DNA (Valko, Izakovic et al. 2004; Lenaz 2012). What's more, the production of superoxide anion (O_2) easily converts the molecule to a hydroxyl radical. Due to this fact, mtDNA undergoes the reaction with hydroxyl radical

promoting deletions and substitutions. In addition, mtDNA damage generates changes in the respiratory chain, elevates the ROS formation and leads to genetic disorders (Yakes and Van Houten 1997).

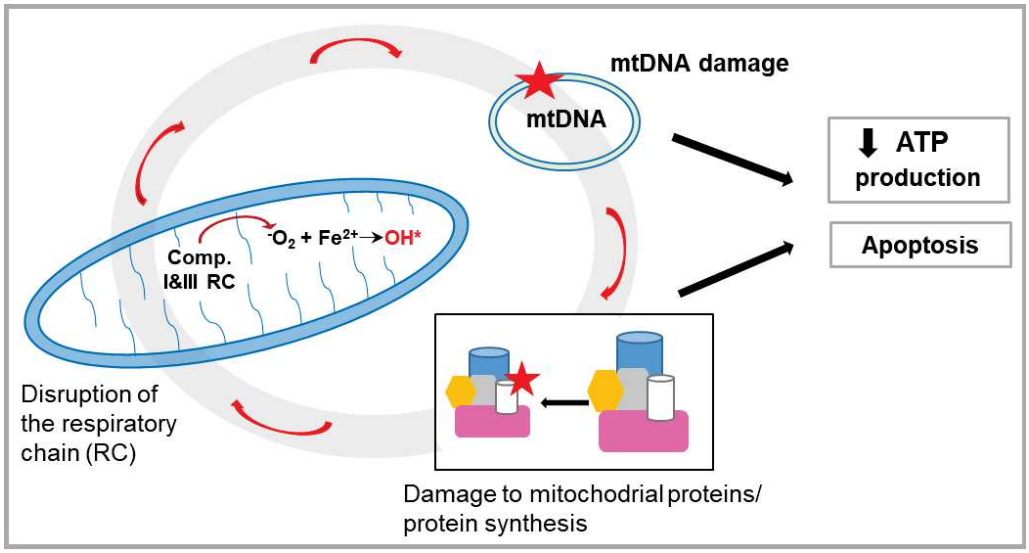

Fig. 2 The detrimental effect of ROS generation on mitochondria and mtDNA damage. Based on "The Mitochondrial Hypothesis of Ageing". Bender et al. 2009.

Altogether, enhanced ROS generation stimulates negative responses such as cell death or induction of cancer cells. To this fact, ROS are also generated in the cancer cells. A higher amount of ROS formation is necessary in tumor cells than in normal cells to provide their biological function, however rapid and uncontrolled ROS generation may potentiate cancer cell death in either normal or tumor cells (Lenaz 1998; Das and White 2002; Nicco, Laurent et al. 2005).

3.3. Antioxidant defense

3.3.1. Enzymatic antioxidants

This group consists of enzymes which remove the ROS from the human body. Superoxide dismutase catalyses the dismutation reaction of superoxide to hydrogen peroxide. This enzyme occurs in three isoforms in humans: cytosolic (Cu, Zn-SOD; SOD1), mitochondrial (Mn-SOD; SOD2) and extracellular (Cu, Zn-SOD; SOD3). The enzymes are obliged to collaborate with concomitant enzymes, in order to prevent the accumulation of hydrogen peroxide, which in the presence of reduced metal ion

promotes the Fenton, Haber-Weiss reaction and generates hydroxyl radical (Wardman and Candeias 1996). In addition, catalase (CAT) is an enzyme that provides the reaction where hydrogen peroxide is decomposed to water and oxygen. Furthermore, glutathione peroxidase (GPx) reduces hydrogen peroxide to water in the presence of glutathione (GSH), which becomes and oxidized form. The GSH must then, be reduced by glutathione reductase using NADPH as the reductant. It is important, as oxidized GSH may react with proteins and imply toxic effect on them. There are two main form of this enzyme including selenium-dependent one and independent one (Mates and Sanchez-Jimenez 1999). In addition, four different Se-GPx exist, which are placed in different cellular locations i.e extracellular, plasma or phospholipids.

3.3.2. Non-enzymatic Antioxidants

Small molecules having antioxidant activities are named "scavengers" and play an important role in scavenging or neutralizing the free radicals from the human body. Hence, they mediate in potentiating the antioxidant effect of the above mentioned enzymes, as their main function is to remove ROS and RNS from the cells, which are the precursors for the free radicals generation. It is worth mentioning that some of these representatives are either produced naturally in the body or occur in the dietary products or are synthesized (Lenaz 2012). Moreover, their solubility differentiates the environment they can work into. The principal water-soluble antioxidants are: vitamin C and glutathione, whereas the most potent lipid- soluble macromolecule is Vitamin E (tocopherol) (Valko, Izakovic et al. 2004), subsequently, Vitamin A (Sies 1997), and Coenzyme Q ($CoQH_2$) (Orlando, Silvestri et al. 2018). In addition, these two groups of antioxidants collaborate with each other, conducting the redox reactions such as NADPH-GSH-ascorbate-tocopherol, where NADPH enables the reduction of membranous α-tocopherol reduction. Thus, the effect of these antioxidant micro molecules is synergistic (Fang, Yang et al. 2002; Valko, Rhodes et al. 2006; Lenaz 2012). Interestingly, a numerous studies have presented an abundant group of dietary antioxidants included in fruit and vegetables such as: polyphenols: resveratrol (Ferraz da Costa, Fialho et al. 2017), flavonoids: quercetin, genistein (Aufderklamm, Miller et al. 2014; Ward, Mir et al. 2018), isothicyanates: sulforaphane (Pawlik, Wiczk et al. 2013) as well as diallyl trisulphate (DATS) derived from the garlic (Borkowska,

Sielicka-Dudzin et al. 2012; Borkowska, Knap et al. 2013). Above all, there are also complex molecules such as: ceruloplasmin, ferritin, transferrin or lactoferrin, which bind an excess of labile iron pool and therefore prevent from Fenton reaction and hydroxyl radical formation. (Wardman and Candeias 1996). It's worth to mention, another antioxidant agent in quenching free radicals and showing antioxidant activity is ebselen, which is a chemically obtained compound (Sies 1993).

3.3.3. Repair line

Despite the enzymatic and non-enzymatic antioxidants, there is also third line referred as "repair line " involved in repairing DNA damage –induced by oxidative stress. The cells contain repair systems, which are capable of for example removing damaged bases via base excision repair (BER) and other enzymes, during DNA replication (de Souza-Pinto, Wilson et al. 2008). Indeed, this process is essential as it protects from DNA mutations during replications. In consequence, the enzymes; DNA glycosylases and AP endonucleases repair and further eliminate the damaged region in DNA. Subsequently, exonucleases and ligases replace the damaged base with new nucleotide and join the DNA fragments. Hence, this process leads to cleavage of damaged DNA nucleotides and substituting them with new ones and therefore "guarding" from dangerous free radicals' deleterious effects.(de Souza-Pinto, Wilson et al. 2008). However, in proteins minor errors are removed by augmented proteolysis as compared to DNA repair.

3.4. Oxidative stress and signaling pathways

As the above mentioned, ROS and RNS are essential in mediating in multiple fundamental, biological and physiological processes in the cell, in physiological concentrations. In particular H_2O_2 acts as chemical messenger activating protein kinases and various intracellular signaling pathways.(Thannickal and Fanburg 2000). However, enhanced ROS and RNS formation directly influences the macromolecules such as lipids, proteins or nucleic acids, which are encountered in the generation of cellular signals correlated with promotion and progression of cancer. ROS and RNS in the

presence of metal ions inhibit phosphatases: phosphoserine/threonine, phosphotyrosine and phospholipid, and oxidize their sulfhydryl groups (Schieber and Chandel 2014). The chemical modification is accompanied by the alternation of the protein conformation and activation of the specific signaling cascades. Among them, the major ones are the signaling pathways – dependent: growth factors, mitogen-activated protein kinases (MAPK) and Pl3k/Akt kinases. For that reason, these pathways –induced transcriptional factor for example ; NF-κB, p-53 or HIF-1 (Thannickal and Fanburg 2000; Valko, Rhodes et al. 2006).

NF-κB is a transcriptional, protein complex factor, which regulates some genes linked with the cell proliferation and angiogenesis (Xie, Xia et al. 2010). In addition, the protein is established to correlate with the process of carcinogenesis since it activates cell differentiation, cell growth or inflammation. Interestingly, the enhanced level of NF-κB was detected in blood, breast, colon and pancreas tumors (Biswas, Shi et al. 2004; Xia, Shen et al. 2014).

On the contrary, p-53 is the transcriptional factor involved in protecting the cells against cancer development. The protein is defined as the: "guardian of the genome,, (Dixit, Sharma et al. 2012; Wade, Li et al. 2013) as it possess a well determined tumor - suppressed function. In addition, it plays an important role in the induction of apoptosis and inhibition of the cell cycle in damaged cells. Normally, p-53 occurs in a wild type and has a short life-span. However, in cancer cells, most of this protein is inactive due to its gene mutation. (Muller and Vousden 2013; Soga 2013; Wade, Li et al. 2013). p-53 may induce cell apoptosis or cell cycle arrest through direct or indirect pathway(Wang, Simpson et al. 2015). The correlation between ROS and apoptosis -induced p53 , seems to have beneficial effect on eliminating damaged cells, although uncontrolled apoptosis may promote damage in normal cells (Valko, Rhodes et al. 2006).

3.5. Akt

Akt kinase protein kinase B (PKB) is a protein serine/threonine protein kinase, which plays a vital role in regulating the cell cycle and cell proliferation progression through the PI3K/Akt signaling pathway. It conducts extracellular signals from the cell membrane to the nucleus (Song, Ouyang et al. 2005; Manning and Cantley 2007). Akt kinase has been detected as a cellular homologue of the viral oncogene v-Akt. Later, it

was identified as that this protein is a principal stimuli of phosphatidylinositol 3-kinase–PI3K, which contributes to the cell survival thorough growth factor responses. Nowadays, there is a well-established evidence that Akt kinase consists of three isoforms Akt1 (PKBα), Akt2 (PKBβ), Akt3 (PKBɣ), where all of the isoforms exhibit similar chemical structure. They are composed of three domains : the plecstrin homology domain placed at the N-terminal, the central kinase domain, where the region of the threonine residue (eg T308 in Akt1) is responsible for the kinase activation and the hydrophobic regulatory domain, which similarly to kinase domain includes the serine (Ser473 in Akt1) essential for the activation.(Song, Ouyang et al. 2005; Manning and Cantley 2007). Akt is present in the most of the cellular tissues for example: muscles, prostate, breast, fat tissue, etc. Akt is a key protein activated on the Pl3K signaling pathway. In particular, insulin, cytokines or growth factors binding to the threonine kinase like receptors stimulate the phosphorylation of Pl3K and transport to cellular membrane. Pl3K triggers phosphatidylinositol-4,5-bisphosphate- PIP2 to phosphatidylinositol-3,4,5-triphosphate- PIP3, which further transfers Akt kinase and phosphoinositide-dependent kinase 1 (PDK1) into the membrane. What's more, Akt must be phosphorylated in order to occur in the active form. PDK1 plays an important role in phosphorylating the threonine located in the domain of the kinase protein. In addition, PDK2 is responsible for the phosphorylation od the serine472 on the regulatory domain. It can be also activated by kinase related protein (PLK), mTORC2, DNA-PK (Hers, Vincent et al. 2011).

An active form of Akt dissociates from the cell membrane and is transported to the cytoplasm or cell nucleus, where it modulates signaling pathways associated with growth, survival, metabolism, proliferation or migration of cells. Reversely, inactivation of Akt kinase is mediated through the dephosphorylation by Protein Phosphatase 2 - PP2 (Brunet, Datta et al. 2001).

3.5.1. Akt and its anti-apoptotic mechanism in cancers

It has been established that in may cancers such as ovarian, breast and prostate, there is an elevated expression and the synthesis of PKB. Enhanced Akt activity and its expression is commonly associated with the mutation in the gene encoding Akt isoforms, mutations in Pl3K gene or most importantly mutation or deletions in the gene

encoding phosphatase, and enzyme functioning as the tumor suppressor phosphatidylinositol phosphatase-3,4,5-triphosphate (PTEN). Akt themself does not generate the oncogenesis. However, in the increased level it contributes to the development of cancer by inhibiting apoptosis, promoting cancer cell proliferation and the changes in metabolism, regulating migration and invasion of cancer cells, and participating in the process of angiogenesis (Song, Ouyang et al. 2005; Manning and Cantley 2007). As above mentioned, Akt is involved in the induction of apoptosis, either directly or indirectly. In addition, Akt directly suppresses the activity of pro-apoptotic proteins and promotes the cell survival of cancer cells. For that reason, the negative regulation of pro-apoptotic proteins such as Bcl-2 (Brunet, Datta et al. 2001). Indirectly, Akt modulates the transcriptional factors involved in the process of apoptosis by ameliorating the genes associated with the cell survival or by aggravating the specific factors, which stimulate the genes related with induction of apoptosis (Song, Ouyang et al. 2005; Manning and Cantley 2007). According to this, Akt prompts the transcriptional factor NFκB, which induces the genes encoding, in this case the cell survival of cancer cells. On the other hand, Akt regulates the activity of transcriptional factor - forkhead box O transcription factor (FOXO), that promotes the genes- induced apoptosis (Brunet, Bonni et al. 1999). In consequence, Akt phosphorylates the nuclear FOXO1, FOXO3 and FOXO4 proteins, which bind to protein 14-3-3 forming complex. These complexes are transported from the nucleus to the cytoplasm, inhibiting genes promoting apoptosis (Hers, Vincent et al. 2011).

It is important to note that, the Akt signaling pathway plays a crucial role in the development of cancer. Since, Akt is believed to be the “guardian of the tumor cell”, the inhibiton of its activity leads to the induction of the cell proliferation, generation of oxidative stress and induction of apoptosis, and in the consequence to the decreased cell survival of cancer cells. (Mundi, Sachdev et al. 2016). Therefore, Akt is considered as an attractive approach in finding the therapeutics that would be able to inhibit the Akt activity and the signaling pathway.

3.6. The cell cycle

The essential process in developing the eukaryotic cell is conjugated with the cell cycle. Cells' proliferation is based on the cell division, which is a part of the cell cycle. Each cell must undergo the cell cycle, in order to raise, copy the genetic material and split into two daughter cells. The cell cycle consists of two major phases such as: the interphase and the mitotic (M) phase. The interphase is assembled of G1, S and G2 phase. In particular, in G1 phase the growth of the cells is maintained, for that reason to efficiently complete the synthesis of copied DNA in the nucleus in S phase. Afterwards, the G2 phase prepares the cells by the separation and reorganization to enter the M phase. Finally, nuclear and cytoplasmic division of the two new cells is conducted in the M phase. Moreover, the cell cycle is strictly regulated and modulated by specific proteins like cyclins and cyclin –dependent kinases such as (Cdk) or inhibitors. Another approach in modulating the cell cycle is the reversible phosphorylation of several proteins (Rhind and Russell 2012). It has been demonstrated that various dietary compounds have an anti-proliferative effect as they influence the cell cycle through inhibition of G1/S and or G2/M phase (Pawlik, Wiczk et al. 2013). In addition, isothiocynates and flavonoids have been shown to inhibit G2/M cell cycle arrest and modulate the anti-apoptotic pathways (Anwar, Uddin et al. 2018; Ward, Mir et al. 2018). Moreover, selenium was shown to regulate the cell cycle and cell growth in prostate cancer cells (Menter, Sabichi et al. 2000; Zhong and Oberley 2001).

3.7. Mechanisms of cell death

3.7.1. Apoptosis

Apoptosis is defined as the programmed cell death, where redundant or pathologically damaged cell are eliminated. It plays a fundamental role in physiological processes and allows the cellular organisms grow properly. There are two main pathways, which activate the apoptosis: extrinsic (death receptors) and intrinsic (mitochondrial). The first one includes death receptors, that are tumor participants of the tumor necrosis factor (TNF-α) receptor gene family (Elmore 2007). The intrinsic

signaling pathway that prompts the apoptosis is associated with non-receptor-initiated intracellular signals, which are directly within the cell and mitochondrial-induced factors. What's more, these factors generate alternations in the inner mitochondrial membrane and lead to opening of the mitochondrial permeability transition pore (MPT) and to loss of mitochondrial transmembrane potential. As a consequence, cytochrome c and the caspases-dependent mitochondrial pathway are activated and cytochrome c leakage from mitochondria occurs (Hacker 2000; Elmore 2007). Another important factor involved in the regulation of apoptosis pathway is the antiapoptotic family of Bcl2 proteins. The decreased level of the ratio between antiapoptotic proteins (eg Bcl-2, Bcl-xL) to pro-apoptotic ones (eg Bax, Bak, Bid) is one of the indicators of apoptosis induction. It is important to note, that much evidence shows that higher ROS generation is correlated with process of apoptosis. Nevertheless, ROS and RNS may demonstrate a dual approach on apoptosis, whereas low concentration of ROS and RNS are crucial for the cell survival (Laurent, Nicco et al. 2005; Nicco, Laurent et al. 2005). Oxidative stress plays a key role in induction of apoptosis in the cancer cells. Moreover, a rapid growth in ROS and RNS concentration causes the loss of mitochondrial potential and leads to mitochondrial-dependent apoptosis. However, the process of stimulating apoptosis seems to initiate the beneficial strategy for cancer therapy.

3.7.2. Necrosis

Another type of cell death is necrosis. As opposed to apoptosis, necrosis is a rapid and irreversible cell death, usually caused by some harmful stimuli such as fungi, viruses and bacteria or by extreme environmental conditions including heat, radiation and hypoxia. What's more, cells which undergo necrosis, increase their volume, lose their integrity of the cell membrane, and permeability of lysosomes and endoplasmic reticulum. As a consequence, dead tissues are dissolved and then transformed into a liquid mass to the environment. In addition, activation of receptor interacting proteins (RIP1 and RIP3) and forming necrosome are one of the main factors involved in the necrosis induction. Moreover, necrosome by interacing with glutamate dehydrogenase and glycogen phosphorylase potentiates their activity and the number of substrates for the respiratory chain, which leads to elevated ROS formation- induced mitochondria. ROS increase the permeability of mitochondrial membrane and translocate the

apoptosis inducing factor (AIF) to the cell nucleus, where DNA is degraded. Subsequently, DNA damage leads to PARP activation, which results in more rapid ATP and NAD+ uptake "energy drop", and therefore necrosis-induced. Recently, it has been shown, that primary necrosis may be regulated and, thus have some positive effect in cancer therapy.

3.7.3. Ferroptosis

The term ferroptosis refers to the form of nonapoptotic cell death, which can be characterized by the iron- dependent accumulation of lipid reactive oxygen species or depletion of plasma membrane polyunsaturated fatty acids (Cao and Dixon 2016). Moreover, it is accompanied by the inactivation of glutathione peroxidase 4 (GPx4) and/or GSH group depletion. In particular, some of the compounds-inducing ferroptosis, including erastin or sulfasalazine inhibit glutathione biosynthesis, which leads to depravation of its enzymatic activity. However, small molecules defined as iron chelators such as ferrostatin-1, liproxstatin-1 or desferoxamine (DFO), are essential to prevent from ferroptosis, since they possess the ability to attenuate the pathological cell death events in brain, kidney and other tissues. Elevated iron accumulation in tissues-triggers iron-dependent oxidative stress (Cao and Dixon 2016). Iron can be stored in a „safe" form, bonded by the specific protein- ferritin. However, excess iron overload may liberate as intracellular free, 'redox active' iron pool, which stimulates iron-dependent cell damage and forms lipid radicals that initiate oxidative stress. The insight into mechanism of ferroptosis is crucial in cancer treatment.

It is worth to mention that there are also some other cell death types including autophagy, anoikis, mitotic catastrophe or ferritinophagy, however, in this study the three principal kinds of cell death were examined.

3.8. PARP

Poly (ADP-ribose) polymerase- 1 is a remarkable enzyme existing in all somatic cells. This enzyme identifies the DNA damage and mediates in the signaling of the chromosomal DNA damage to the cellular repair mechanisms. Moreover, PARP is activated, when DNA damage occurs. Polymerase-1 is involved in repair processes,

where it detects damaged DNA fragments, majorly DNA strand breaks, and transfers the information to effector proteins through poly (ADP-ribose) acceptor proteins. Despite this, PARP also directly interacts with other repair proteins. In particular, the amino acid sequence aspartic acid-glutamine-valine-aspartic acid (DEVD) localized in the B domain region of PARP, during apoptosis, is recognized by caspases 3 and 7, which subsequently cause PARP cleavage into 89 and 24 kDa molecular fragments (Boulares, Yakovlev et al. 1999; Morales, Li et al. 2014). PARP cleavage, activated by the caspase 3, appears during programmed cell death- apoptosis modulated by a variety of stimuli. The process of PARP polymerase degradation by caspases is considered as a marker of apoptosis According to this fact, agents – inducing programed cell death are being considered as novel and therapeutic factors in cancer treatment as the induction of this process would lead to explicit decrease in tumor mass.

It is worth mentioning that another type of cell death process refers to necrosis. Necrosis (accidental death) is characterized by the rapid cell death due to detrimental factors for example: toxins or infection. As the consequence, cell components undergo unregulated digestion. The induction of necrosis-requires receptor interacting protein (RIP1 and RIP3) activation, and formation of necrosome (Galluzzi, Kepp et al. 2009). Necrosome by interacting with enzymes such as: glycogen phosphorylase, glutamate dehydrogenase, increases their activity. Furthermore, elevated the number of substrates for the respiratory chain may enhance ROS generation in the mitochondria. Moreover, the overproduction of ROS may increase mitochondrial membrane permeability and transport of apoptosis inducing factor (AIF) to the nucleus. Consequently, DNA is degraded by EndoG nucelases accompanied by AIF. DNA damage causes activation of PARP, which leads to rapid uptake of NAD^+ and uncontrolled use of ATP. Hence this leads to energy deficiency and induction of necrosis (Nicotera, Leist et al. 1998; Kung, Konstantinidis et al. 2011).

3.9. Anticancer and chemopreventive activities of organoselenium compounds

Selenium is an essential element that plays a multiple and vital role in the human body. It regulates the proper function of thyroid hormone, potentiates the immune system and moderates the risk of cancer development. It was identified in 1817 by the

Swedish chemist Berzelius. It is very important to control the concertation of selenium in the blood, as its deficiency may lead to cardiovascular diseases, thyroid dysfunction or it is associated with carcinogenesis. On the contrary, an extensive level of selenium may result in cancer development. Daily dose should be 50 µg. In addition, selenium builds up the active side of many enzymes for example : gluthatione peroxidase or thioredoxin reductase and other proteins, which are responsible for the biological and physiological function (Hatfield, Tsuji et al. 2014). It augments the scavenging of ROS and protects from free radicals formation and oxidative stress. Due to this fact, compounds containing selenium have been studied for their therapeutic potential, namely anticancer (Roman, Jitaru et al. 2014; Wang, Sun et al. 2014). In particular, selenium compounds such as: selenocysteine, sodium selenite, diallyl selenite, triphenylselenium chloride, ebselen and many others have been examined.

3.9.1. Antioxidant and cytoprotective activites of ebselen

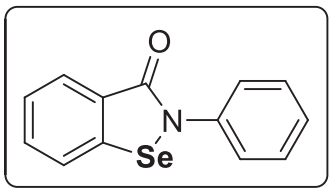

Fig. 3 Structural formula of ebselen

Ebselen [2-phenyl-1,2-benzisoselenazol-3(*2H*)-one] is an organoselenium compound, that is obtained in chemical synthesis. It was first discovered in 1980s as the drug candidate for curing brain ischema and stroke by the German scientists, who further explored its antioxidant mechanism of action. Hence, Sies and co-workers determined that ebselen catalyzes the reduction reaction of hydroperoxides namey H_20_2 (Sies 1995; Parnham and Sies 2013). Ebselen was shown to reveal a multiple spectrum of biological activities, including chemopreventive, anti-inflammatory, neuroprotective, and anticancer activity. Moreover, ebselen exhibits a potent antioxidant activity as it mimics GPx, and therefore possess the ability to regulate redox homeostasis and protect the cells against oxidative stress. (Sies 1993; Sies 1994; Steinbrenner, Speckmann et al. 2016). The organoselenium compound has been studied extensively and there are of abundant studies concerning its pleiotropic activity.

It has been demonstrated that ebselen protected numerous cell cultures and animals from the induction of the oxidative stress and damage due to scavenging peroxides and peroxynitrates (Briviba, Roussyn et al. 1996; Masumoto and Sies 1996; Sies and Masumoto 1997). However, some studies indicate that ebselen exhibits prooxidant activity, which leads to inhibition of cancer development. In addition, Zhang and co-authors showed that in multiple myeloma cancer cells, ebselen significantly enhanced the ROS formation, induced apoptosis-related with increased Bax level, and attenuated the cell proliferation (Zhang, Zhou et al. 2014). Organoselenium compound also induces apoptosis in the liver cancer cells (Yang, Shen et al. 2000), pancreatic cancer cells (Santofimia-Castano, Garcia-Sanchez et al. 2014) and leukemic cancer cells (Maraldi, Prata et al. 2009). Sharma et al. showed that ebselen sensitizes glioblastoma cancer cells to tumor necrsosis factor – induced apoptotic death though two distnitc pathways involving NFκB regulation and Fas-mediated formation of death inducing signaling complex (Sharma, Tewari et al. 2008). Despite of apoptosis, ebselen was indicated to cause rapid necrosis in hybridoma cells (Guerin and Gauthier 2003).

The search for new chemotherapeutics in cancer treatment has been underway for many decades and yet the progress in finding a novel and effective drugs against malignancies have been marginal. In particular, understanding of the regulatory mechanisms and identification of the proteins mediated in carcinogenesis, and chemotherapeutics-induced apoptosis are considered to be a foremost target on the way develop potent anticancer drugs. However, there is relatively enough data indicating that organoselenium compounds could fulfil this need of drugs with versatile target action. We have recently published the data, concerning newly synthesized N-substituted ebselen derivatives. (Pacula, Kaczor et al. 2017; Pacula, Kaczor et al. 2017). Therefore, newly synthesized ebselen derivatives with antitumor potential and their mechanism of action were investigated in this doctoral dissertation.

4. Aims

The main objective of this study was to investigate the antitumor activity of ebselen derivatives in two phenotypically different prostate cancer cell lines and to learn their potential mechanism as anticancer agents.

In particular, the aims of the dissertation were:

1. To determine whether *N*-allyl-BS and *N*-(3-m)-b-BS inhibited cell viability in prostate cancer cells and whether they would be less toxic towards normal prostate cells.
2. To investigate if the inhibition of cell growth was associated with cell cycle arrest and ROS generation.
3. To study if *N*-allyl-BS and *N*-(3-m)-b-BS induced cell death through apoptosis or ferroptosis.
4. To determine if down-regulation of the Akt signalling pathway was associated with the cytotoxic effect of *N*-allyl-BS and *N*-(3-m)-b-BS.
5. To determine if DNA damage was associated with the cytotoxic activity of *N*-allyl-BS and *N*-(3-m)-b-BS.
6. To investigate if hypoxic conditions potentiated the cytotoxic activity of *N*-allyl-BS compared to normoxic conditions.
7. To examine whether PTEN-negative PC-3 cells were more sensitive to *N*-allyl-BS and *N*-(3-m)-b-BS as compared to PTEN-positive DU 145.

5. Materials

5.1. Cell lines

In this doctoral dissertation two prostate cancer cells lines phenotypically different from each other were used in the experiments. DU145 cancer cell line purchased from the American Type Culture Collection (ATCC, Manassas, VA), derived from metastatic site –brain (grade II) from Caucasian man. The first time isolated by Stone (Stone, Mickey et al. 1978). Highly metastatic adenocarcinoma PC-3 cell (Kaighn, Narayan et al. 1979) line (grade IV) was also purchased from ATTC. Noncancerous, prostate epithelial PNT1A cell line was purchased from the European Collection of Authenticated Cell Cultures (ECACC, France, Paris). The first time described by Cussenot (Cussenot, Berthon et al. 1991) immortalised with SV40.

5.2. Tested chemical compounds

The newly synthesized ebselen derivatives were obtained from the collaboration with prof. Ścianowski from Department of Organic Chemistry, Nicolaus Copernicus University in Torun (Pacula, Kaczor et al. 2017; Pacula, Kaczor et al. 2017).

5.3. Reagents

5.3.1. Cell culture media and reagents

1. RPMI 1640 (Sigma Aldrich, USA)
2. MEME 6526 (Sigma Aldrich, USA)
3. Phosphate buffered saline (PBS), pH-7.4

   2.68 mM KCl, 137 mM NaCl, 1.76 mM KH_2PO_4, 10 mM Na_2HPO_4
4. 1 x Trypsin-EDTA (Sigma Aldrich, USA)

5.3.2. Supplements:

1. 10% Heat-inactivated fetal bovine serum (FBS) (Sigma Aldrich, USA)
2. Mixture of antibiotics penicillin/streptomycin (Sigma Aldrich, USA)
3. L-glutamine (Sigma Aldrich, USA)
4. Sodium pyruvate (Sigma Aldrich, USA)

5.4. Buffers and reagents:

5.4.1. SRB assay:

1. 20% Trichloroacetic acid (TCA) (Sigma Aldrich, USA)
2. 0.4% Sulforhodamine (SRB) (Sigma Aldrich, USA) in 1% acetic acid (POCH, (Avantor Performance Materials Poland S.A., Polska)
3. 10mM Trisma-base solution, pH 10.5 (Sigma Aldrich, USA)

5.4.2. Commercial assay kits:

1. Muse® Cell Cycle Assay Kit, (Merck Millipore, Germany)
2. Annexin-V & Dead Cell Assay Kit (Merck Millipore, Germany)
3. Guava Viacount (Merck Millipore, Germany)

5.4.3. Western blot analysis:

Lysis buffer:

1% Triton® X-100,

0.1% SDS,

50 mM TRIS,

150 mM NaCl; pH 7.5

Ripa buffer (Sigma Aldrich, USA)

Loading buffer (SDS-sample buffer):

250 mM TRIS; pH 6.8
8% SDS,
40% glicerol,
0.4% bromophenol blue,
400 mM DTT

Running buffer (gel):

1.5 M TRIS, 0.4% SDS; pH 8.8
Stacking buffer (gel):
0.5 M TRIS, 0.4% SDS; pH 6.8

1. 10% Running gel: 4 x TRIS/SDS, pH 8.8; 1.25 ml, 40% acrylamide 1.25 ml, 2% bis-acrylamide 0.67 ml, H_2O 1.825 ml, TEMED 2.5 µl, 10 % APS 37.5 µl
2. Stacking gel: 4 x TRIS/SDS, pH 6.8; 0.562 ml, 40% acrylamide 326.25 µl, 2% bis-acrylamide 0.150 µl, H_2O 1.44 ml, TEMED 2.5 µl, 10 % APS 25 µl

Running buffer:

25 mM TRIS; pH 8.3
192 mM Glicyne,
0.01% (x/v) SDS
Transfer buffer:

25 mM TRIS,
200 mM glycine,
20% methanol
Blocking buffer:

5% non-fat milk
1x TBST
TBST buffer:
5 mM TRIS, pH 7.4
15 mM NaCl,
0.01% Tween 20

5.4.4. Primary antibodies:

Rabbit; Anti-Akt (Santa Cruz Biotechnology, USA) dilution: 1:1000

Rabbit; anti-P-Akt (Ser473) (Santa Cruz Biotechnology, USA) dilution: 1:1000

Rabbit; anti-PARP (Cell signalling, USA) dilution: 1:1000

Mouse; anti-β actin (Sigma Aldrich, USA) dilution: 1:25 000

5.4.5. Secondary antibodies:

Anti-rabbitIgG (Sigma Aldrich, USA) dilution: 1:12 000

Anti-mouseIgG (Sigma Aldrich, USA) dilution: 1: 20 000

5.4.6. Comet assay:

Freezing solution:

Albumin (7%),
DMSO (20%)
1:1 ratio

Thawing solution: Albumin (2.5%), Dextran (50%), in PBS

FOR THE GEL: LMA (Low Melting Agarose; 0.7%)

Lysis solution:

NaCl (2.5 M), pH 10.0

Na_2EDTA (100 mM),

Tris-HCl (10 mM),

Triton X-100 (1%)

DMSO (10%)

Electrophoretic Buffer:

Na_2EDTA (1mM), pH 13

Neutralization Buffer:

TRIS-HCl (300mM), pH 7.5

Other reagents:

Methanol (70%) (Sigma Aldrich)

Ethidium bromide (Sigma Aldrich)

5.5. Other reagents:

Amonium persulfate

Phosphatase and protease inhibitor cocktail (Roche, Germany)

2',7'-dichloro-fluorescein diacetate (2',7'-DCFHDA)

Chemiluminescene reagents

Dimethyl sulfoxide (DMSO)

5.6. Evaluation of maximum tolerated dose (MTD)

Dimethyl sulfoxide (DMSO)

PEG 400 (Sigma-Aldrich)

Water (Water for injection, Polpharma)

6. Methods

6.1. Cell culture

The cell lines PC-3 and PNT1A were cultured in RPMI 1640 medium (Sigma) supplemented with 10% fetal bovine serum (FBS, Sigma) and a mixture of the antibiotics penicillin and streptomycin (Sigma). The DU145 cell line was cultured in MEME medium (Sigma) containing 10% fetal bovine serum (FBS, Sigma), a mixture of the antibiotics penicillin and streptomycin (Sigma), sodium pyruvate (Sigma) and L-glutamine (Sigma). All cell lines were cultured at 37°C, in a humidified atmosphere saturated in 5% CO_2 in the incubator.

6.2. Cell treatment

Before each experiment the cells were washed with PBS and then trypsinized with a solution of 0.25% and 0.02% EDTA trypsin. Next, the cells were cultured for 24 h, and subsequently seeded for the experiments. Each experiment was performed after 24h. The cells were seeded into cell culture plates- depending on the experiments and time incubation, each time before 24h. After 24h, proper concertation was added to cells. Ebselen derivatives were dissolved in a freshly prepared 100% DMSO, where the

final concertation of DMSO added to cells was lower than 0.01 %. Stock solution of 100 mM *N*-allyl-BS and *N*-(3-m)-b-BS was prepared in 0.1% DMSO and stored at 4°C.

6.3. Cell viability assay using Sulforhodamine B (SRB)

In order to check the cytotoxic effect of ebselen derivatives, the SRB viability assay was applied in which the colorimetric sulphordamine B dye was used. PC-3, PNT1A and DU145 cells were seeded in 96-well plates at $6x10^3$ cells per well for 24h. The medium was removed and the cells were then treated with various concentrations (2.5, 5, 10, 20, 30, or 40 μM) of *N*-allyl-BS or *N*-(3-m)-b-BS for additional 24h. After incubation, 100 μl of 20% trichloroacetic acid (TCA) was added to the cells and fixed for 1h. Plates were then washed with distilled water, air-dried for 10 minutes at 37 ° C. The cells were then stained with 100 μl of 0.4% solution of SRB (Sigma-Aldrich) in 1% acetic acid, for 15 minutes. The cells were washed four times with 1% acetic acid and dried. SRB was then solubilized in 200 μl of 10 mM Trisma-base solution and sample absorbance was measured at 570 nm using a microplate reader (EPOCH, BioTek). The results were expressed as IC_{50} values (50% of effective concentration). Each experiment was performed at least three times.

6.4. Cell cycle assay

For the experiment, the cells (3×10^5 cells/well) were seeded in 6 well plates for 24h, and then exposed to recently prepared solution of 40 μM *N*-allyl-BS or *N*-(3-m)-b-BS for the next 8h. Subsequently, both floating and attached cells were trypsinized and collected by centrifugation at 500 x g for 5 minutes. The supernatant was removed and the pellet was then washed with 1 ml of PBS, and fixed with 70% ethanol overnight at –20°C. Next the cells were centrifuged at 500 x g for 5 miutes and washed with 1 ml of PBS again. The pelleted cells were stained with 200 μl of MuseTM Cell Cycle Reagent with propidium iodide (PI) and incubated for 30 minutes at room temperature in the dark. The cell cycle (G0/G1, S, and G2/M) phase distributions were determined using flow Muse Cytometr™. The obtained results showed the percentage of the cells in each phase. Each experiment was performed at least three times.

6.5. Assessment of cell death using Muse Anaylzer

The cells were seeded into 6 well plates (3×10^5 cells/well) for 24 h. Next, the cells were incubated with freshly prepared solution of 40 μM *N*-allyl-BS or *N*-(3-m)-b-BS for another 24h. The medium and trypsinized cells were collected, and centrifuged at 300 x g for 10 minutes. Subsequently, the pelleted cells were resuspended in 100 μl of medium containing 1% of BSA, and 100 μl Muse® Annexin V & Dead Cell Assay Kit was addaded for 20 minutes. After incubation, the early and late apoptic, and necrtoic cells were detected using flow Muse Cytomtr™. Each experiment was performed at least three times.

6.6. Cell viability assay

Prior to the experiment, cells cultured both, in normoxic and hypoxic conditions were seeded (3×10^5 cells/well) in 6 well plates for 24h. After 24h of culture in normal growth medium, the cells were treated with 40 μM *N*-allyl-BS or *N*-(3-m)-b-BS for another 24h. The medium and trypsinized cells were collected and centrifuged at 500 x g for 5 minutes. Next, the cell pellet was resuspended in 50 μl of fresh medium. In order, to determine the viability, 15 μl of the cell suspension was added to 135μl of a Guava ViaCount solution (Merck Millipore), in the final volume of 150 μl for each sample. The cells were analyzed by the Guava EasyCyte flow cytometer (Merck Millipore) using an excitation wavelength of 488 nm. The red and yellow fluorescence intensity was recorded on an average of 5 000 cells from each sample.

6.7. Detection of intracellular reactive oxygen species (ROS) by flow cytometry

For the experiment, 3×10^5 cells/well were seeded in a 6 well plate and allowed to attach overnight. After 24h, the cells were exposed to freshly prepared solution of 40 μM *N*-allyl-BS or *N*-(3-m)-b-BS for 2h. Next, 10 μl solution of 2',7'-dichloro-fluorescein diacetate (2',7'-DCFHDA) was added to each well for 30 minutes, in order to allow the reagent detecting the reactive oxidative cellular populations. Both, floating

and trypsinized cells were collected and centrifuged at 500 x g for 5 minutes. Subsequently, the supernatant was removed and the pellet was washed twice with 1ml of PBS. The cells were then resuspended in 100µl of PBS and the samples were placed on ice. Immidiately afterwards, cell fluorescene was measured using BD LSR II flow cytometer. Fluorescence of unstained cells was also measured and subtracted as the background. Each experiment was performed at least three times.

6.8. Protein lysate preparation

In order to determine the changes in the protein level, Western blotting was performed. The cells were incubated with 40 uM *N*-allyl-BS or *N*-(3-m)-b-BS at different time points for appropriate time conditions, and then lysed. The medium and the cells were collected using scrapers, and centrifuged at 2250 rpm at 4°C for 5 minutes The supernatant was then removed and the pelleted cells were washed twice in 1ml of PBS. Subsequently, the cells were centrifuged at 1500 rpm at 4°C for 5 minutes and PBS was removed. 60 µl of protease and phosphatase inhibitor cocktails dissolved in Ripa lysis buffer (Sigma) were added to the pellets and the resuspennded cells were lysed for 30 minutes at -80°C. Afterwards, the suspension was placed in new Eppendorf tubes and centrifuged at
16 000 x g at 4°C for 20 minutes. The supernatant was gently moved to another new Eppendorf tube and the protein concentration was measured in the given samples.

6.8.1. Protein concentration using Bradford protein assay

Total protein concentration was determined using the Bradford method (Bradford 1976). To 1ml of Bradford reagent (Sigma), 2 µl of cell lysate was added mixed and transferred to spectrophotometric cuvettes. The absorbance was measured at a wavelength $\lambda = 595$ using a spectrophotometer (DR 3900, Hach Lange). The protein concentration was analyzed by previously prepared standard curve using bovine albumin (BSA).

6.9. Western blotting - One gel electrophoresis

Protein samples were prepared in 1.5 ml volume Eppendorf, containing 60 µg of total protein lysates. All samples were normalized using lysis buffer and subsequently, diluted in the loading buffer. The samples were vortexed, placed on thermoblock and then incubated at 95ºC for 10 minutes, in order to denaturate proteins. Moreover, equal amounts of protein samples were loaded into the wells of previously prepared 10% SDS-polyacrylamide gels, along with molecular weight marker (Page Ruler Plus-Fermentas). The proteins were separated by vertical electrophoresis in the running buffer, using Mini PRTOTEAN III Electrophoresis System (Bio-Rad) 75 V for running gel and 130 V for stacking gel.

6.9.1 Transfer protein from gel to membrane

The resolved proteins were then transferred onto polyvinyli-dene difluoride (PVDF) membrane using Bio-Rad (Trans-Blot SD Semi-Dry Transfer Cell) system at a constant current of 260 mA and a voltage of 25 V for 1 hour, in the presence of transfer buffer. PVDF membrane was activated with methanol for 1 minute, and rinsed in transfer buffer before preparing the stack. The stack consisted of lawyers: Whatman paper, methanol-activated PVDF, gel and second Whatman paper respectively. The membranes were then blocked with a solution containing 10 mM Tris-buffered saline, 0.05% Tween 20, and 5% nonfat dry milk for 1h. The membranes were then incubated with primary antibodies over night at 4ºC. After incubation with primary antibodies the memmbranes were washed with TBST 4 x 5 minutes. The membranes were treated with secondary antibodies conjugated with horseradish peroxidase for 1h at room temperature. Following treatment with the appropriate secondary anti-body, the membranes were washed with TBST 4 x 5 minutes and the bands were visualized using ImageQuant LAS 500 (GE Healthcare). The changes in the protein level were quantified by densitometric method using the LASImage software. β-tubulin was used as a loading control.

6.10. Comet assay

The comet assay was carried out to measure DNA damage as previously desrbied (Orlando, Silvestri et al. 2018). Briefly, aliquots of treated and control cells containing 10 000 cells from each sample were transferred to Eppendorf tubes and centrifuged for 10 min at 800 g/4°C. The supernatant was removed and cells were resuspended in 0.7% low melting agarose from which 0.035 ml were taken and placed on pre-coated, high throughput, comet assay slides (Trevigen). Trevigen Comet hightrouput microscope slides are characterized by clean area separated by silicon barriers in order to allow simultaneous layering of ten different samples on each slide. Clean areas are manufactured with a dried agarose coating, in oroder to enhance adhesity. The microgels on the slides were then allowed to solidify at 4°C. Subsequently, the slides were immersed overnight at 4°C in the dark, in ice-cold, freshly prepared lysis solution (2.5 M NaCl, 100 mM Na_2EDTA, 10 mM Tris-HCl, 1% Triton X-100 and 10% DMSO, adjusted to pH 10). in order to lyse the embedded cells and to allow DNA unfolding. After incubation in lysis solution, the slides were exposed to alkaline buffer (1 mM Na_2EDTA, 300 mM NaOH buffer, pH for 30 minutes to allow DNA unwinding. Electrophoresis was then performed for 20 min at 1 V/cm in the same buffer. After neutralization in Tris buffer (pH 7.5) and dehydration in 75% methanol, the DNA on each slide was stained with 0.015 ml ethidium bromide (20 µg/ml) and viewed under fluorescent light using an Olympus BX51 fluorescence microscope connected to a PC.

6.10.1 Evaluation of DNA damage

For each sample, Fifteen randomly acquired images were recorded and processed using a custom made software (Tiano, Littarru et al. 2005) developed by the Department in collaboration with the Engineering Department of the Polytechnic University of the Marche based on Labview programming platform (National Instruments) that enables automatic identification of the comets, greatly reducing operator-dependent variability. A key feature of the software is its ability to identify the comets from the background and to estimate the commonly used DNA-damage indexes, including tail length, tail intensity, tail moment. Comet specific DNA-damage indexes

and images of 150 nucleoids for each slide were fed to a Microsoft Access database; in this manner data and images were easily traceable for subsequent evaluation and statistical analysis. Three slides were analysed for each treatment condition and a total of 450 comets were saved.

6.11. Statistical analysis

Data were analyzed using GraphPad Prism 6. One-way ANOVA followed by Dunnett's or Bonferroni's multiple comparison test was used to determine statistical significance of the differences in measured variables between the control and treated groups. Differences were considered significant at $*P < 0.05$, $*P<0.01$, $**P<0.001$.

7. Animal study

7.1. Determination of Maximum Tolerated Dose (MTD) after single administration

The study was performed on BALB/c mice (n = 10), aged 18 – 19 weeks at the beginning of the study and with average body weight (BW) 24.4 g. Mice were purchased from Tri-City Academic Laboratory Animal Centre – Research and Services Centre. All experiments were carried out according to protocol approved by the Local Ethical Committee for Animal Research (approval no.1/2016). During the study mice were fed with standard diet *ad libitum* and had free access to water, and were maintained on a 12h light/dark cycle, temperature 22°C, and humidity 50–55% in the home cages.

7.2. Evaluation of Maximum Tolerated Dose – study design

Animals used in experiment were randomly divided into two groups. In the first part of the experiment mice were treated orally with escalating doses of *N*-allyl-BS aliquot (n = 1 per single dose), until apparent signs of toxicity, but not lethality, were noticed. In this study, it corresponded to a range from 10 to 100 mg/kg doses. In the next stage, the highest established single dose was administered to another 4 mice, in

order to confirm the toxic effect. Also, control animals (n = 3) receiving vehicle only, were included in this study.

During the experiments, mice were weighted prior to compound administration, and then every day for another two weeks. In the first hour after *N*-allyl-BS administration, animals were constantly observed and the symptoms of toxicity were noticed every 15 minutes. Symptoms were categorized into following: appearance and hair condition, breath, environment, behavior and moving ability. In each category, animals were scored from 0 to 3, where 0 means normal and 3 strongly impaired. In case of severe toxic symptoms, human endpoint was also considered. After first hour of administration, animals were assessed daily in each of the above mentioned category. Study design was identical for preliminary and main part of the study.

7.2.1 Drug preparation

N-allyl-BS was administered by oral gavage in the volume 10 ml/kg of BW. Solution was prepared each time right before the administration. In order to prepare solution, certain amount of *N*-allyl-BS powder was dissolved in the mixture of DMSO: PEG 400: water (0,1:0,6:0,3, v/v/v) and vortex mixed.

8. Results

The results are divided into 4 sections:

1. The antitumor activity of *N*-substituted ebselen derivatives.
2. The influence of *N*-allyl-BS on DU 145, PC-3 cells and PNT1A.
3. The influence of *N*-(3-m)-b-BS on DU 145, PC-3 cells and PNT1A.
4. The MTD of *N*-allyl-BS *in vivo*.

8.1. 1. Antitumor activity of *N*-substituted ebselen derivatives

A series of newly synthesized *N*-alkyl and *N*-aryl ebselen derivatives and corresponding diselenides were examined for their anticancer activity expressed as IC_{50} valuess in prostate cancer cells DU 145 and non-cancer PNT1A. Some of them have been published in the articles below:

Pacula, A. J., **Kaczor K. B**., Wojtowicz A., Antosiewicz J., Janecka A., Dlugosz A., Janecki T., Scianowski J. New glutathione peroxidase mimetics-Insights into antioxidant and cytotoxic activity. Bioorg. Med. Chem. 2017; vol. 25, nr 1, s. 126-13125(1): 126-131.

Pacula, A. J., **K. B. Kaczor**, Antosiewicz J., Janecka A., Dlugosz A., Janecki T., Wojtczak A, Scianowski J. New Chiral Ebselen Analogues with Antioxidant and Cytotoxic Potential. Molecules 2017; vol. 22, nr 3, art. ID 492

Pacula, A. J. Obieziurska M., **Kaczor K. B**., Antosiewicz J., J Scianowski J. Water-dependent synthesis of biologically active diaryl diselenides. Arkivoc 2018; part iii, s. 153-164,

Two of the ebselen derivatives were further examined as potential anticancer agents.

Chemical structure	Chemical name	DU 145	PC-3
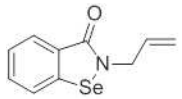	*N*-allyl-1,2-benzisoselenazol-3(2*H*)-one	10,30 ±0,1454	20,49 ±0,1569
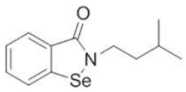	*N*-(3-methyl)-butyl-1,2-benzisoselenazol-3(2*H*)-one	30,39± 0,1291	30,29±0,1579

Table 1. IC_{50} (μM) values are means ±SD measured using SRB assay.

8.2. Cytotoxic activity of *N*-allyl-BS in DU 145, PC-3 and PNT1A cells

8.2.1. Influence of *N*-allyl-benzisoselenazol-3(*2H*)-one on cell viability in prostate cancer cell lines DU 145 and PC-3, and in the non-cancer cell line PNT1A

The first goal was to determine the cytotoxic effect of *N*-allyl –BS on the DU 145 (PTEN-positive) cell line with normal Akt kinase activity and PC-3 (PTEN-negative) cell line with high Akt kinase activity. The cells were treated with a series of dilutions (2.5-40 μM) of *N*-allyl-BS for 24h. The cell viability was measured using the SRB assay. As presented in Fig. 4, *N*-allyl-BS significantly inhibited cell proliferation in all concentrations tested in both cancer cell lines. In addition, the highest anti-proliferative activity was observed after incubation in the presence of 40 μM. Moreover, a higher cytotoxic effect was observed in PC-3 cells than in DU 145, where the viability was reduced by 80% in PC-3. In DU 145, the viability was reduced by 70% (Fig. 4A, B). Interestingly, the cytotoxicity of *N*-allyl-BS in the normal prostate cell line PNT1A was significantly lower than that observed with cancer cells, especially at lower concentrations (5–10 μM).

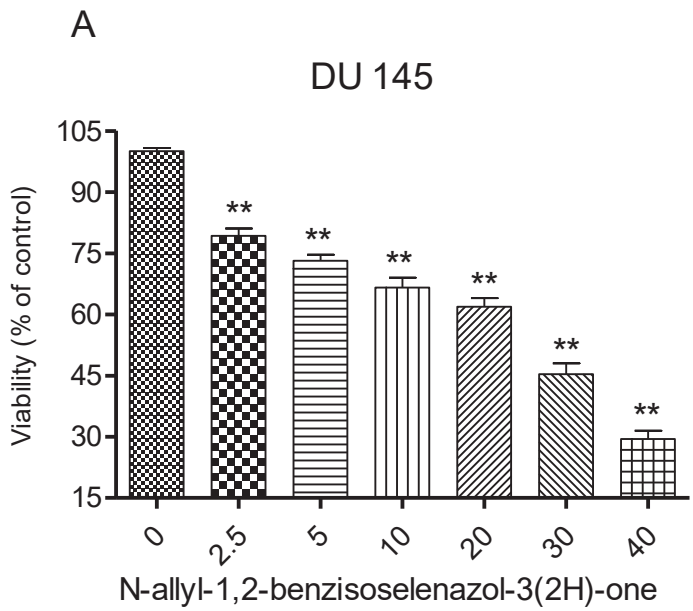

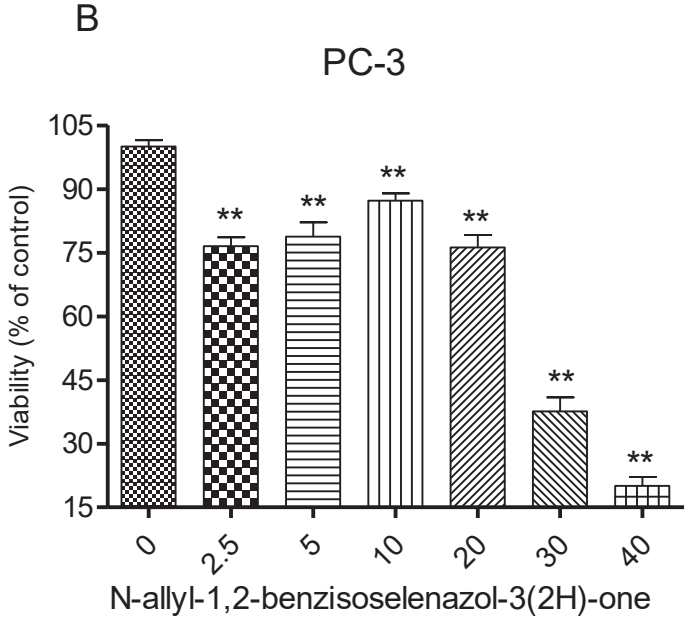

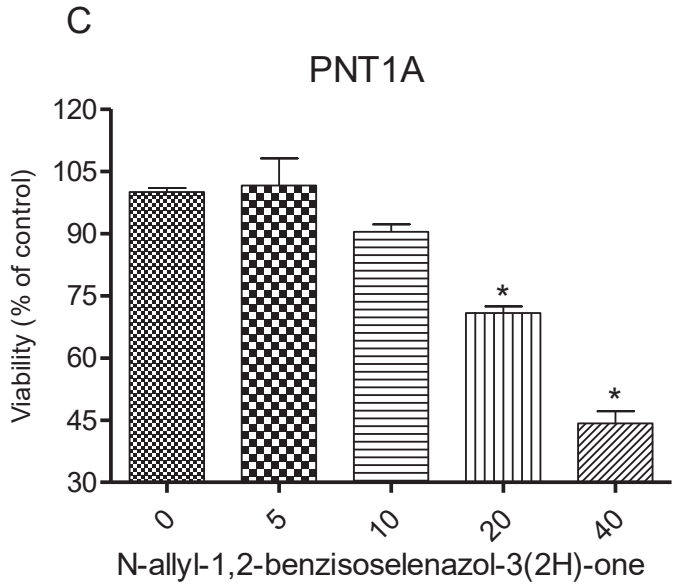

Fig. 4 *N*-allyl-BS decreased cell viability in prostate cancer cells

A. DU 145, **B.** PC-3, **C.** PNT1A were treated with the indicated concentrations of *N*-allyl-BS for 24h. Cell viability was measured using SRB assay. Results are presented as a mean ± SE of three independent experiments, where (n=6). A significant difference at (**P<0.001), (*P< 0.01) was calculated using one-way ANOVA followed by Dunnett's multiple comparison test.

8.2.2. Influence of *N*-allyl-BS on the cell cycle in prostate cancer cells

The inhibitory effect of *N*-allyl-BS on the cell cycle was measured using flow cytometry. DU 145 and PC-3 cancer cells were exposed to 40 μM *N*-allyl-BS for 8h. A significant increase in the percentage of the cells in the G2/M phase was observed. (Fig. 5). The percentage of the control cells in G2/M reached 30%, whereas after incubation with *N*-allyl-BS it increased to 50% in the case of DU145 (Fig. 5A). In PC-3, the percentage changed from 33% (in the control) to 57% (treated cells) (Fig. 5B). In addition, a stronger cytostatic effect of *N*-allyl-BS was observed in PC-3 than in DU 145 cells. Moreover, the phenomenon determined in both cancer cells lines (Fig. 5) showed that *N*-allyl-BS significantly induced G2/M cell cycle arrest.

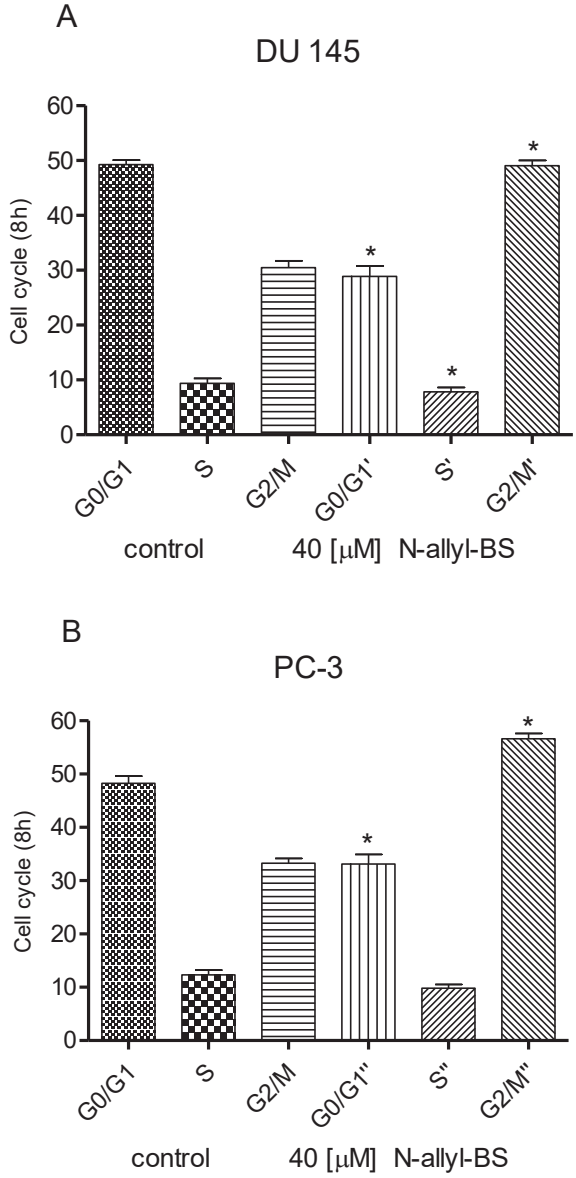

Fig. 5 *N*-allyl-BS induced G2/M cell cycle arrest in prostate cancer cells

A. DU 145, **B.** PC-3 cells were incubated with 40 μM *N*-allyl-BS for 8h. Cell cycle arrest was determined using flow cytometry. Data are presented as a mean ± SE from at least three independent experiments (n=3). There was a significant difference at (*P< 0.001) compared with control using one-way ANOVA followed by Bonferroni's multiple comparison test.

8.2.3. Influence of *N*-allyl-BS on apoptosis and necrosis in prostate cancer cells

The cells were treated for 24h with 40 μM *N*-allyl-BS and then analyzed. As presented (Fig. 6), *N*-allyl-BS induced apoptosis and necrosis in DU 145 and PC-3 cells (Fig. 7A, B). In particular, the percentage of apoptotic and necrotic cells in the control was under 10%, however the increase in apoptotic cells in DU 145 reached 25%, and necrotic 38%. Moreover, the pro-apoptotic and necrotic effect of *N*-allyl-BS was more prominent in PC-3 cells, where the percent of apoptotic and necrotic cells was each around 40%. These data clearly show that *N*-allyl-BS significantly increased the level of apoptotic and necrotic cells as compared to the control, both in DU 145 and PC-3 (Fig. 6A, B).

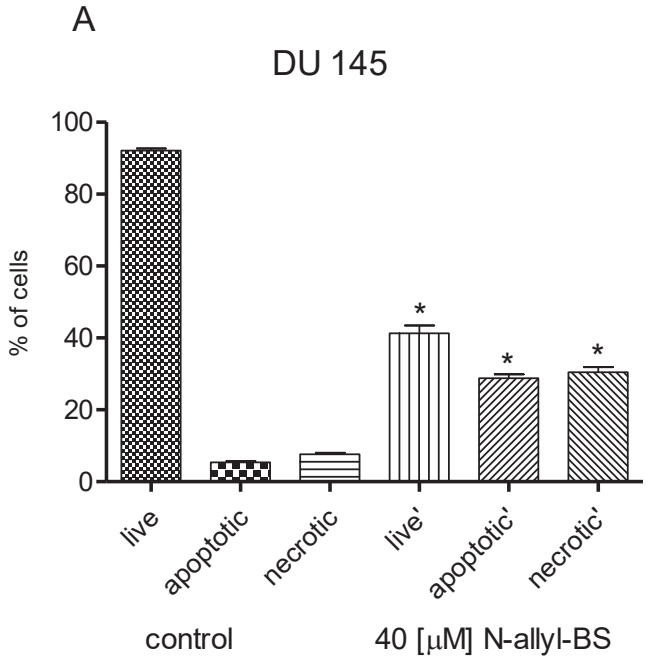

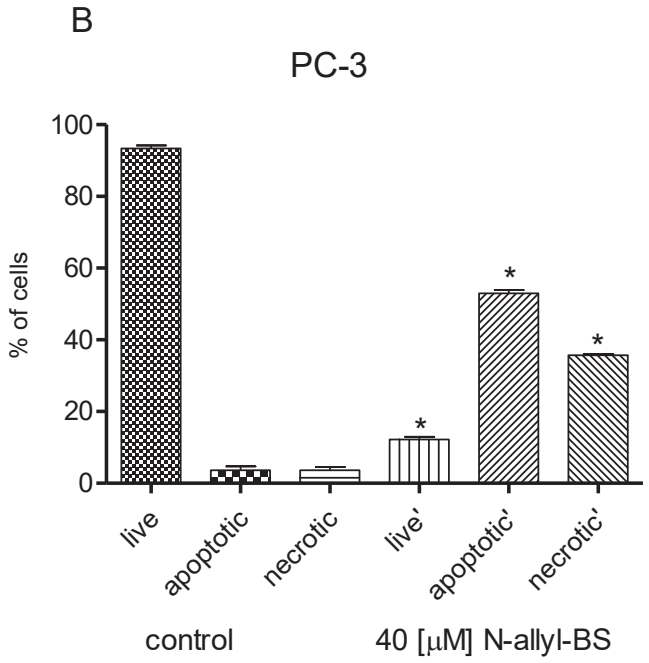

Fig. 6 *N*-allyl-BS significantly increased the number of apoptotic and necrotic cells in prostate cancer cells

Induction of apoptosis and necrosis of **A.** DU 145, **B.** PC-3 cells treated with 40 μM *N*-allyl-BS for 24h. The total number of apoptotic and necrotic cells was determined using flow cytometry. Results are presented as a mean ± SE of three independent experiments. A significant difference at (*P< 0.001) was determined by one-way ANOVA followed by Bonferroni's multiple comparison test.

In order to confirm the induction of apoptosis and necrosis by *N*-allyl-BS, the level of caspase- dependent cleaved PARP, which is the marker of apoptosis and the enzyme responsible for DNA repair, was measured. The changes in the level of PARP-cleavage were determined in the cells incubated with 40 μM *N*-allyl-BS at different time points (4-24 h). As shown in (Fig. 7A, B) the highest significant level of cleaved PARP in DU 145 was observed after the 8h treatment with 40μM *N*-allyl-BS, where it increased to a relative level of 2.25. Subsequently, PARP-cleavage level significantly declined after 24h (Fig. 7A). However, in PC cells the level of cleaved PARP significantly reached the highest point after 4h (2.75), and dropped after 8 and 24h (Fig. 7B). The obtained results confirm that *N*-allyl-BS induced apoptosis and necrosis in both cancer cell lines.

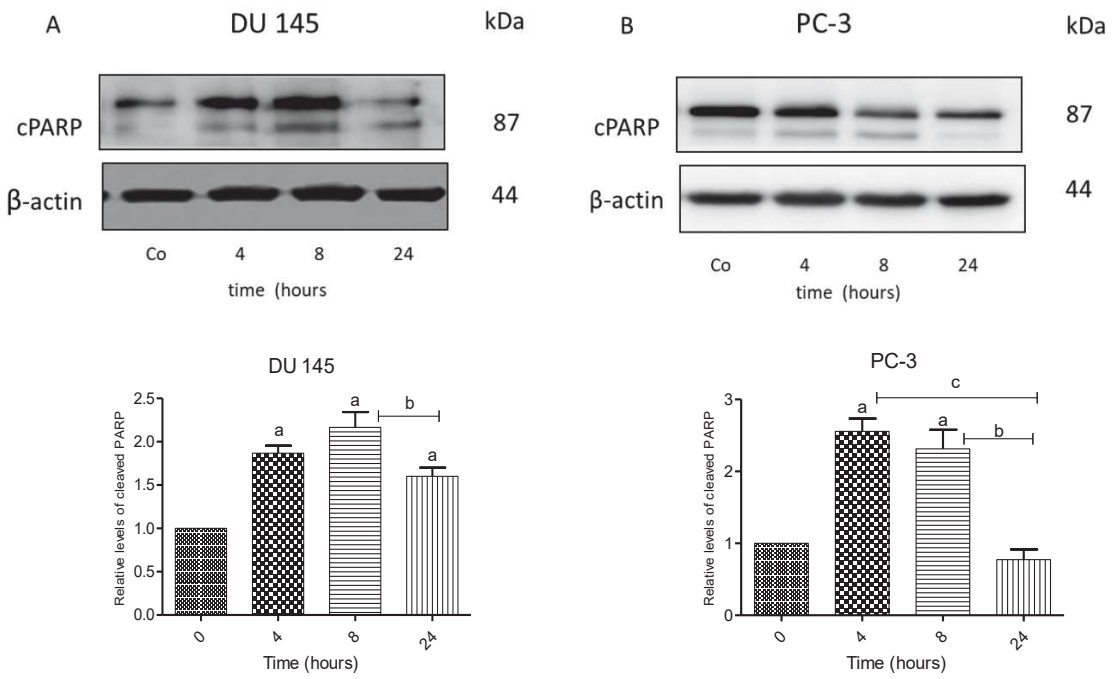

Fig. 7 Western blot analysis of cleaved PARP

A. DU 145, **B.** PC-3 cells treated with 40 μM *N*-allyl-BS at the indicated time points. β-actin was used as a lane loading control. Data are presented as a mean ±SE of three independent experiments. The statistical significance of differences between respective samples was determined by one-way ANOVA followed by Bonferroni's multiple comparison test, where (a) indicates significant difference between control and treated cells (*P < 0.05) and (b, c) indicates significant difference between 4, 8 and 24h of 40 μM *N*-allyl-BS-treated cells (*P < 0.05).

8.2.4. Effect of DFO and Ferr-1 on cell death induced by *N*-allyl-BS

To investigate if *N*-allyl-BS induced ferroptosis in both cancer cell lines, flow cytometry was used. The cells were treated for 24h with 40 μM *N*-allyl-BS only, and in the presence of iron chelators including desferoxamine (DFO) and ferrostatin-1, and then analyzed. As presented (Fig. 8), DFO and Ferr-1 (Fig. 9) had no effect on the cells treated with *N*-allyl-BS in DU 145 and PC-3 cells (Fig. 8A, B), (9A, B). Moreover, no significant difference was observed in neither DU 145 nor PC-3 cells. Therefore, *N*-allyl-BS did not influence the induction of ferroptosis in prostate cancer cell lines (Fig. 8, 9).

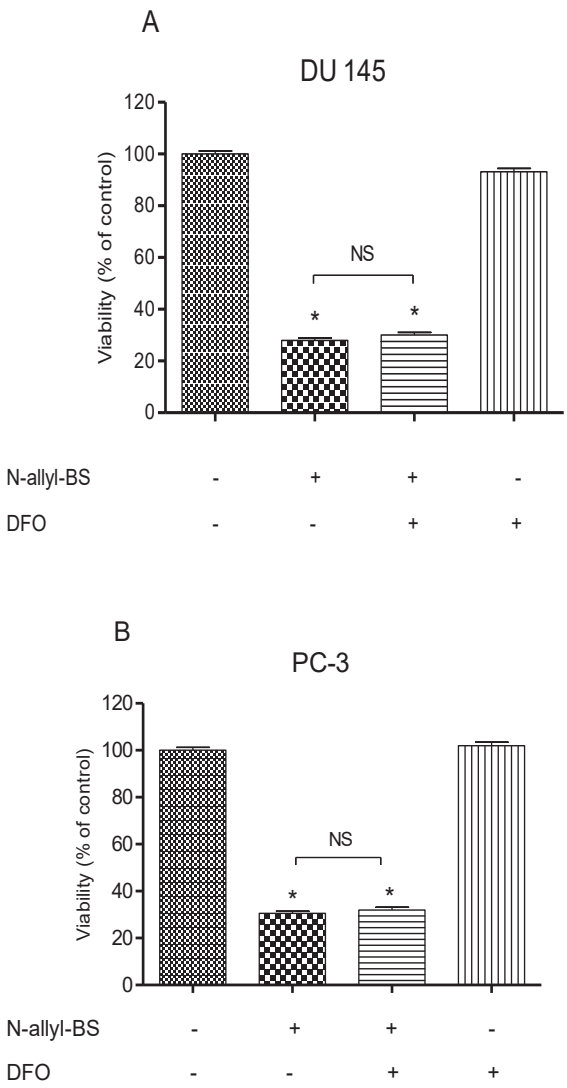

Fig. 8 DFO had no effect on *N*-allyl-BS-induced cell death

A. DU 145, **B.** PC-3 cells were treated with 40 μM *N*-allyl-BS and 25 μM DFO for 24 h. Cell viability was measured using SRB assay. Results are presented as a mean ± SE of three independent experiments. No significant difference was determined by one-way ANOVA followed by Bonferroni's multiple comparison test.

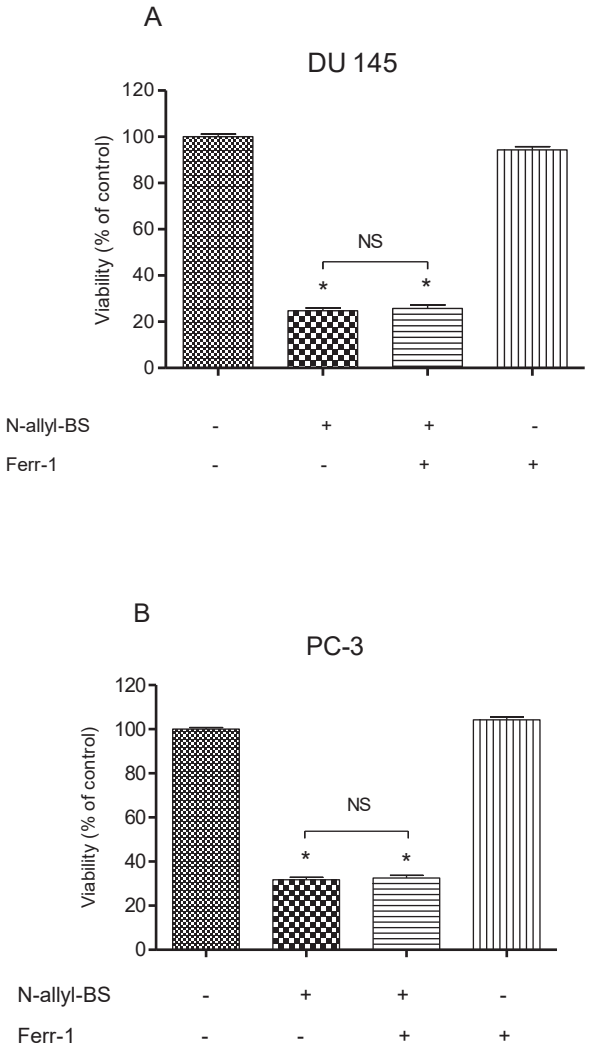

Fig. 9 Ferr-1 had no effect on *N*-allyl-BS-induced cell death

A. DU 145, **B.** PC-3 cells were treated with 40 μM *N*-allyl-BS and 2 μM Ferr-1 for 24 h. Cell viability was measured using SRB assay. Results are presented as a mean ± SE of three independent experiments. No significant difference was determined by one-way ANOVA followed by Bonferroni's multiple comparison test.

8.2.5. Influence of *N*-allyl-BS on ROS generation in prostate cancer cells

To examine whether oxidative stress is involved in the cytotoxic effect of *N*-allyl-BS, the intracellular level of ROS was determined. As presented (Fig. 10A, B), a significant increase in ROS generation was noticed after 2h treatment of 40 μM *N*-allyl-BS in both cancer cell lines. Moreover, the results show that *N*-allyl-BS elevated the

level of ROS by 15% in DU 145 and by 22% in PC-3 at the 2h time point as compared to control. (Fig. 10A, B).

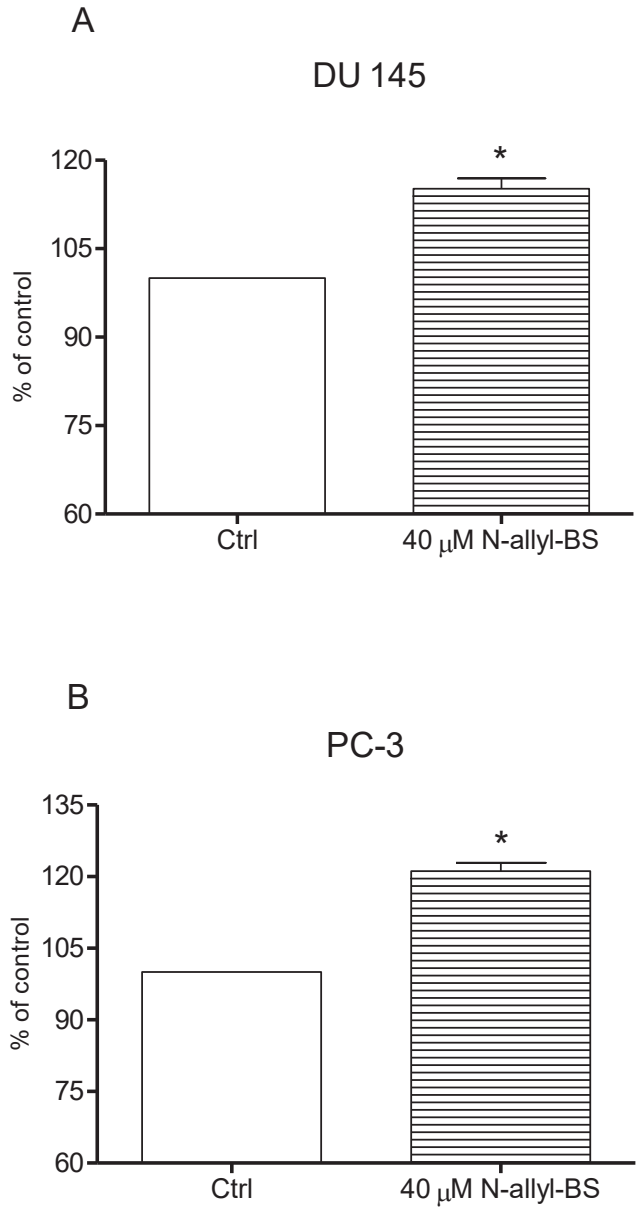

Fig. 10 *N*-allyl-BS increased the level of ROS generation in prostate cancer cell lines

A. DU 145, **B.** PC-3 cells were incubated with 40 μM *N*-allyl-BS for 2h. The level of ROS generation was analyzed using flow cytometry. Results are presented as a mean ± SE of three independent experiments (n=3), where there was a significant difference at (*P < 0.001) compared with control, as determined by ANOVA followed by Dunnett's multiple comparison test.

8.2.6. Influence of *N*-allyl-BS on DNA damage in prostate cancer cells

Oxidative stress and apoptotic cell death is strictly linked with DNA damage in cancer cells. In order to estimate whether *N*-allyl-BS induced DNA damage, the Comet Assay was performed. In addition, 40 µM *N*-allyl-BS significantly induced DNA damage after 8h and 24h incubation in PC-3 cells. This was highlighted by a significant increase of the upper third (+33%) and fourth quartile (+88%) of tail intensity, a parameter indicating the percentage of DNA fluorescence in the tail of comet images proportional to the amount of damaged DNA (Fig. 12C, D) On the contrary, no significant effect was observed in DU 145 (Fig. 11A, B).

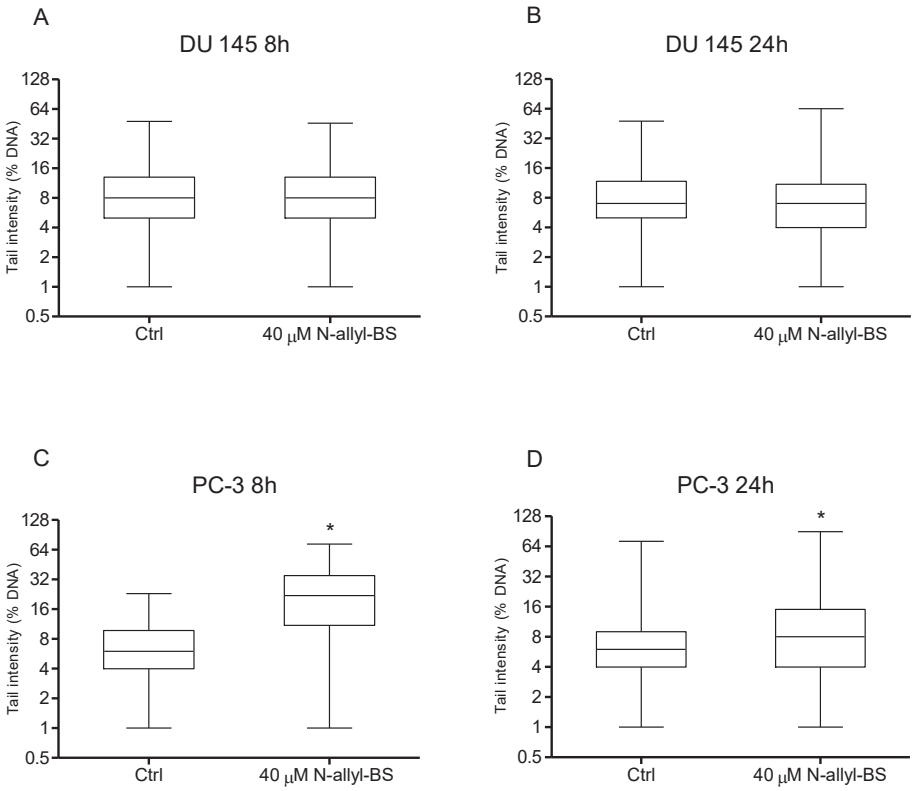

E

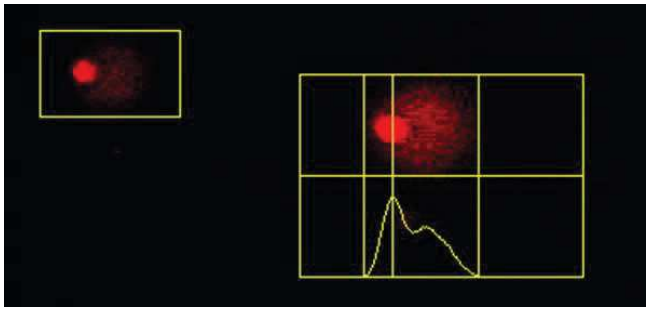

Fig. 11 The analysis of DNA damage

A. The influence of 40 μM *N*-allyl-BS on DNA damage in DU 145 (A, B) and PC-3 (C, D) cells after 8h and 24h treatment was determined using comet assay. Results are presented as the percentage of DNA in Tail Intensity ± SE (n=3). The significance of each difference compared with control was calculated by ANOVA followed by Dunnet's multiple comparison test (*P< 0.05) in PC-3 cells. A representative picture of PC-3 cells in the upper 90th percentile of tail intensity is shown in E.

8.2.7. Influence of *N*-allyl-BS on the level of the active form of Akt in prostate cancer cells

In order to determine whether *N*-allyl-BS decreased Akt phosphorylation in prostate cancer cells, Western blotting was employed. The cells were exposed to 40 μM *N*-allyl-BS for different time periods and the changes in the level of phosphorylated Akt were measured. Indeed, Akt phosphorylation declined slightly after treatment for 0.5h and a high drop was observed after 4h treatment in DU 145 (Fig.12A, B). Furthermore, *N*-allyl-BS slightly elevated the level of Akt phosphorylation after treatment for 0.5h in PC-3 cells (Fig. 12B), and after treatment for 1h, there was a decreased level of Akt phosphorylation. The changes in Akt phosphorylation were statistically significant in both cancer cell lines. (Fig. 12A, B).

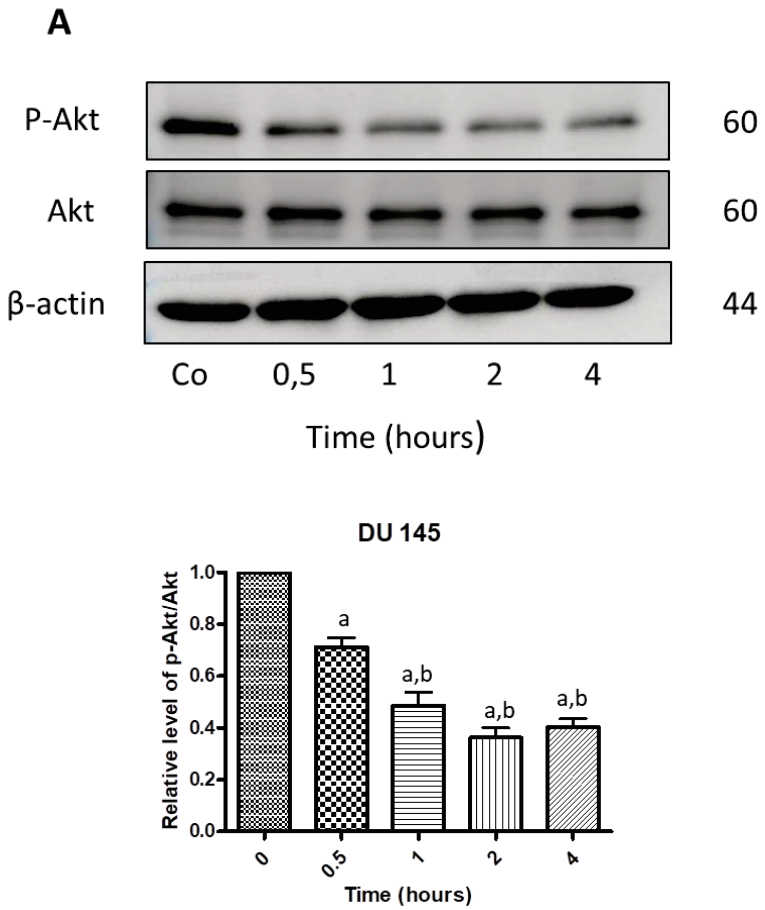

B

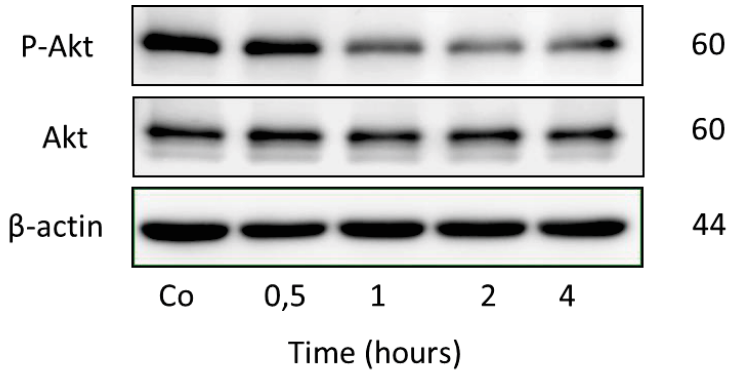

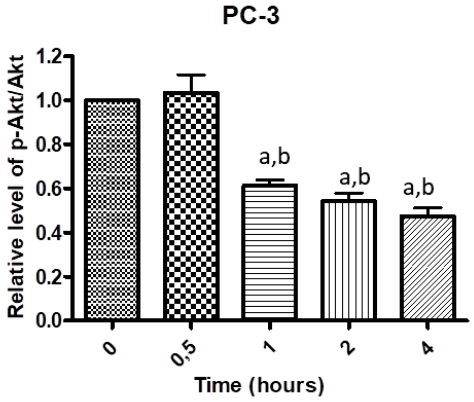

Fig. 12 Western blot analysis of p-Akt and Akt kinase in DU145 (A) and PC-3 (B) cells were treated with 40 μM *N*-allyl-BS for the indicated periods of time. β-actin was used as a lane loading control. Results are presented as a mean ± SE (n=3). The statistical difference between respective samples was determined by one-way ANOVA followed by Bonferroni's multiple comparison test, where (a) indicates a significant difference between control and treated cells (*P<0.01) and (b, c) indicates a significant difference between 4, 8 and 24h treatments of 40 μM *N*-allyl-BS (*P<0.01).

8.2.8. Cytotoxic activity of *N*-allyl-BS in PC-3 cells-effects of different oxygen tension

To analyze whether the different oxygen concentrations influenced cell sensitivity to *N*-allyl-BS, the experiments were performed in atmospheres of 4 and 21% oxygen concentration. The cytotoxic activity was measured using flow cytometry. PC-3 cells with higher metastatic potential were treated for 24h with 40 μM *N*-allyl-BS under hypoxic and normoxic conditions (Fig. 13). A similar fraction of apoptotic and necrotic cells was determined under the two conditions. Significant changes were observed, however the lower oxygen condition did not induce a stronger cytotoxic effect of *N*-allyl-BS as compared to normal oxygen conditions (Fig. 13A, B).

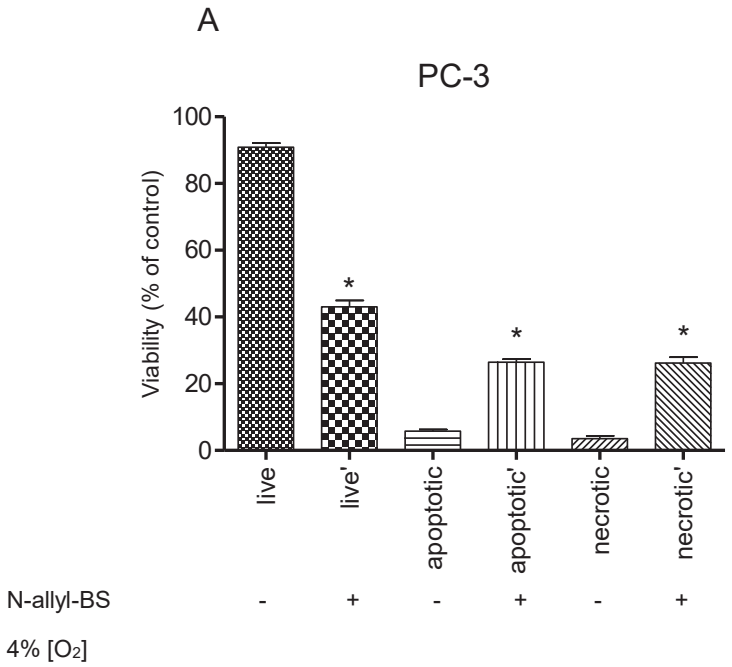

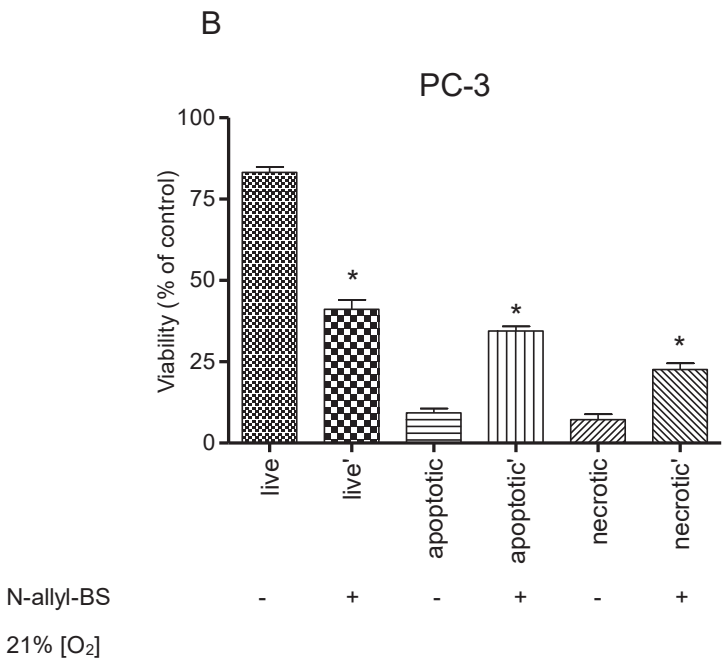

Fig. 13 Different oxygen tension had no effect on *N*-allyl-BS-induced apoptosis and necrosis

40 µM *N*-allyl-BS exhibits similar cytotoxic activity towards PC-3 cells in hypoxic and normoxic conditions (A, B). The cells were treated with the indicated concentration of *N*-allyl-BS for 24h. The viability was assessed using flow cytometry. Data are presented as a mean ± SE (n=3); a significant difference at (*P < 0.001) was calculated using one-way ANOVA followed by Bonferroni's multiple comparison test.

8.3. Cytotoxic activity of *N*-(3-m)-b-BS in DU 145 and PC-3 cells and PNT1A

8.3.1. The influence of *N*-(3-methyl)-butyl- benzisoselenazol-3(*2H*)-one on cell viability in prostate cancer cell lines DU 145 and PC-3, and in the non-cancer PNT1A

As previously described, the cytotoxic effect of *N*-3-m-b-BS was detected on PTEN-positive (DU 145) cell line with normal Akt kinase activity and PTEN-negative (PC-3) cell line with high Akt kinase activity using SRB assay. The cells were treated with a series of dilutions (2.5 – 40 μM) of *N*-(3-m)-b-BS for 24h. As shown, (Fig. 14) *N*-(3-m)-b-BS significantly decreased the cell viability in all concentrations. In particular, the highest anti-proliferative activity was observed in the presence of 40 μM, where the cell viability dropped by 70% in the case of DU 145 (Fig. 14A). However, in PC-3 the cell viability dropped by 80% (Fig. 14B). The stronger cytotoxic effect was observed in PC-3 cells. Interestingly the anti-proliferative activity of *N*-(3-m)-b-BS in the normal prostate cell line PNT1A was significantly lower than that observed with cancer cells, especially at lower concentrations (5–10 μM).

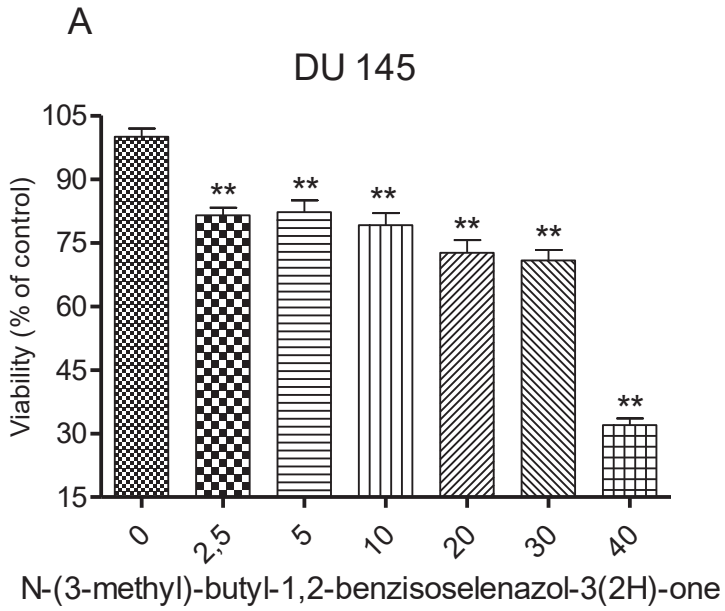

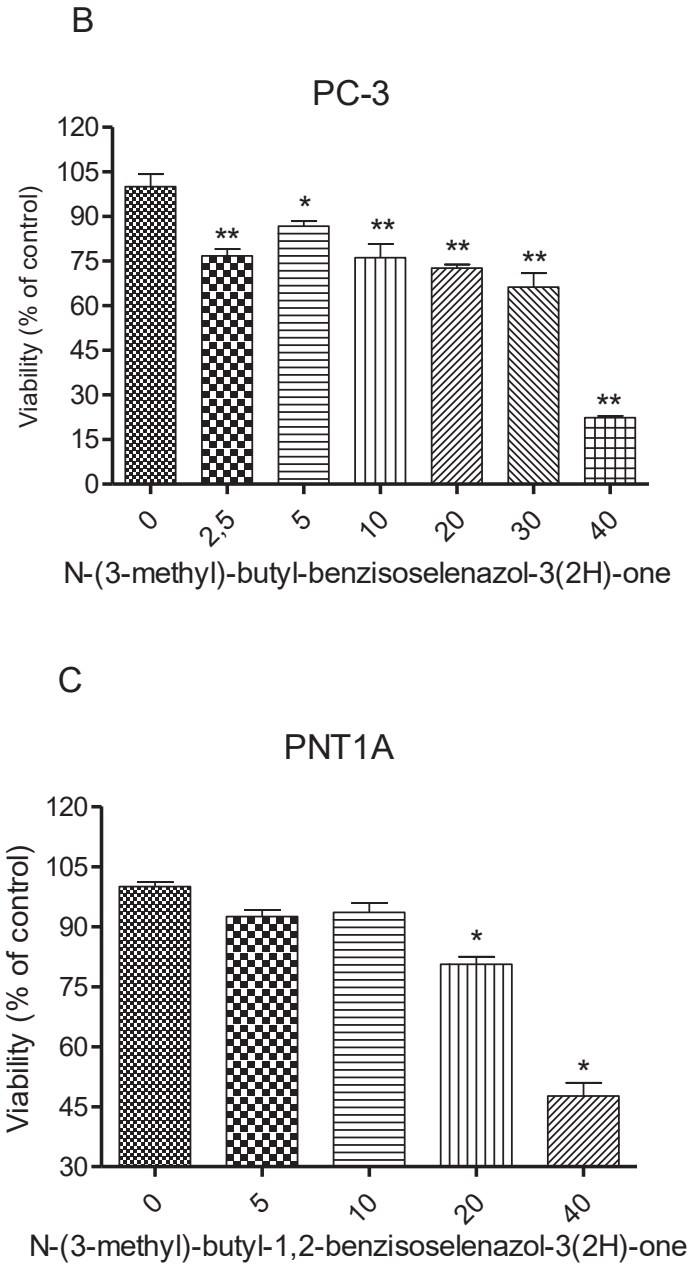

Fig. 14 *N*-(3-m)-b-BS decreased cell viability in prostate cancer cells

A. DU 145, **B.** PC-3, **C.** PNT1A were treated with indicated concentrations of *N*-(3-m)-b-BS for 24 h. The cell viability was measured using SRB assay. Results are presented as a mean ± SE of three independent experiments, where (n=6). A significant difference at (**P<0.001), (*P<0.01) was calculated using one-way ANOVA followed by Dunnett's multiple comparison test.

8.3.2. Influence of *N*-(3-m)-b-BS on the cell cycle in prostate cancer cells

Again, the inhibitory effect of *N*-(3-m)-b-BS on the cell cycle was analyzed using flow cytometry. The experiment showed that after 8 h incubation of DU 145 cells with 40 μM *N*-(3-m)-b-BS induced a slight increase by 15% in the G2/M phase as compared to the control (30%). Statistically significant difference was observed (Fig. 15A). Moreover, *N*-(3-m)-b-BS significantly increased the percentage of the PC-3 cells in G2/M phase (Fig. 15B). The percentage from control 33% raised to 56% in treated cells. Again, the stronger cytostatic effect was observed in PC-3 cells than in DU 145. Indeed, *N*-(3-m)-b-BS significantly induced G2/M cell cycle arrest in both, cancer cell lines (Fig. 15 A, B).

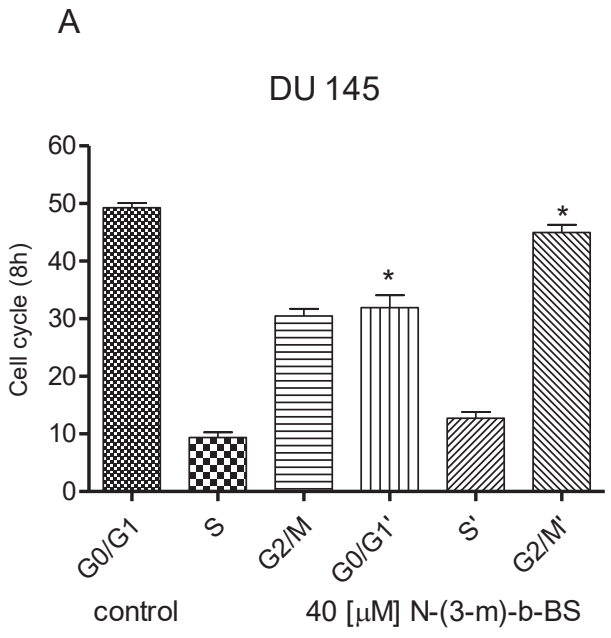

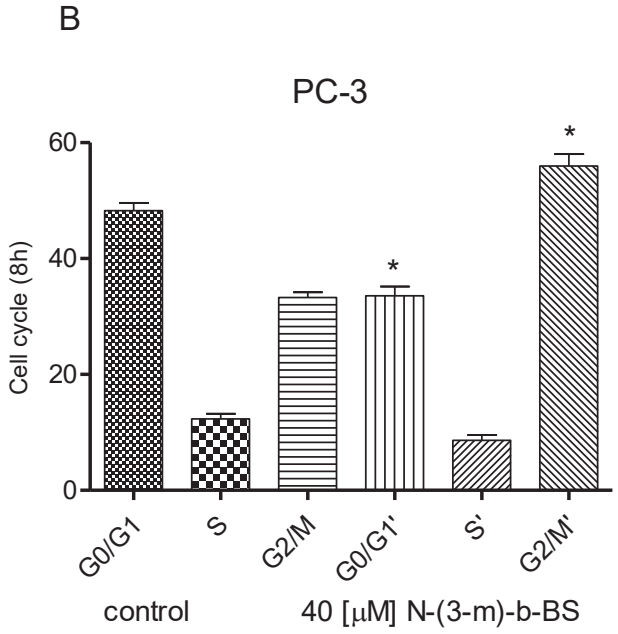

Fig. 15 *N*-(3-m)-b-BS induced G2/M cell cycle arrest in prostate cancer cells

A. DU 145, **B.** PC-3 cells were incubated with 40 μM *N*-(3-m)-b-BS for 8h. Cell cycle arrest was determined using flow cytometry. Data are presented as a mean ± SE from at least three independent experiments (n=3). There was a significant difference at (*P< 0.001) compared with control using one-way ANOVA followed by Bonferroni's multiple comparison test.

8.3.3 Influence of *N*-(3-m)-b-BS on apoptosis and necrosis in prostate cancer cells

To investigate, whether *N*-(3-m)-b-BS induced apoptosis and necrosis in both cancer cell lines, the cells were exposed to 40 μM *N*-(3-m)-b-BS for 24h, and then analyzed using flow cytometry. As shown (Fig. 16) *N*-(3-m)-b-BS induced apoptosis and necrosis in both cancer cell lines. In DU 145 the total number of apoptotic cells was 35%, and in PC- 3 around 20%. However, the total number of necrotic cells reached similar amount as apoptotic in case of DU 145 cells and around 20% in PC-3.

Moreover, the pro-apoptotic and necrotic effect of *N*-(3-m)-b-BS was more prominent in DU 145 cells. Therefore, *N*-(3-m)-b-BS significantly increased the level of apoptotic and necrotic cells as compared to the control, both in DU 145 and PC-3. (Fig.16A, B).

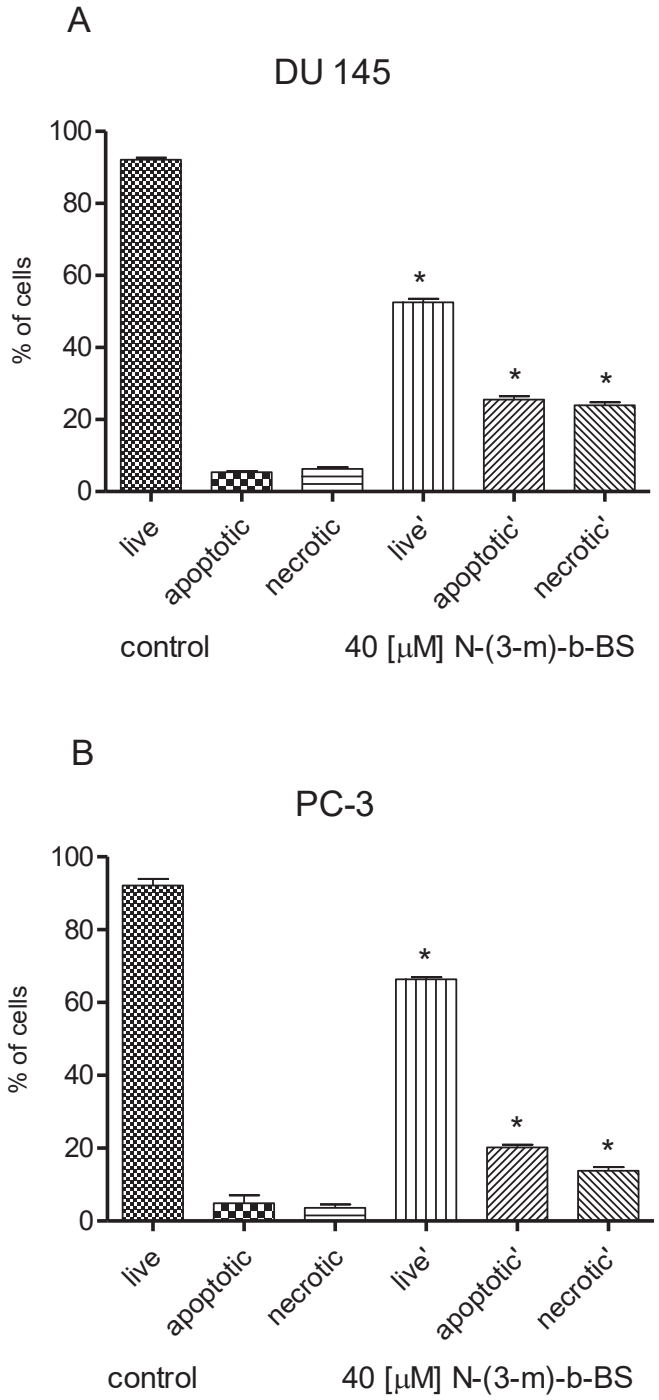

Fig. 16 *N*-(3-m)-b-BS significantly increased the level of apoptotic and necrotic cells in prostate cancer cells

Induction of apoptosis and necrosis of **A.** DU 145, **B.** PC-3 cells treated with 40 μM *N*-(3-m)-b-BS for 24h. The total number of apoptotic and necrotic cells was determined using flow cytometry. Results are presented as a mean ± SE of three independent experiments. A significant difference at (*P< 0.001) was determined by one-way ANOVA followed by Bonferroni's multiple comparison test.

In order to confirm the induction of apoptosis and necrosis by *N*-(3-m)-b-BS, the level of caspase- dependent cleaved PARP, which is the apoptosis marker and enzyme responsible for DNA repair, was analyzed. The changes in the level of PARP-cleavage were determined in the cells incubated with 40 µM *N*-(3-m)-b-BS in different time point (4-24 hrs). As shown, in (Fig. 17A, B) the highest, significant level of cleaved PARP in DU 145 was observed after 8h treatment with 40 µM *N*-(3-m)-b-BS, where it increased to a relative level of 3,5. Subsequently, PARP-cleavage level significantly declined after 24h (Fig. 17A, B). The obtained results confirm that *N*-(3-m)-b-BS induced apoptosis and necrosis in both cancer cell lines.

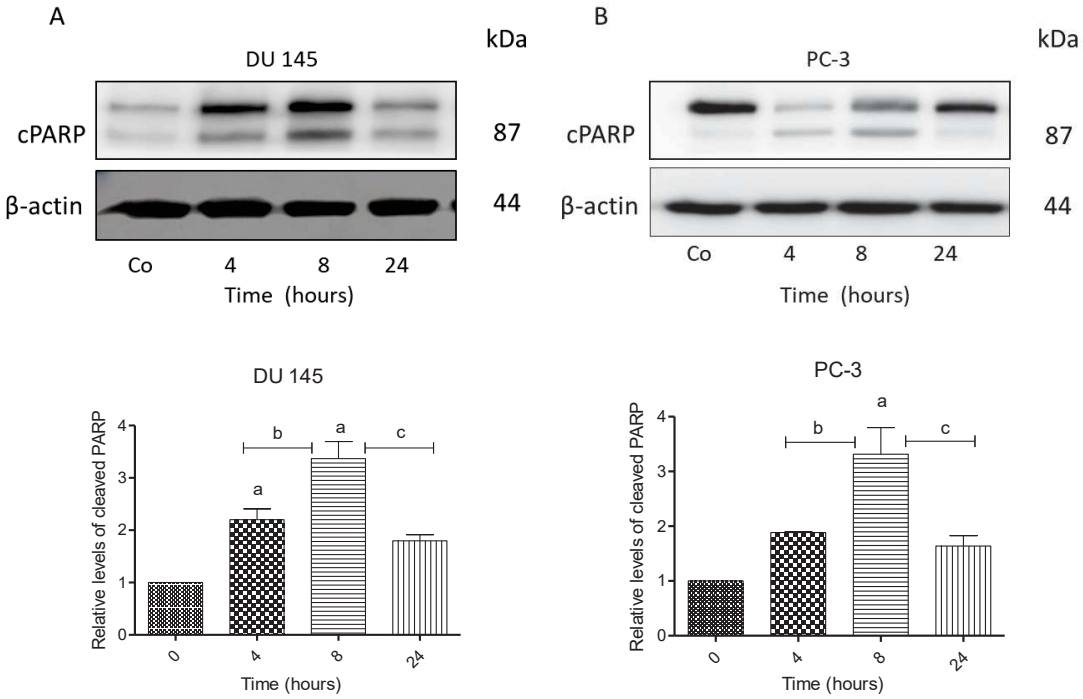

Fig. 17 Western blot analysis of cleaved PARP

A. DU 145, **B.** PC-3 cells treated with 40 µM *N*-(3-m)-b-BS at the indicated time points. β-actin was used as a lane loading control. Data are presented as a mean ±SE of three independent experiments. The statistical significance of differences between respective samples was determined by one-way ANOVA followed by Bonferroni's multiple comparison test, where (a) indicates significant difference between control and treated cells (*P < 0.05) and (b, c) indicates significant difference between 4, 8 and 24h of 40 µM *N*-(3-m)-b-BS treated cells (* P < 0.05).

8.3.4 Effect of DFO and Ferr-1 on cell death induced by *N*-(3-m)-b-BS

To investigate, if *N*-(3-m)-b-BS induced ferroptosis in both cancer cell lines, flow cytometry was used. The cells were treated for 24h with 40 µM *N*-allyl-BS only, and in the presence of iron chelators including desferoxamine (DFO) and ferrostatin-1, and then analyzed. As presented, (Fig. 18) DFO and Ferr-1 (Fig. 19) had no effect on the cells treated with *N*-(3-m)-b-BS in DU 145 and in PC-3 cells (Fig. 18A, B), (19A, B). Moreover, no significant difference was observed in neither DU 145 nor PC-3 cells. Therefore, *N*-(3-m)-b-BS did not influence the induction of ferroptosis in prostate cancer cell lines (Fig. 18, 19).

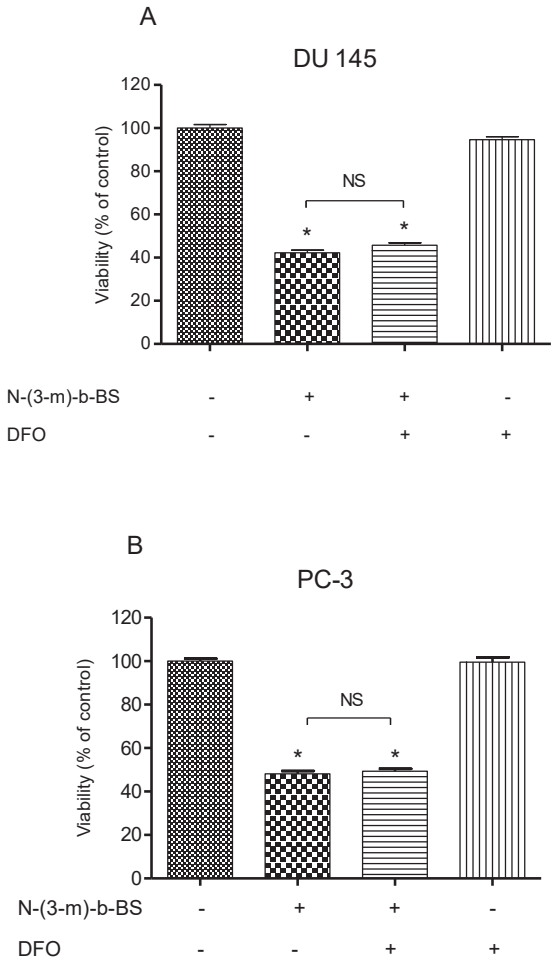

Fig. 18 DFO had no effect on *N*-(3-m)-b-BS-induced cell death

A. DU 145, **B.** PC-3 cells treated with 40 µM *N*-(3-m)-b-BS and 25 µM DFO for 24h. Cell viability was measured using SRB assay. Results are presented as a mean ± SE of three independent experiments. No significant difference was determined by one-way ANOVA followed by Bonferroni's multiple comparison test.

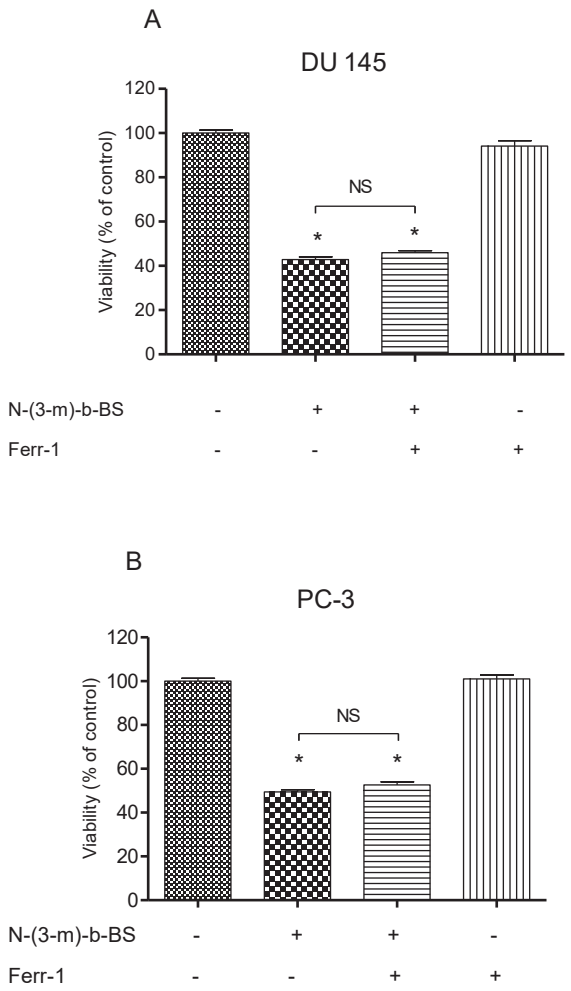

Fig. 19 Ferr-1 had no effect on *N*-(3-m)-b-BS-induced cell death

A. DU 145, **B.** PC-3 cells treated with 40 µM *N*-(3-m)-b-BS and 2 µM Ferr-1 for 24h. Cell viability was measured using SRB assay. Results are presented as a mean ± SE of three independent experiments. No significant difference was determined by one-way ANOVA followed by Bonferroni's multiple comparison test.

8.3.5. Influence of *N*-(3-m)-b-BS on ROS generation in prostate cancer cells

Again, to detect whether the oxidative stress is involved in the cytotoxic effect of *N*-(3-m)-b-BS, intracellular level of ROS was determined. As shown (Fig. 20A, B) a significant increase in ROS generation was observed after 2h treatment of 40 µM *N*-(3-m)-b-BS in both cancer cell lines. Moreover, the results show that *N*-allyl-BS elevated

the level of ROS by 24% in DU 145 and in PC-3 at 2h time point as compared to control (Fig. 20A, B).

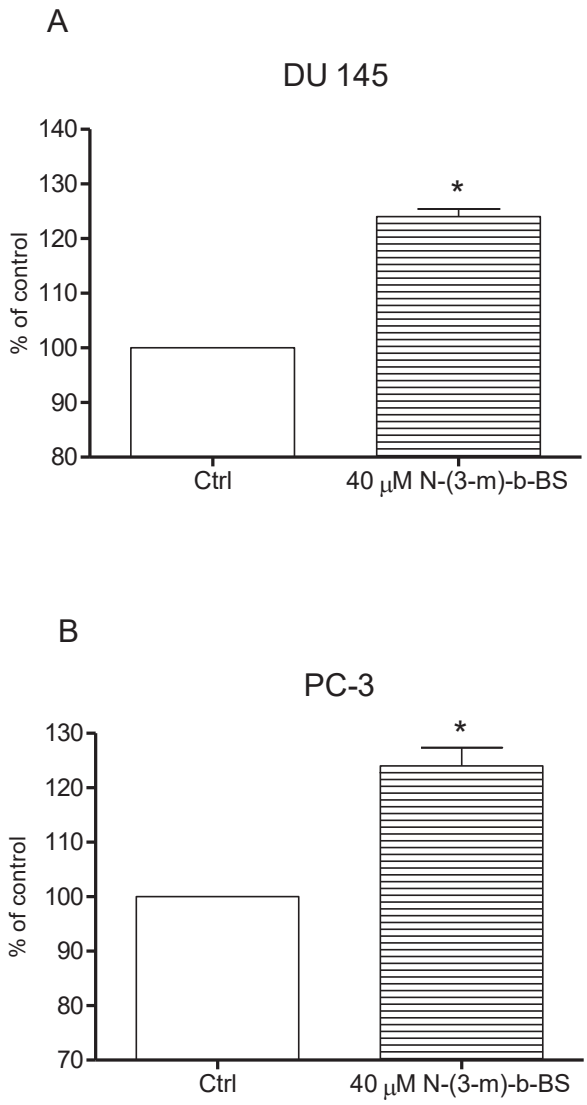

Fig. 20 *N*-(3-m)-b-BS increased the level of ROS generation in prostate cancer cells **A.** DU 145, **B.** PC-3 cells were incubated with 40 μM *N*-(3-m)-b-BS for 2h. The level of ROS-induced formation was analyzed using flow cytometry. Results are presented as a mean ± SE of three independent experiments (n=3), where significantly different at (*P<0.001) compared with control by ANOVA followed by Dunnett's multiple comparison test.

8.3.6. Influence of *N*-(3-m)-b-BS on DNA damage in prostate cancer cells

As mentioned above, oxidative stress and apoptotic cell death is strictly linked with DNA damage in cancer cells. For that, to estimate whether *N*-(3-m)-b-BS induced DNA damage, the cells were treated with 40 μM *N*-(3-m)-b-BS for 8 and 24h. DNA damage was assessed using Comet assay. However, no significant effect was observed neither in DU 145 nor in PC-3 cells after 8 and 24h incubation (Fig. 21A, B, C, D).

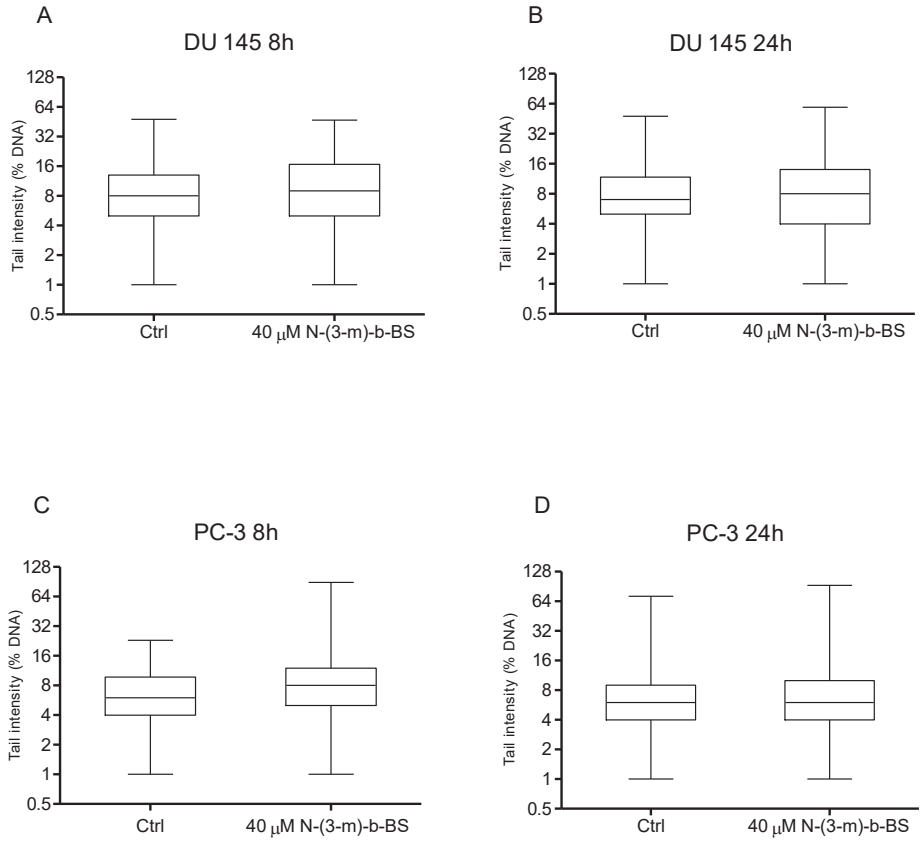

E

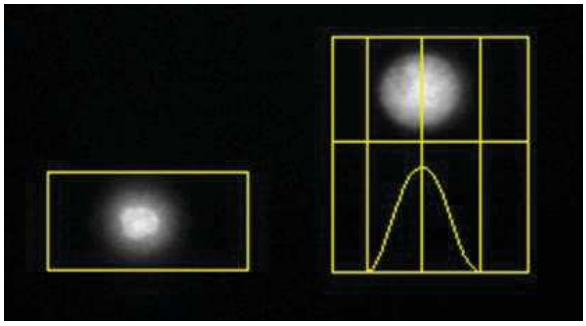

Fig. 21 The analysis of DNA damage

The influence of 40 μM *N*-(3-m)-b-BS on DNA damage in DU 145 (A, B) and PC-3 (C, D) cells after 8 and 24h treatment was determined using comet assay. Results are presented as the percentage of DNA in Tail Intensity ± SE (n=3). No significance of differences compared with control was calculated by ANOVA followed by Dunnet's multiple comparison test. Representative picture of DU 145 (E) and PC-3 (E) cells.

8.3.7. Influence of *N*-(3-m)-b-BS on the level of active form of Akt in prostate cancer cells

In order, to determine whether *N*-(3-m)-b-BS decreased Akt phosphorylation in prostate cancer cells, Western blotting was performed. The cells were exposed to 40 μM *N*-(3-m)-b-BS for different time periods and the changes in the level of phosphorylated Akt were determined. Indeed, Akt phosphorylation declined slightly after 0.5h treatment and a high drop was observed after 4 h treatment in DU 145 (Fig. 22A). Furthermore, *N*-(3-m)-b-BS decreased the level of Akt phosphorylation after 0.5h treatment in PC-3 cells (Fig. 22B), and after 1h treatment decreased the level of Akt phosphorylation. The changes in the Akt phosphorylation were statistically significant in both cancer cell lines (Fig. 22A, B).

A

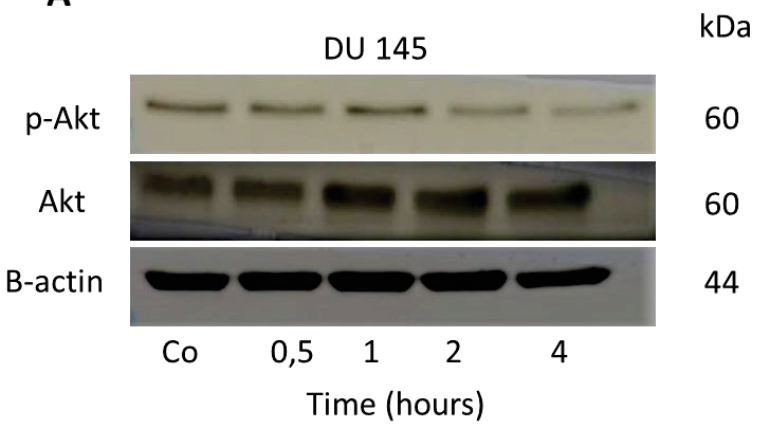
DU 145
kDa
p-Akt
60
Akt
60
B-actin
44
Co
0,5
1
2
4
Time (hours)

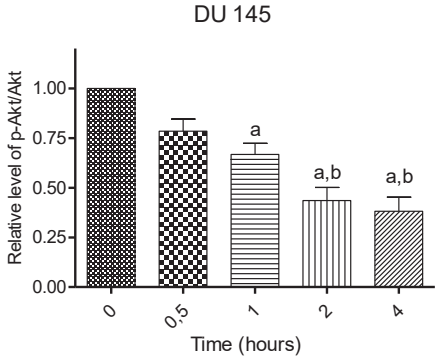
DU 145
Relative level of p-Akt/Akt
1.00
0.75
0.50
0.25
0.00
a
a,b
a,b
0
0,5
1
2
4
Time (hours)

B

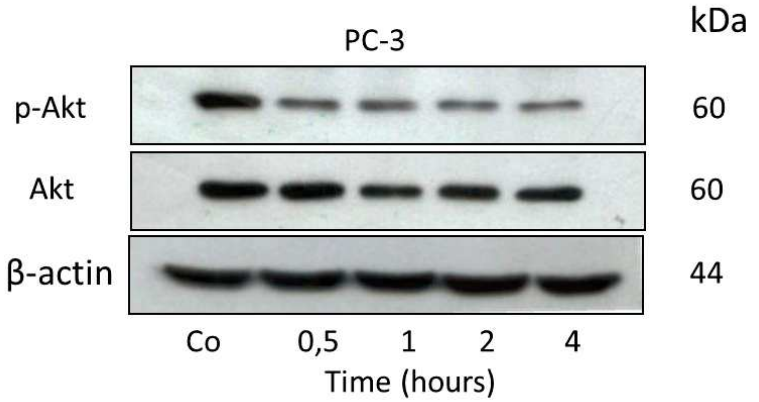
PC-3
kDa
p-Akt
60
Akt
60
β-actin
44
Co
0,5
1
2
4
Time (hours)

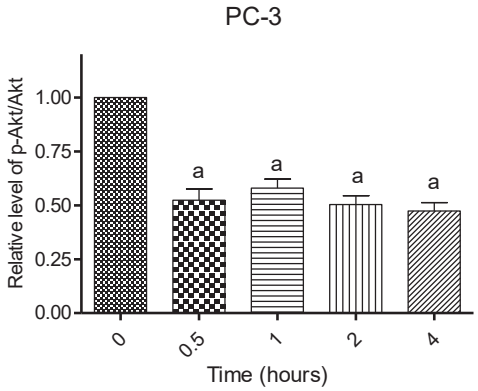
PC-3
Relative level of p-Akt/Akt
1.00
0.75
0.50
0.25
0.00
a
a
a
a
0
0.5
1
2
4
Time (hours)

Fig. 22 Western blot analysis of p-Akt and Akt kinase in DU145 (A) and PC-3 (B) cells treated with 40 μM *N*-(3-m)-b-BS for the indicated periods of time. β-actin was used as a lane loading control. Results are presented as a mean ± SE (n=3). The statistical difference between respective samples was determined by one-way ANOVA followed by Bonferroni's multiple comparison test, where (a) indicates significant difference between control and treated cells (*P< 0.01) and (b, c) indicates significant difference between 4, 8 and 24h treatments of 40 μM *N*-(3-m)-b-BS (*P< 0.05).

8.3.8. Cytotoxic activity of *N*-(3-m)-b-BS in PC-3 cells-effects of different oxygen tension

To analyze, whether the different oxygen concentrations influenced the cell sensitivity to *N*-(3-m)-b-BS, the experiments were performed in atmospheres of 4 and 21% oxygen concertation. The cytotoxic activity was measured using flow cytometry. PC-3 cells with higher metastatic potential were treated for 24 h with 40 μM *N*-(3-m)-b-BS under hypoxic and normoxic conditions (Fig. 23). A similar fraction of apoptotic and necrotic cells was determined under the two conditions. Significant changes were observed, however lower oxygen condition did not induce the stronger cytotoxic effect of *N*-(3-m)-b-BS as compared to normal oxygen conditions (Fig. 23A, B).

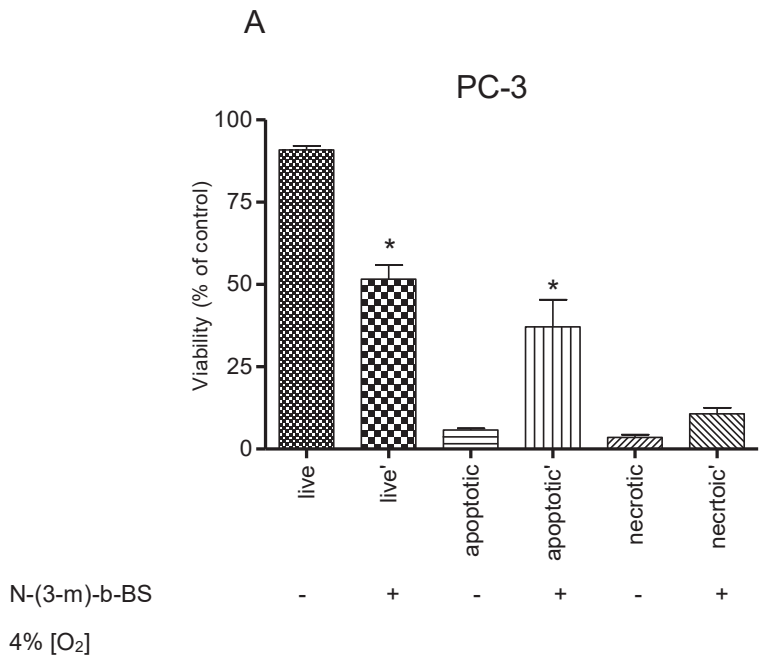

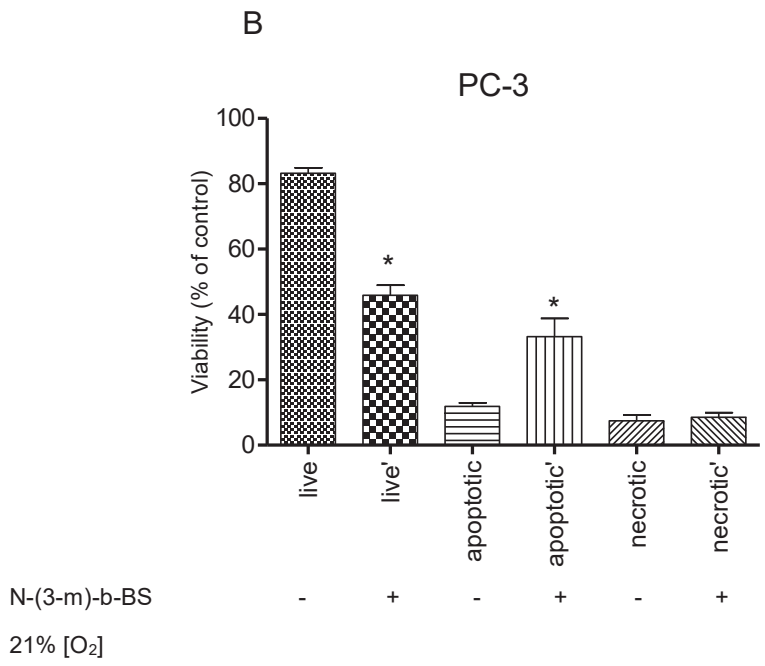

Fig. 23 Different oxygen tension had no effect on *N*-(3-m)-b-BS-induced apoptosis and necrosis

40 µM *N*-(3-M)-b-BS exhibits similar cytotoxic activity towards PC-3 cells in hypoxic and normoxic conditions (23A, B). The cells were treated with indicated concentration of *N*-(3-m)-b-BS for 24h. The viability was assessed using flow cytometry. Data are presented as mean ± SE (n=3); significant difference at (*P <0.01), was calculated using one-way ANOVA followed by Bonferroni's multiple comparison test.

8.3.9. Influence of *N*-allyl-BS and *N*-(3-m)-b-BS on DNA damage in PNT1A

In order to, estimate whether *N*-allyl-BS and *N*-(3-m)-b-BS induced DNA damage in normal prostate cells PNT1A, the cells were treated with 40 µM *N*-allyl-BS and *N*-(3-m)-b-BS for 8 and 24 h. DNA damage was assessed using Comet assay. Surprisingly, no significant effect was observed in PNT1A cells after 8 and 24h incubation (Fig. 24A, B, C, D).

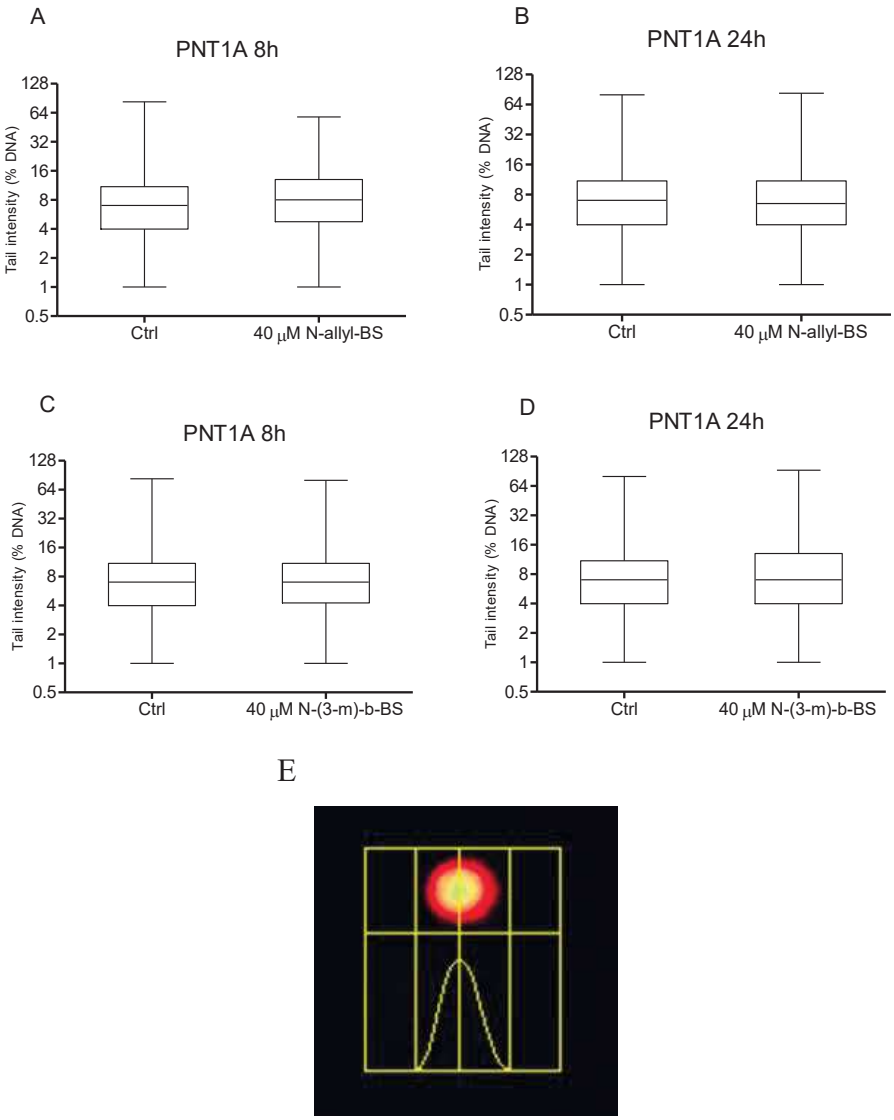

Fig. 24 *N*-allyl-BS and *N*-(3-m)-b-BS did not induce genotoxic DNA damage in PNT1A

The influence of 40 µM *N*-allyl-BS and *N*-(3-m)-b-BS on DNA damage PNT1A (Fig. 24) cells after 8 and 24h treatment was determined using comet assay. Results are presented as the percentage of DNA in tail intensity ± SE (n=3). No significance of differences compared with control was calculated by ANOVA followed by Dunnet's multiple comparison test. Representative picture of PNT1A (E).

8.4. Result of MTD determination of *N*-allyl-BS *in vivo*.

8.4.1. Evaluation of MTD of *N*-allyl-BS *in vivo*

Table 2.

ID Mouse	**Parameter**	0 min	15'	30'	45'	60'	5h'
KK_Tox_Veh	**Body weight - (grams)**	24,6	-	-	-	-	24,4
	Body weight- change in %	-	-	-	-	-	-0,81
	Appearance	0	-	-	-	-	0
	Hair condition	0	0	0	0	0	0
	Breath	0	0	0	0	0	0
	Environment	0	0	0	0	0	0
	Behaviour	0	0	0	0	0	0
	Moving ability	0	0	0	0	0	0
	Total value	**0**	**0**	**0**	**0**	**0**	**0**

Table 2. Control mouse (n = 1) receiving vehicle only. The animal was scored from 0 to 3, where 0 corresponded with normal condition and 3 with strongly impaired. No signs of toxicity were observed.

Table 3.

ID Mouse	**Parameter**	0 min	15'	30'	45'	60'	5h'
KK_Tox_2b_10_mg/kg	**Body weight - (grams)**	28,6	-	-	-	-	28
	Body weight- change in %	-	-	-	-	-	-2,10
	Appearance	0	-	-	-	-	0
	Hair condition	0	0	0	0	0	0
	Breath	0	0	0	0	0	0
	Environment	0	0	0	0	0	0
	Behaviour	0	1	1	1	1	0
	Moving ability	0	1	1	1	1	0
	Total value	**0**	**2**	**2**	**2**	**2**	**0**

Table 4.

ID Mouse	Parameter	0 min	15'	30'	45'	60'	5h'
KK_Tox_2b_ 50_mg/kg	**Body weight - (grams)**	27,6	-	-	-	-	25,4
	Body weight- change in %	-	-	-	-	-	-7,97
	Appearance	0	-	-	-	-	1
	Hair condition	0	0	0	0	0	0
	Breath	0	0	1	1	1	1
	Environment	0	0	0	0	0	0
	Behaviour	0	1	1	1	1	0
	Moving ability	0	0	1	2	1	0
	Total value	**0**	**1**	**3**	**4**	**3**	**2**

Table 5.

ID Mouse	Parameter	0 min	15'	30'	45'	60'	5h'
KK_Tox_2b_ 100_mg/kg	**Body weight - (grams)**	23,4	-	-	-	-	22,2
	Body weight- change in %	-	-	-	-	-	-5,13
	Appearance	0	-	-	-	-	1
	Hair condition	0	0	0	0	0	0
	Breath	0	1	1	0	0	0
	Environment	0	0	0	0	0	0
	Behaviour	0	3	3	2	1	0
	Moving ability	0	2	2	2	1	0
	Total value	**0**	**6**	**6**	**4**	**2**	**1**

Tables 3-5 The evaluation of mice (n =1 per dose), during the first day after oral administration of *N*-allyl-BS in escalating doses. The most apparent signs of toxicity were observed after the dose of 100mg/kg. The scoring increased during the first 45 minutes and after that, the animal started to recover from the toxic effect of *N*-allyl-BS.

Before Administration

After administration

Fig. 25 Representative pictures of mice before and after treatment of *N*-allyl-BS.

9. Discussion

It is widely known that cancer cells possess some unique characteristics that differentiate them from normal cells. In particular, the essential features are: self-sufficiency in growth signals, enhanced proliferation and resistance to its inhibition, evasion of apoptosis-uncontrolled replicative potential, ability to induce angiogenesis, penetration of tissues, and metastasis (Hanahan and Weinberg 2000). The goal of anti-cancer therapies is to trigger the "pro survival" cellular cancer mechanisms that participate in the limitless cell division and metastasis. Moreover, the parameters that should be considered as targets in anti-cancer therapies are: inhibition of cell proliferation, induction of apoptosis, inhibition of cell cycle progression, and induction of ROS production, all of which lead to cancer cell death. The effect of many chemotherapeutics is to decrease the proliferation of cancer cells and eliminate them. However, cancer cells, due to their plasticity, become resistant to drugs and thus the invasion of tissues and metastasis are not inhibited. Furthermore, scientific research for the development of more effective chemotherapeutics in the case of prostate cancer has been underway for decades, and yet the progress is marginal.

Many chemotherapeutics applied in prostate cancer treatment (such as cisplatin, carboplatin, docetaxel, cyclophosphamide, and doxorubicin), besides their efficacy towards malignancies, cause side effects and attack normal cells (Hilkens, Pronk et al. 1997; Hilkens, Verweij et al. 1997). Numerous studies show that cisplatin dosing is limited in usage due to its toxicity. In particular, there have been reports of cisplatin-induced nephrotoxicity in rats (Salem, Helmi et al. 2018) and in many others (Miller, Tadagavadi et al. 2010). Miller and co-authors have reported that cisplatin-associated nephrotoxicity is mediated through mitochondrial and nuclear DNA damage, elevated ROS formation and induction of oxidative stress. What's more, cisplatin promotes apoptosis and renal injury *in vivo* (Miller, Tadagavadi et al. 2010). Thus, it is important to identify chemotherapeutics that would be less toxic towards normal cells. Hu and colleagues reported that selenium applied during cisplatin therapy prevented nephrotoxicity in patients with cancer (Hu, Chen et al. 1997).

Another problem in the curing of tumors is cancer cells' ability to develop resistance against anti-cancer drugs, which makes them less effective. Some findings have presented that selenium played a preventive role in the development of cisplatin

resistance in human ovarian tumors (Caffrey and Frenkel 2000). This was confirmed by Yousef, who reported that selenium enhanced the efficiency and reduced the toxicity of studied anti-cancer drugs (Yousef and Hussien 2015).

Ebselen acts as an artificial selenocysteine. This selenocysteine builds up the active side of GPx and works as a strong antioxidant agent. Both of these roles eliminate ROS generation and protect against oxidative stress. This process is directly associated with the prevention of carcinogenesis as high oxidative stress leads to apoptosis, DNA damage and cancer development. In particular, ebselen has been shown to abrogate oxidative stress and inhibit apoptosis via eliminating ROS in PC12 cells (Yoshizumi, Kogame et al. 2002). Ebselen decreased TNF-α mediated NF-κB activity and exerted induction of apoptosis in tumor cells (Sharma, Tewari et al. 2008). Furthermore, ebselen demonstrates protective effects against toxic compounds and impairs the genotoxic influence of cyclophosphamide in mice (Tripathi and Jena 2008).

Therefore, the first aim of this study was to assess the antiproliferative and cytotoxic effect of newly synthesized N-substituted ebselen dervatives. In addition, the groups of newly synthesized ebselen derivatives bearing aliphatic or aromatic moiety structures were examined against prostate cancer cells with different genetic backgrounds (ie. PTEN –positive DU 145, and PTEN-negative PC-3), and towards normal epithelial prostate cells PNT1A. Indeed, many of these ebselen derivatives revealed strong antioxidant activities, which are similar to or even stronger than the activity of ebselen. Furthermore, some of them exhibited a strong cytotoxic effect towards prostate cancer cells, and a less toxic effect towards normal prostate cells (Pacula, Kaczor et al. 2017; Pacula, Kaczor et al. 2017). Two ebselen N-substituted derivatives were selected to further investigate their antitumor potential mechanism. For this reason, it was decided to examine if both *N*-allyl-BS and *N*-(3-m)-b-BS exerted stronger cytotoxic effects on the prostate cancer cell lines PC-3 and DU 145 than in the normal prostate cells PNT1A. Surprisingly, PC-3 cells seemed to be more sensitive to the exposure to *N*-allyl-BS and *N*-(3-m)-b-BS than DU 145 cells. These data indicate that cell viability of PC-3 cells is more Akt-dependent than in DU 145 cells. What's more, both organoselenium compounds showed more cytotoxic effects on prostate cancer cells than in non-cancer cells.

The cell cycle is a vital process in cell division and DNA replication. Due to this fact, inhibition of cell cycle progression is considered an important part of the preventive effect of cancer therapy. Therefore, the next purpose was to determine if *N*-

allyl-BS and *N*-(3-m)-b-BS induced cell cycle arrest in the G2/M phase, after treatment of 8h in the case of two cancer cell lines. It was demonstrated for the first time that newly synthesized ebselen derivatives induced arrest in the G2/M phase in both prostate cancer cell lines. These data are in line with Venkateswaran and co-authors, who pointed out that PC-3 transfected with the androgen receptor (PC3-AR2) induced a G2/M arrest (Venkateswaran, Klotz et al. 2002). Selenomethionine caused G2/M arrest in colon cancer cells (Goel, Fuerst et al. 2006), however there is limited data showing that organoselenium compounds may induce G2/M arrest.

ROS in physiological concentrations play an important role in regulating a broad range of biological processes. Numerous studies also show that enhanced ROS formation leads to structural changes in lipids, proteins, and nucleic acids. Consequently, oxidative stress generation promotes cardiovascular diseases, neurodegenerative diseases such as Alzheimer's or Parkinson's, and the development of cancer (Halliwell 1992; Coyle and Puttfarcken 1993; Beal 2002). It has been reported that in normal cells the level of ROS production is lower than in cancer cells (Halliwell 2003). Hence, cancer cells require higher concentrations of ROS in order to function properly. The obtained results might explain the inhibition of the G2/M cell cycle phase in prostate cancer cells and in the modulation of the apoptotic pathway.

As was mentioned above, ebselen has been identified as a strong antioxidant molecule, as it mimics the activity of GPx. For this reason, another goal of the current study was to determine whether *N*-allyl-BS and *N*-(3-m)-b-BS would act as pro-oxidants or antioxidants. PC-3 and DU 145 cancer cell lines were incubated with *N*-allyl-BS and *N*-(3-m)-b-BS and the level of ROS generation was examined. Two of the studied ebselen derivatives increased ROS generation to a similar extent in both of the cancer cell lines. It has been shown that selenium compounds may alter the redox status of cells by modulating cellular levels of reducing agents (Zhong and Oberley 2001; Hatfield, Tsuji et al. 2014; Roman, Jitaru et al. 2014). What’s more, a strong correlation was found between enhanced ROS generation and DNA damage. These strongly reactive molecules, upon elevated generation, provoke single or double- stranded breaks. Therefore, the cells were incubated with organoselenium compounds for 8h and 24h and the level of DNA damage was measured using comet assay. Interestingly, *N*-allyl-BS caused statistically significant growth in DNA damage in PC-3 after 8h and 24h treatment. Meanwhile, in DU 145 there was no statistical significance reached after neither 8h nor 24h. Moreover, no statistically significant increase was detected in any of

the cancer cell lines exposed to *N*-(3-m-)-b-BS. The above outcome strongly suggests that *N*-allyl-BS caused genotoxic stress in PC-3 cells. Ebselen in higher concentrations causes cellular toxicity. It was demonstrated that ebselen induced DNA fragmentation in HepG2 cells (Yang, Shen et al. 2000; Yang, Shen et al. 2000). Another study showed that selenocystamine caused DNA damage in mouse keratinocytes and this was detected by a high concentration of 8-OHdG, which is one of the markers of DNA damage (Shigenaga and Ames 1991; Stewart, Spallholz et al. 1999). In the present study, the differences in the extent of DNA damage induced by *N*-allyl-BS and *N*-(3m-b)-BS could not be explained by the changes of ROS generation, due to the fact that only *N*-allyl-BS caused significant DNA damage in PC-3 cells. These findings are in agreement with data showing that other organoselenium compounds promoted DNA damage in human prostate, colon, and cells, as well as mouse keratinocytes and mammary cancer cells (Sinha and Medina 1997; Stewart, Spallholz et al. 1999; Menter, Sabichi et al. 2000; Chigbrow and Nelson 2001) .

Akt kinases are the proteins involved in the regulation of the apoptosis process. As described above, apoptosis is an essential phenomenon that removes pathologically altered cells that are caused by intrinsic and extrinsic factors. In addition, an amplified Akt level and mutated PTEN are observed in various types of aggressive cancer, including that of the prostate (Noguchi, Ropars et al. 2007). Due to this fact, the importance of finding a potent agent that would regulate the Akt signaling pathway is considered a major target for anti-cancer therapies. As mentioned above, PC-3 cells are PTEN-negative and it has been shown that the growth of cancer cells depends principally on the activation of the Akt pathway. Hence, it was hypothesized that some of the *N*-allyl-BS and *N*-(3-m)-b-BS anticancer activities (apoptosis induction and/or cell cycle arrest) could correlate with the inhibition of Akt kinase. In fact, the presented data confirmed the hypothesis that the level of Akt phosphorylation was significantly decreased in DU145 and PC-3 cells treated with *N*-allyl-BS and *N*-(3-m)-b-BS in a time-dependent manner. In addition, these results suggested that the higher sensitivity of PC-3 than DU145 cells to *N*-allyl-BS and *N*-(3-m)-b-BS was associated with Akt inactivation. There is relatively little data referring to the knock-down of the Akt kinase pathway, however our data are in line with Wang and colleagues, who reported that methylselenic acid down-regulated the Akt dependent pathway in vascular endothelial cells (Wang, Jiang et al. 2001). Nevertheless, we demonstrated for the first time that newly synthesized ebselen derivatives inhibited the Akt signaling pathway in prostate

cancer cells. This may be an outcome of cell cycle arrest, elevated ROS production, oxidative stress, DNA damage and the induction of apoptosis.

It is important to know that the induction of apoptosis and inhibition of cell proliferation by selenium-containing compounds seem to be relevant cellular targets in the prevention of cancers. As mentioned above, tumor transformation correlates with point mutations, deletions, amplifications and changes in the promotor sequences, resulting in elevated expression or lack of expression of specific genes. For this reason, another aim of the present study was to determine whether both organoselenium compounds induced apoptosis in both of the analyzed cancer cell lines that are phenotypically different. It was demonstrated that *N*-allyl-BS and *N*-(3-m)-b-BS significantly increased the apoptotic fraction in both cancer cell lines. Surprisingly, higher apoptosis was observed in the PC-3 line as compared to DU 145, in the case of both ebselen derivatives. The presented results are consistent with previously published data showing that organoselenium compounds induce cell death via apoptosis in cancer cells (Yang, Shen et al. 2000; Wang, Jiang et al. 2002; Chen and Wong 2008). Zhang and colleagues reported that ebselen induced apoptosis in multiple myeloma cells by enhancing endogenous ROS production. This data was confirmed by flow cytometry, Bax translocation, and mitochondrial membrane potential depolarization (Zhang, Zhou et al. 2014). Furthermore, another study suggested a strong correlation between mitochondrial ROS generation and the induction of apoptosis in pancreatic AR42J cancer cells (Santofimia-Castano, Garcia-Sanchez et al. 2014). Interestingly, Sharma and co-authors described the pro-apoptotic effect of ebselen in human acute myeloid leukemia cell lines due to inhibition of ROS production (Maraldi, Prata et al. 2009). What's more, when apoptosis was induced in HepG2 cells via depletion of intracellular thiols and through mitochondrial permeability, this lead to cell death (Yang, Shen et al. 2000; Yang, Shen et al. 2000). Despite this fact, numerous studies highlight that organoselenium compounds such as ebselen, selenadiazole, methylselenic acid, Se-methylselenocysteine (MSC), selenezaine derivatives and many others prompt cell death via apoptosis (Stewart, Spallholz et al. 1999; Goel, Fuerst et al. 2006; Chen and Wong 2008; Maraldi, Prata et al. 2009). Taken together, these data are in agreement with data presented in this dissertation, which confirm that *N*-allyl-BS and *N*-(3-m)-b-BS promote apoptosis through elevated ROS formation and therefore oxidative stress generation. It is worth mentioning that the use of apoptosis- and necrosis-inducing agents is more often being considered as a therapeutic approach in cancer treatment

because induction of these processes would result in a pronounced reduction of tumor mass. In the current study, a Western blot analysis of cleaved PARP levels was used as the marker of apoptosis. As described above, PARP is an abundant enzyme that exists in all somatic cells. PARP promotes a variety of cellular processes, including modulation of chromatin structure, transcription, replication, recombination, and DNA repair (Whitacre, Zborowska et al. 1999; Morales, Li et al. 2014). Due to this fact, PARP determines DNA damage and signals to the cellular repair mechanism. Since PARP-cleavage is catalyzed by caspase 3, which is observed during cell death modulated by various apoptotic stimuli, it is considered an apoptotic marker. In the current study, it was shown that both analyzed compounds caused PARP-cleavage. The highest level of degraded PARP was noticed after 4h and 8h exposure of both cancer cells. Moreover, it has been reported that organoselenium compounds induced PARP-cleavage in human breast and ovarian cancer cells through caspase-3 activation (Yeo, Cha et al. 2002). Another study demonstrated that methylselenic acid and its metabolite methylselenol induced apoptosis via cleavage of PARP-mediated caspase activation in prostate cancer cells (Menter, Sabichi et al. 2000; Jiang, Wang et al. 2001). Taken together, results obtained from this study and the data reported by others are in agreement, strongly suggesting that *N*-allyl-BS and *N*-(3-m)-b-BS promote apoptosis in cancer cells by an intrinsic pathway (Zhang, Zhou et al. 2014). Notwithstanding, after 24h treatment of PC-3 and DU 145 cells with *N*-allyl-BS and *N*-(3-m)-b-BS, the level of cleaved PARP was significantly diminished. This phenomenon may be a result of necrosis induction. It has been detected that necrosis is associated with a loss of membrane integrity, intracellular organelle swelling and adenosine triphosphate (ATP) depletion leading to alternations in energy –required apoptotic cell death to necrotic cell death (Nicotera, Leist et al. 1998). Furthermore, it has also been shown that during necrosis, subsequent cleavage of PARP occurs, with small PARP fragments (Mr 50,000, 40,000, and 35,000) identified (Whitacre, Zborowska et al. 1999). Despite the fact that necrosis is defined as an uncontrolled type of cell death correlated with peripheral tissue damage and increased inflammation, nowadays it has been highlighted as a positive phenomenon induced in cancer therapy. In fact, HMGB1 (a biochemical marker of necrosis) may be able to stimulate an antitumor immune system. Moreover, studies in fibroblasts *in vivo* imply that immunization with HMGB1 can augment antitumor immunity against poorly immunogenic apoptotic tumors (Rovere-Querini, Capobianco et al. 2004). Interestingly, Guerin and Gauthier demonstrated that ebselen induced

prominent necrotic cell death in Sp2/0-Ag14 hybridoma cells, which was proven by fluorescence microscopy (Guerin and Gauthier 2003). Again, these findings are consistent with the hypothesis that *N*-allyl-BS and *N*-(3-m)-b-BS induced necrosis in both of the cancer cell lines analyzed.

Ferroptosis plays a crucial role in cancer treatment, since it is accompanied by an excessive accumulation of iron (Cao and Dixon 2016). Thus, another goal was to determine if *N*-allyl-BS and *N*-(3-m)-b-BS induced ferroptosis. Cell viability was measured using SRB assay after treatment with iron chelators including DFO and ferrostatin-1. In particular, DU145 and PC-3 were first treated with 25 uM DFO in the presence of 40 uM *N*-allyl-BS. The same experiment was performed with *N*-(3-m)-b-BS. However, no significant difference was observed in the case of the two cancer cell lines. Hence, another step was to confirm that *N*-allyl-BS and *N*-(3-m)-b-BS did not induce ferroptosis, so the cells were treated with ferrostatin-1. The hypothesis was confirmed since there was no significant increase in the viability of the cells after treatment with *N*-allyl-BS and *N*-(3-m)-b-BS in the presence of ferrostatin-1, in both cancer cell lines DU 145 and PC-3. These data demonstrated that ebselen derivatives did not induce cell death via ferroptosis.

Some studies concerning cell culture, including our own, are performed in 21% oxygen concentration, while tissue oxygen concentration is between 3 and 8%. There is some evidence suggesting that the increased oxygen concentration normally employed in cell cultures may initiate alternations in cellular pathways *in vitro* (Miller, Genbacev et al. 2005; Al-Ani, Toms et al. 2018). In addition, hypoxia has been demonstrated to elevate the level of ROS. Therefore, another goal of this study was to investigate the cytotoxicity of *N*-allyl-BS and *N*-(3-m)-b-BS towards prostate cells with higher metastatic potential upon 21% and 4% oxygen. We hypothesized that the cytotoxic effect of *N*-allyl-BS and *N*-(3-m)-b-BS would be lower under 21% due to the adaptation of greater free radical formation under this condition than under 4% oxygen (Bourdeau-Heller and Oberley 2007). Surprisingly, the obtained results did not confirm the hypothesis since both compounds induced similar cytotoxic effects under both 21% and 4% oxygen concentration. Thus, the cytotoxic effect of *N*-allyl-BS and *N*-(3-m)-b-BS was not associated with different oxygen concentration.

N-allyl-BS, which revealed the most promising antitumor activity in prostate cancer cells and the least toxic effect in normal prostate cells, was further considered to be evaluated *in vivo*. The first step of this evaluation was to determine the maximum

tolerated dose (MTD). Since *N*-allyl-BS exhibits a stronger cytotoxic effect than *N*-(3-m)-b-BS, it has been studied *in vivo*. Animals were orally administered *N*-allyl-BS in escalating doses (Table 3-5) until the apparent symptoms of toxicity appeared. These severe toxic, but not lethal, effects were considered as the endpoint. At first only one mouse was administered *N*-allyl-BS in order to reduce the amount of animals exposed to toxic symptoms. What's more, prominent signs of toxicity were observed in a range of doses from 10 to 100 mg/kg. Animals that received the highest dose (100mg/kg) presented severe toxic effects during the first 15 minutes after administration. Those effects included severely impaired breathing and moving ability, as well as changes in behavior. After reaching the highest intensity of symptoms (30 minutes after administration), mice started to recover. During the following 14-day observation, animal presented full recovery from toxic effect.

In order to confirm this finding of the preliminary experiment, the same dose (100 mg/kg) was administered to another four mice. Animals demonstrated similar signs of toxicity as compared to the first one. The most severe toxic effects were observed during the first 15 minutes after administration of *N*-allyl-BS and the intensity of symptoms started to reduce after 30 minutes post-administration. Again, during the 14-day observation, the animals presented full recovery from toxic sympotoms. In summary, this tested dose (100mg/kg per mouse) was determined to be the single maximum tolerated dose (MTD).

Taken together, the data obtained in this study suggest that newly synthesized ebselen derivatives *N*-allyl-BS and *N*-(3-m)-b-BS possess antitumor potential in the prostate cancer model (Fig. 25).

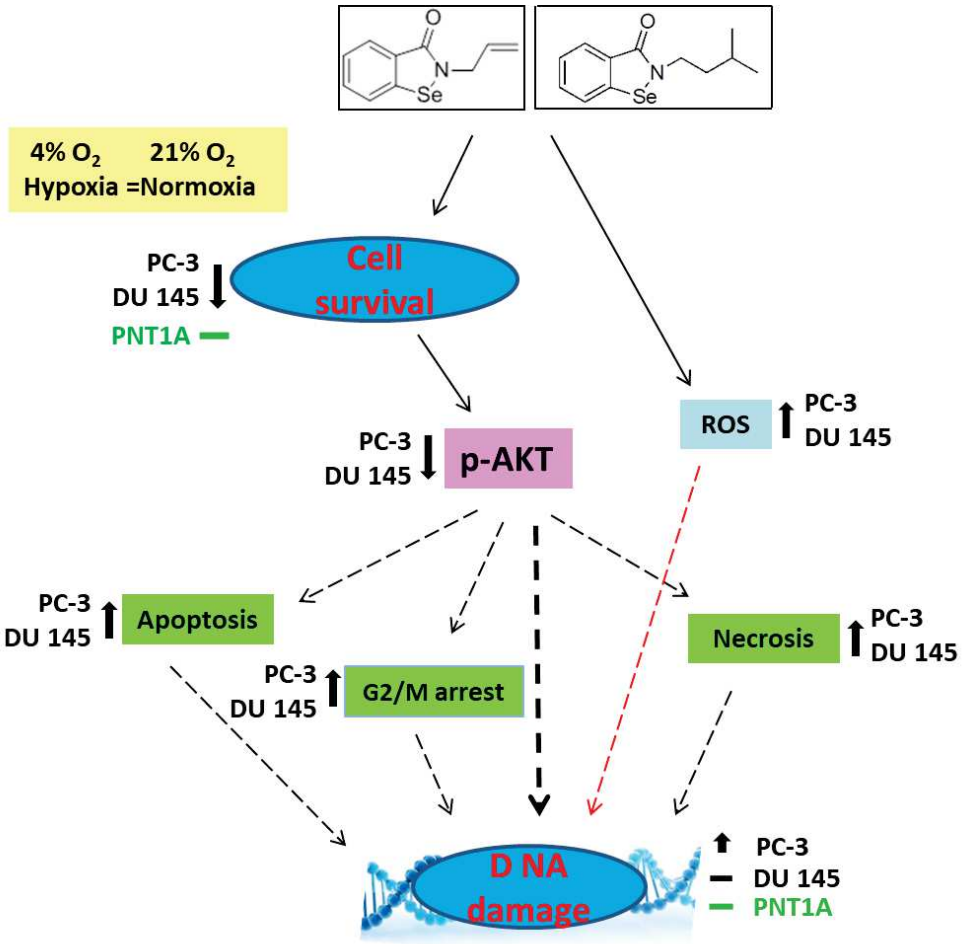

Fig. 26 The potential mechanism of studied compounds

The cytotoxic effect of *N*-allyl-BS and *N*-(3-m-)-b-BS is associated with:

- Increased ROS production
- Induction of G2/M cell cycle arrest
- Induction of apoptosis and necrosis
- Down-regulation of the Akt signalling pathway
- *N*-ally-BS-induced DNA damage

10. Conclusions

1. *N*-allyl-BS and *N*-(3-m)-b-BS exhibited cytotoxicity and decreased cell growth in both prostate cancer cell lines, and demonstrated less toxic effects towards normal cell lines.
2. *N*-allyl-BS and *N*-(3-m)-b-BS induced cell cycle arrest in the G2/M phase and increased the level of ROS generation in both studied cancer cell lines.
3. No effect of Ferr-1 and DFO on cell death induced by *N*-allyl-BS and *N*-(3-m)-b-BS indicates that ferroptosis was not induced in both cancer cell lines.
4. *N*-allyl-BS and *N*-(3-m)-b-BS reduced Akt phosphorylation, and therefore down-regulated the activation of the Akt signaling pathway in both cancer cell lines.
5. *N*-allyl-BS and *N*-(3-m)-b-BS promoted apoptosis and necrosis, and this was associated with the increase in ROS production and genotoxic stress-induced DNA damage.
6. Hypoxic conditions did not potentiate the cytotoxic activity of *N*-allyl-BS and *N*-(3-m)-BS in PC-3 cells.
7. PTEN-negative PC-3 cells were more sensitive to *N*-allyl-BS and *N*-(3-m)-b-BS than PTEN- positive DU 145.
8. The maximum tolerated dose of *N*-allyl-BS after a single oral administration in mice was determined as 100 mg/kg.

11. Bibliography

Al-Ani, A., D. Toms, et al. (2018). "Oxygenation in cell culture: Critical parameters for reproducibility are routinely not reported." PLoS One **13**(10): e0204269.

Anwar, A., N. Uddin, et al. (2018). "A natural flavonoid lawsonaringenin induces cell cycle arrest and apoptosis in HT-29 colorectal cancer cells by targeting multiple signalling pathways." Mol Biol Rep **45**(5): 1339-1348.

Aufderklamm, S., F. Miller, et al. (2014). "Chemoprevention of prostate cancer by isoflavonoids." Recent Results Cancer Res **202**: 101-108.

Avery, J. C. and P. R. Hoffmann (2018). "Selenium, Selenoproteins, and Immunity." Nutrients **10**(9).

Beal, M. F. (2002). "Oxidatively modified proteins in aging and disease." Free Radic Biol Med **32**(9): 797-803.

Biswas, D. K., Q. Shi, et al. (2004). "NF-kappa B activation in human breast cancer specimens and its role in cell proliferation and apoptosis." Proc Natl Acad Sci U S A **101**(27): 10137-10142.

Borkowska, A., N. Knap, et al. (2013). "Diallyl trisulfide is more cytotoxic to prostate cancer cells PC-3 than to noncancerous epithelial cell line PNT1A: a possible role of p66Shc signaling axis." Nutr Cancer **65**(5): 711-717.

Borkowska, A., A. Sielicka-Dudzin, et al. (2012). "Diallyl trisulfide-induced prostate cancer cell death is associated with Akt/PKB dephosphorylation mediated by P-p66shc." Eur J Nutr **51**(7): 817-825.

Boulares, A. H., A. G. Yakovlev, et al. (1999). "Role of poly(ADP-ribose) polymerase (PARP) cleavage in apoptosis. Caspase 3-resistant PARP mutant increases rates of apoptosis in transfected cells." J Biol Chem **274**(33): 22932-22940.

Bourdeau-Heller, J. and T. D. Oberley (2007). "Prostate carcinoma cells selected by long-term exposure to reduced oxygen tension show remarkable biochemical plasticity via modulation of superoxide, HIF-1alpha levels, and energy metabolism." J Cell Physiol **212**(3): 744-752.

Bradford, M. M. (1976). "A rapid and sensitive method for the quantitation of microgram quantities of protein utilizing the principle of protein-dye binding." Anal Biochem **72**: 248-254.

Bray, F., J. Ferlay, et al. (2018). "Global cancer statistics 2018: GLOBOCAN estimates of incidence and mortality worldwide for 36 cancers in 185 countries." CA Cancer J Clin **68**(6): 394-424.

Briviba, K., I. Roussyn, et al. (1996). "Attenuation of oxidation and nitration reactions of peroxynitrite by selenomethionine, selenocystine and ebselen." Biochem J **319 (Pt 1)**: 13-15.

Brunet, A., A. Bonni, et al. (1999). "Akt promotes cell survival by phosphorylating and inhibiting a Forkhead transcription factor." Cell **96**(6): 857-868.

Brunet, A., S. R. Datta, et al. (2001). "Transcription-dependent and -independent control of neuronal survival by the PI3K-Akt signaling pathway." Curr Opin Neurobiol **11**(3): 297-305.

Burton, G. J. and E. Jauniaux (2011). "Oxidative stress." Best Pract Res Clin Obstet Gynaecol **25**(3): 287-299.

Cao, J. Y. and S. J. Dixon (2016). "Mechanisms of ferroptosis." Cell Mol Life Sci **73**(11-12): 2195-2209.

Chen, Q., E. J. Vazquez, et al. (2003). "Production of reactive oxygen species by mitochondria: central role of complex III." J Biol Chem **278**(38): 36027-36031.

Chen, T. and Y. S. Wong (2008). "Selenocystine induces apoptosis of A375 human melanoma cells by activating ROS-mediated mitochondrial pathway and p53 phosphorylation." Cell Mol Life Sci **65**(17): 2763-2775.

Chiang, K. C., H. Y. Chen, et al. (2015). "PTEN insufficiency modulates ER+ breast cancer cell cycle progression and increases cell growth in vitro and in vivo." Drug Des Devel Ther **9**: 4631-4638.
Chigbrow, M. and M. Nelson (2001). "Inhibition of mitotic cyclin B and cdc2 kinase activity by selenomethionine in synchronized colon cancer cells." Anticancer Drugs **12**(1): 43-50.
Choi, B. H., S. Xie, et al. (2017). "PTEN is a negative regulator of mitotic checkpoint complex during the cell cycle." Exp Hematol Oncol **6**: 19.
Churg, A. (2003). "Interactions of exogenous or evoked agents and particles: the role of reactive oxygen species." Free Radic Biol Med **34**(10): 1230-1235.
Cooke, M. S., M. D. Evans, et al. (2003). "Oxidative DNA damage: mechanisms, mutation, and disease." FASEB J **17**(10): 1195-1214.
Coyle, J. T. and P. Puttfarcken (1993). "Oxidative stress, glutamate, and neurodegenerative disorders." Science **262**(5134): 689-695.
Cussenot, O., P. Berthon, et al. (1991). "Immortalization of human adult normal prostatic epithelial cells by liposomes containing large T-SV40 gene." J Urol **146**(3): 881-886.
Dalle-Donne, I., D. Giustarini, et al. (2003). "Protein carbonylation in human diseases." Trends Mol Med **9**(4): 169-176.
Daniyal, M., Z. A. Siddiqui, et al. (2014). "Epidemiology, etiology, diagnosis and treatment of prostate cancer." Asian Pac J Cancer Prev **15**(22): 9575-9578.
Das, K. C. and C. W. White (2002). "Redox systems of the cell: possible links and implications." Proc Natl Acad Sci U S A **99**(15): 9617-9618.
Davies, M. J. (2016). "Protein oxidation and peroxidation." Biochem J **473**(7): 805-825.
de Souza-Pinto, N. C., D. M. Wilson, 3rd, et al. (2008). "Mitochondrial DNA, base excision repair and neurodegeneration." DNA Repair (Amst) **7**(7): 1098-1109.
Dixit, D., V. Sharma, et al. (2012). "Inhibition of Casein kinase-2 induces p53-dependent cell cycle arrest and sensitizes glioblastoma cells to tumor necrosis factor (TNFalpha)-induced apoptosis through SIRT1 inhibition." Cell Death Dis **3**: e271.
Elmore, S. (2007). "Apoptosis: a review of programmed cell death." Toxicol Pathol **35**(4): 495-516.
Fang, Y. Z., S. Yang, et al. (2002). "Free radicals, antioxidants, and nutrition." Nutrition **18**(10): 872-879.
Ferlay, J., M. Colombet, et al. (2018). "Estimating the global cancer incidence and mortality in 2018: GLOBOCAN sources and methods." Int J Cancer.
Ferlay, J., I. Soerjomataram, et al. (2015). "Cancer incidence and mortality worldwide: sources, methods and major patterns in GLOBOCAN 2012." Int J Cancer **136**(5): E359-386.
Ferraz da Costa, D. C., E. Fialho, et al. (2017). "Cancer Chemoprevention by Resveratrol: The p53 Tumor Suppressor Protein as a Promising Molecular Target." Molecules **22**(6).
Galluzzi, L., O. Kepp, et al. (2009). "RIP kinases initiate programmed necrosis." J Mol Cell Biol **1**(1): 8-10.
Goel, A., F. Fuerst, et al. (2006). "Selenomethionine induces p53 mediated cell cycle arrest and apoptosis in human colon cancer cells." Cancer Biol Ther **5**(5): 529-535.
Gomez-Cabrera, M. C., C. Borras, et al. (2005). "Decreasing xanthine oxidase-mediated oxidative stress prevents useful cellular adaptations to exercise in rats." J Physiol **567**(Pt 1): 113-120.
Guerin, P. J. and E. R. Gauthier (2003). "Induction of cellular necrosis by the glutathione peroxidase mimetic ebselen." J Cell Biochem **89**(1): 203-211.
Hacker, G. (2000). "The morphology of apoptosis." Cell Tissue Res **301**(1): 5-17.
Halliwell, B. (1992). "Reactive oxygen species and the central nervous system." J Neurochem **59**(5): 1609-1623.
Halliwell, B. (2003). "Oxidative stress in cell culture: an under-appreciated problem?" FEBS Lett **540**(1-3): 3-6.
Hatfield, D. L., P. A. Tsuji, et al. (2014). "Selenium and selenocysteine: roles in cancer, health, and development." Trends Biochem Sci **39**(3): 112-120.
Hers, I., E. E. Vincent, et al. (2011). "Akt signalling in health and disease." Cell Signal **23**(10): 1515-1527.

Hilkens, P. H., L. C. Pronk, et al. (1997). "Peripheral neuropathy induced by combination chemotherapy of docetaxel and cisplatin." Br J Cancer **75**(3): 417-422.
Hilkens, P. H., J. Verweij, et al. (1997). "Clinical characteristics of severe peripheral neuropathy induced by docetaxel (Taxotere)." Ann Oncol **8**(2): 187-190.
Hollander, M. C., G. M. Blumenthal, et al. (2011). "PTEN loss in the continuum of common cancers, rare syndromes and mouse models." Nat Rev Cancer **11**(4): 289-301.
Hopkins, B. D., C. Hodakoski, et al. (2014). "PTEN function: the long and the short of it." Trends Biochem Sci **39**(4): 183-190.
Hrycay, E. G. and S. M. Bandiera (2015). "Involvement of Cytochrome P450 in Reactive Oxygen Species Formation and Cancer." Adv Pharmacol **74**: 35-84.
Javeshghani, D., S. A. Magder, et al. (2002). "Molecular characterization of a superoxide-generating NAD(P)H oxidase in the ventilatory muscles." Am J Respir Crit Care Med **165**(3): 412-418.
Jiang, C., Z. Wang, et al. (2001). "Caspases as key executors of methyl selenium-induced apoptosis (anoikis) of DU-145 prostate cancer cells." Cancer Res **61**(7): 3062-3070.
Kaighn, M. E., K. S. Narayan, et al. (1979). "Establishment and characterization of a human prostatic carcinoma cell line (PC-3)." Invest Urol **17**(1): 16-23.
Klaunig, J. E. and L. M. Kamendulis (2004). "The role of oxidative stress in carcinogenesis." Annu Rev Pharmacol Toxicol **44**: 239-267.
Klaunig, J. E., L. M. Kamendulis, et al. (2010). "Oxidative stress and oxidative damage in carcinogenesis." Toxicol Pathol **38**(1): 96-109.
Kung, G., K. Konstantinidis, et al. (2011). "Programmed necrosis, not apoptosis, in the heart." Circ Res **108**(8): 1017-1036.
Laurent, A., C. Nicco, et al. (2005). "Controlling tumor growth by modulating endogenous production of reactive oxygen species." Cancer Res **65**(3): 948-956.
Lenaz, G. (1998). "Role of mitochondria in oxidative stress and ageing." Biochim Biophys Acta **1366**(1-2): 53-67.
Lenaz, G. (2012). "Mitochondria and reactive oxygen species. Which role in physiology and pathology?" Adv Exp Med Biol **942**: 93-136.
Lenaz, G. and M. L. Genova (2009). "Structural and functional organization of the mitochondrial respiratory chain: a dynamic super-assembly." Int J Biochem Cell Biol **41**(10): 1750-1772.
Manning, B. D. and L. C. Cantley (2007). "AKT/PKB signaling: navigating downstream." Cell **129**(7): 1261-1274.
Maraldi, T., C. Prata, et al. (2009). "Induction of apoptosis in a human leukemic cell line via reactive oxygen species modulation by antioxidants." Free Radic Biol Med **46**(2): 244-252.
Marnett, L. J. (2000). "Oxyradicals and DNA damage." Carcinogenesis **21**(3): 361-370.
Masumoto, H. and H. Sies (1996). "The reaction of ebselen with peroxynitrite." Chem Res Toxicol **9**(1): 262-267.
Mates, J. M. and F. Sanchez-Jimenez (1999). "Antioxidant enzymes and their implications in pathophysiologic processes." Front Biosci **4**: D339-345.
Menter, D. G., A. L. Sabichi, et al. (2000). "Selenium effects on prostate cell growth." Cancer Epidemiol Biomarkers Prev **9**(11): 1171-1182.
Miller, R. K., O. Genbacev, et al. (2005). "Human placental explants in culture: approaches and assessments." Placenta **26**(6): 439-448.
Morales, J., L. Li, et al. (2014). "Review of poly (ADP-ribose) polymerase (PARP) mechanisms of action and rationale for targeting in cancer and other diseases." Crit Rev Eukaryot Gene Expr **24**(1): 15-28.
Muller, P. A. and K. H. Vousden (2013). "p53 mutations in cancer." Nat Cell Biol **15**(1): 2-8.
Mundi, P. S., J. Sachdev, et al. (2016). "AKT in cancer: new molecular insights and advances in drug development." Br J Clin Pharmacol **82**(4): 943-956.
Mylonas, C. and D. Kouretas (1999). "Lipid peroxidation and tissue damage." In Vivo **13**(3): 295-309.

Naderali, E., A. A. Khaki, et al. (2018). "Regulation and modulation of PTEN activity." Mol Biol Rep **45**(6): 2869-2881.
Naskalski, J. W. and G. Bartosz (2000). "Oxidative modifications of protein structures." Adv Clin Chem **35**: 161-253.
Nicco, C., A. Laurent, et al. (2005). "Differential modulation of normal and tumor cell proliferation by reactive oxygen species." Biomed Pharmacother **59**(4): 169-174.
Nicotera, P., M. Leist, et al. (1998). "Intracellular ATP, a switch in the decision between apoptosis and necrosis." Toxicol Lett **102-103**: 139-142.
Noguchi, M., V. Ropars, et al. (2007). "Proto-oncogene TCL1: more than just a coactivator for Akt." FASEB J **21**(10): 2273-2284.
Orlando, P., S. Silvestri, et al. (2018). "Effect of ubiquinol supplementation on biochemical and oxidative stress indexes after intense exercise in young athletes." Redox Rep **23**(1): 136-145.
Pacula, A. J., K. B. Kaczor, et al. (2017). "New Chiral Ebselen Analogues with Antioxidant and Cytotoxic Potential." Molecules **22**(3).
Pacula, A. J., K. B. Kaczor, et al. (2017). "New glutathione peroxidase mimetics-Insights into antioxidant and cytotoxic activity." Bioorg Med Chem **25**(1): 126-131.
Parnham, M. J. and H. Sies (2013). "The early research and development of ebselen." Biochem Pharmacol **86**(9): 1248-1253.
Pawlik, A., A. Wiczk, et al. (2013). "Sulforaphane inhibits growth of phenotypically different breast cancer cells." Eur J Nutr **52**(8): 1949-1958.
Perdomo, H. A. G., J. A. Zapata-Copete, et al. (2018). "Molecular alterations associated with prostate cancer." Cent European J Urol **71**(2): 168-176.
Rhind, N. and P. Russell (2012). "Signaling pathways that regulate cell division." Cold Spring Harb Perspect Biol **4**(10).
Roman, M., P. Jitaru, et al. (2014). "Selenium biochemistry and its role for human health." Metallomics **6**(1): 25-54.
Salem, N., N. Helmi, et al. (2018). "Renoprotective Effect of Platelet-Rich Plasma on Cisplatin-Induced Nephrotoxicity in Rats." Oxid Med Cell Longev **2018**: 9658230.
Santofimia-Castano, P., L. Garcia-Sanchez, et al. (2014). "The seleno-organic compound ebselen impairs mitochondrial physiology and induces cell death in AR42J cells." Toxicol Lett **229**(3): 465-473.
Schieber, M. and N. S. Chandel (2014). "ROS function in redox signaling and oxidative stress." Curr Biol **24**(10): R453-462.
Sharma, V., R. Tewari, et al. (2008). "Ebselen sensitizes glioblastoma cells to Tumor Necrosis Factor (TNFalpha)-induced apoptosis through two distinct pathways involving NF-kappaB downregulation and Fas-mediated formation of death inducing signaling complex." Int J Cancer **123**(9): 2204-2212.
Shichiri, M. (2014). "The role of lipid peroxidation in neurological disorders." J Clin Biochem Nutr **54**(3): 151-160.
Shigenaga, M. K. and B. N. Ames (1991). "Assays for 8-hydroxy-2'-deoxyguanosine: a biomarker of in vivo oxidative DNA damage." Free Radic Biol Med **10**(3-4): 211-216.
Sies, H. (1993). "Ebselen, a selenoorganic compound as glutathione peroxidase mimic." Free Radic Biol Med **14**(3): 313-323.
Sies, H. (1994). "Ebselen: a glutathione peroxidase mimic." Methods Enzymol **234**: 476-482.
Sies, H. (1995). "Ebselen." Methods Enzymol **252**: 341-342.
Sies, H. (1997). "Oxidative stress: oxidants and antioxidants." Exp Physiol **82**(2): 291-295.
Sies, H. and E. Cadenas (1985). "Oxidative stress: damage to intact cells and organs." Philos Trans R Soc Lond B Biol Sci **311**(1152): 617-631.
Sies, H. and H. Masumoto (1997). "Ebselen as a glutathione peroxidase mimic and as a scavenger of peroxynitrite." Adv Pharmacol **38**: 229-246.
Singh, K. B., S. H. Kim, et al. (2018). "Prostate cancer chemoprevention by sulforaphane in a preclinical mouse model is associated with inhibition of fatty acid metabolism." Carcinogenesis **39**(6): 826-837.

Sinha, R. and D. Medina (1997). "Inhibition of cdk2 kinase activity by methylselenocysteine in synchronized mouse mammary epithelial tumor cells." Carcinogenesis **18**(8): 1541-1547.
Smith, C. D., J. M. Carney, et al. (1992). "Protein oxidation in aging brain." Ann N Y Acad Sci **663**: 110-119.
Soga, T. (2013). "Cancer metabolism: key players in metabolic reprogramming." Cancer Sci **104**(3): 275-281.
Song, G., G. Ouyang, et al. (2005). "The activation of Akt/PKB signaling pathway and cell survival." J Cell Mol Med **9**(1): 59-71.
Stadtman, E. R. (1992). "Protein oxidation and aging." Science **257**(5074): 1220-1224.
Steinbrenner, H., B. Speckmann, et al. (2016). "Selenoproteins: Antioxidant selenoenzymes and beyond." Arch Biochem Biophys **595**: 113-119.
Stewart, M. S., J. E. Spallholz, et al. (1999). "Selenium compounds have disparate abilities to impose oxidative stress and induce apoptosis." Free Radic Biol Med **26**(1-2): 42-48.
Stone, K. R., D. D. Mickey, et al. (1978). "Isolation of a human prostate carcinoma cell line (DU 145)." Int J Cancer **21**(3): 274-281.
Thannickal, V. J. and B. L. Fanburg (2000). "Reactive oxygen species in cell signaling." Am J Physiol Lung Cell Mol Physiol **279**(6): L1005-1028.
Tiano, L., G. P. Littarru, et al. (2005). "Assessment of DNA damage in Down Syndrome patients by means of a new, optimised single cell gel electrophoresis technique." Biofactors **25**(1-4): 187-195.
Tikkinen, K. A. O., P. Dahm, et al. (2018). "Prostate cancer screening with prostate-specific antigen (PSA) test: a clinical practice guideline." BMJ **362**: k3581.
Turrens, J. F. (2003). "Mitochondrial formation of reactive oxygen species." J Physiol **552**(Pt 2): 335-344.
Valko, M., M. Izakovic, et al. (2004). "Role of oxygen radicals in DNA damage and cancer incidence." Mol Cell Biochem **266**(1-2): 37-56.
Valko, M., C. J. Rhodes, et al. (2006). "Free radicals, metals and antioxidants in oxidative stress-induced cancer." Chem Biol Interact **160**(1): 1-40.
Vernooij, R. W. M., L. Lytvyn, et al. (2018). "Values and preferences of men for undergoing prostate-specific antigen screening for prostate cancer: a systematic review." BMJ Open **8**(9): e025470.
Vinceti, M., T. Filippini, et al. (2018). "Selenium for preventing cancer." Cochrane Database Syst Rev **1**: CD005195.
Wade, M., Y. C. Li, et al. (2013). "MDM2, MDMX and p53 in oncogenesis and cancer therapy." Nat Rev Cancer **13**(2): 83-96.
Wang, X., E. R. Simpson, et al. (2015). "p53: Protection against Tumor Growth beyond Effects on Cell Cycle and Apoptosis." Cancer Res **75**(23): 5001-5007.
Wang, X., K. Sun, et al. (2014). "Efficacy and safety of selenium nanoparticles administered intraperitoneally for the prevention of growth of cancer cells in the peritoneal cavity." Free Radic Biol Med **72**: 1-10.
Wang, Z., C. Jiang, et al. (2001). "Antimitogenic and proapoptotic activities of methylseleninic acid in vascular endothelial cells and associated effects on PI3K-AKT, ERK, JNK and p38 MAPK signaling." Cancer Res **61**(19): 7171-7178.
Wang, Z., C. Jiang, et al. (2002). "Induction of caspase-mediated apoptosis and cell-cycle G1 arrest by selenium metabolite methylselenol." Mol Carcinog **34**(3): 113-120.
Ward, A. B., H. Mir, et al. (2018). "Quercetin inhibits prostate cancer by attenuating cell survival and inhibiting anti-apoptotic pathways." World J Surg Oncol **16**(1): 108.
Wardman, P. and L. P. Candeias (1996). "Fenton chemistry: an introduction." Radiat Res **145**(5): 523-531.
Weinstein, I. B. (1991). "Cancer prevention: recent progress and future opportunities." Cancer Res **51**(18 Suppl): 5080s-5085s.
Whitacre, C. M., E. Zborowska, et al. (1999). "Detection of poly(ADP-ribose) polymerase cleavage in response to treatment with topoisomerase I inhibitors: a potential surrogate end point to assess treatment effectiveness." Clin Cancer Res **5**(3): 665-672.

Wiseman, H. and B. Halliwell (1996). "Damage to DNA by reactive oxygen and nitrogen species: role in inflammatory disease and progression to cancer." Biochem J **313 (Pt 1)**: 17-29.

Xia, Y., S. Shen, et al. (2014). "NF-kappaB, an active player in human cancers." Cancer Immunol Res **2**(9): 823-830.

Xie, T. X., Z. Xia, et al. (2010). "Constitutive NF-kappaB activity regulates the expression of VEGF and IL-8 and tumor angiogenesis of human glioblastoma." Oncol Rep **23**(3): 725-732.

Yakes, F. M. and B. Van Houten (1997). "Mitochondrial DNA damage is more extensive and persists longer than nuclear DNA damage in human cells following oxidative stress." Proc Natl Acad Sci U S A **94**(2): 514-519.

Yang, C. F., H. M. Shen, et al. (2000). "Ebselen induces apoptosis in HepG(2) cells through rapid depletion of intracellular thiols." Arch Biochem Biophys **374**(2): 142-152.

Yang, C. F., H. M. Shen, et al. (2000). "Intracellular thiol depletion causes mitochondrial permeability transition in ebselen-induced apoptosis." Arch Biochem Biophys **380**(2): 319-330.

Yeo, J. K., S. D. Cha, et al. (2002). "Se-methylselenocysteine induces apoptosis through caspase activation and Bax cleavage mediated by calpain in SKOV-3 ovarian cancer cells." Cancer Lett **182**(1): 83-92.

Yoshida, Y., A. Umeno, et al. (2013). "Lipid peroxidation biomarkers for evaluating oxidative stress and assessing antioxidant capacity in vivo." J Clin Biochem Nutr **52**(1): 9-16.

Zhang, L., L. Zhou, et al. (2014). "Induction of apoptosis in human multiple myeloma cell lines by ebselen via enhancing the endogenous reactive oxygen species production." Biomed Res Int **2014**: 696107.

Zhong, W. and T. D. Oberley (2001). "Redox-mediated effects of selenium on apoptosis and cell cycle in the LNCaP human prostate cancer cell line." Cancer Res **61**(19): 7071-7078.

web side and polish articles:

https://www.cancer.org/cancer/prostate-cancer.html

Didkowska J., Wojciechowska U., Zatoński W. (2009) Prognozy zachorowalności i umieralności na nowotwory złośliwe w Polsce do 2025 roku. Centrum Onkologii-Instytut im. M. Curie-Skłodowskiej, Warszawa 2009

Didkowska J., Wojciechowska U., Zatoński W. (2015) Nowotwory złośliwe w Polsce w 2015 roku. Centrum Onkologii-Instytut im. M. Curie-Skłodowskiej, Warszawa 2017